

### Abstract

At Syowa Station, which was opened in 1957, two diesel electric generators were installed, one of which was always operated as the main energy source. The electric capacity of each generator has been increased from 20 kVA to 110 kVA in accordance with the expansion of the station.

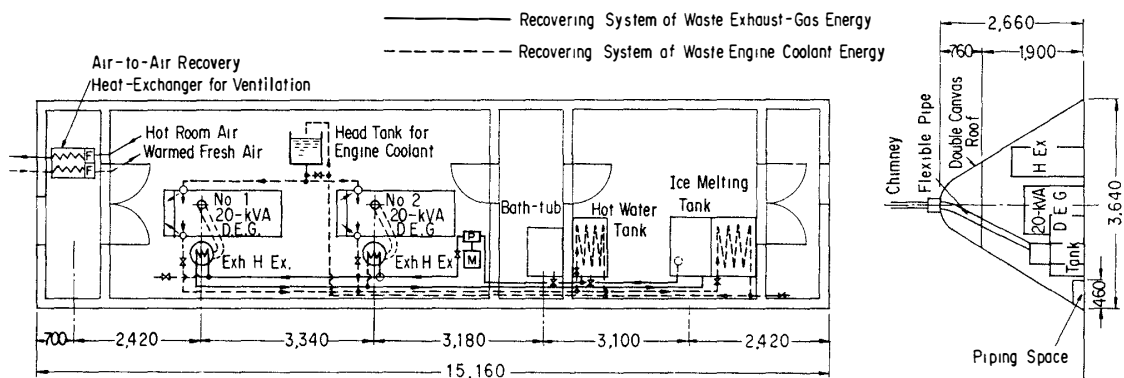
In order to save fuel consumption, the authors have developed some waste heat recovery systems of the diesel engines. By fully utilizing the waste heat of diesel engines, *i.e.*, their exhaust-gas energy and coolant energy, cold and hot water was made from ice or snow even in winter. The hot and cold water was supplied to the living quarters through insulated water pipes. The hot water was also supplied for bathing and heating of apartments of the buildings.

At Mizuho Station, which was opened in 1970, a system for recovering coolant heat of a diesel electric generator was installed. The cold and hot water is made by the similar system. The hot water is supplied to a bathtub and to a fan-coil unit in a trench living room. The heating by utilizing the waste coolant can ensure the safety of the personnel living in the trench room against fire, contamination by CO, CO<sub>2</sub> and lack of oxygen.

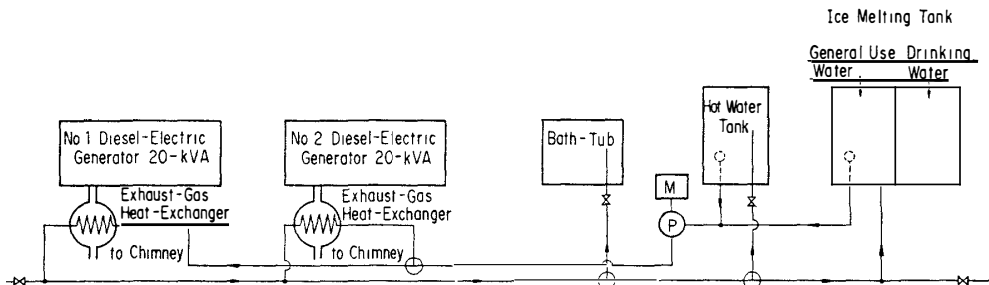
In this report, the technical problems and experiences on waste heat recovering, especially on exhaust-gas heat exchangers are described.

### 1. Historical Review of Development of Syowa Station

In 1955/56, S. AWANO, who was a member of the Special Committee on Mechanical Engineering for Japanese Antarctic Research Expedition (JARE) organized within Japan Society of Mechanical Engineers (JSME), designed and constructed a prototype system for producing cold and hot water as shown in Figs. 1 and 2 for JARE-1 (1956/58), utilizing the waste heat of exhaust gas from diesel engines coupled to 20-kVA electric generators as the main electric power source of Syowa Station.



a. Waste heat recovery system prepared for JARE-1.



b. Waste exhaust-gas energy recovery system actually rebuilt in JARE-1 engine room of Syowa Station.

Fig. 1. 20-kVA diesel-electric generators and waste heat recovery system prepared for JARE-1 (1956/58).

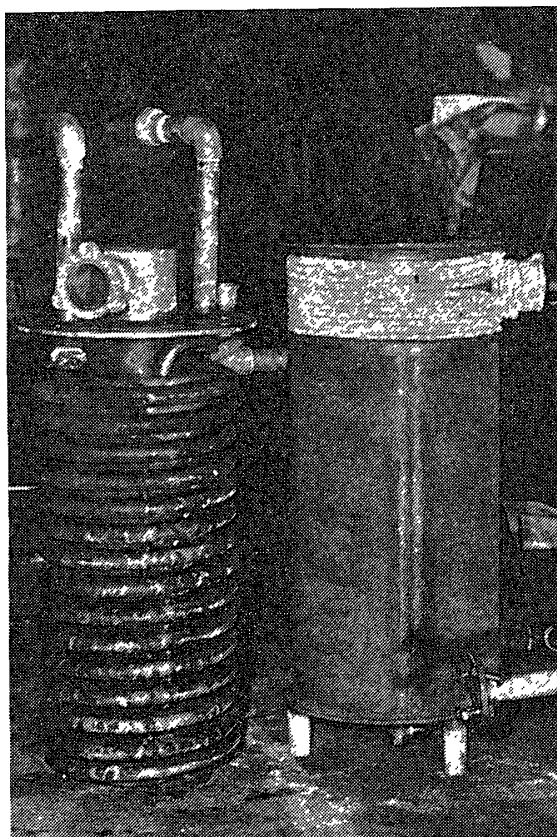


*Fig. 2. Shell-and-coil type exhaust-gas heat exchanger prepared for JARE-1 (1956/58).*

The details of the system have already been reported by AWANO and MAITA (1963) and SPECIAL COMMITTEE ON MECHANICAL ENGINEERING FOR JARE (1959). This system was used satisfactorily from JARE-1 to JARE-5 (1960/62).

Syowa Station was closed from February 1962 to December 1965. During these unmanned years, the system was left as it was. However, it was paid a special attention so as to facilitate the future reopening of the station.

Another JARE-7 engine room was newly built in January 1966. Two 45-kVA diesel-electric generators were set with a new system for making cold and hot water utilizing the waste heat of exhaust gas and coolant of diesel engines. In the 1967 wintering season, to satisfy the expanded requirement for electric power, one of the old two 20-kVA diesel-electric generators was used for scientific purpose. One of the new two 45-kVA generators supplied the electric power for general use.

Another new JARE-9 engine room was built in 1968, which contained two 65-kVA diesel-electric generators and a cold and hot water making system utilizing their waste heat. One of the two 45-kVA generators supplied the electric power for scientific instruments, and one of the two 65-kVA generators supplied the power for general use. The two engine rooms, JARE-7 and JARE-9, were separated about 40 m and connected by a corrugated passage. The surveillance

Table 1. Data on the logistics of JARE.

	Year	Number of wintering members	Total area of laboratories (m <sup>2</sup> )	Total weight of cargo (t)	Total weight of fuels (t)	Water consumption (l/day·person)
JARE-1	1956/58	11	184	141	37	14.5
-2	1957/58	0	184	0	0	0
-3	1958/60	14	194	52	15	15
-4	1959/61	15	251	154	63	21
-5	1960/62	16	256	121	98	21
-6	1961/62	0	256	0	0	0
-7	1965/67	18	778	390	122	40
-8	1966/68	24	1283	463	149	56
-9	1967/69	29	1827	526	235	60
-10	1968/70	29	2322	560	231+ 64*	50
-11	1969/71	30	2772	572	160+ 88*	49.5
-12	1970/72	29	2810	500	270	38.4
-13	1971/73	30	3026	468	258	53.9
-14	1972/74	30	3221	488	258	53.2
-15	1973/75	30	3322	496	283+ 12**	43.2
-16	1974/76	30	3394	473	333+ 11**	42.6
-17	1975/77	29	3422	493	307	77.3
-18	1976/78	30	3522	494	304+ 4**	41.2
-19	1977/79	30	3622	487	290+144*	51.5
-20	1978/80	30	3492	462	237+ 19**	
-21	1979/81	33	3794	459	141+ 54**	

\* Transferred gas oil from the fuel of icebreaker FUJI.

\*\* Aeronautical gasoline.

Table 2. An example of yearly consumed fuel and oil in JARE-19 (1978/79).

Items	Purposes	Consumption (kl/year)
JARE gas oil	Vehicles	30
Gas oil	Diesel-electric generators	150
Kerosene	Hot-air heaters for room-heating	60
Gasoline	Vehicles	30
	Air heaters	
	300 W engine generator	
	1-kVA engine generator	
	Torch lamp	
	Total	270
JARE lubricating oil	Vehicles, 16-kVA diesel-electric generator etc.	4.2
Lubricating oil	110-kVA diesel-elctetric generators	0.4
Anti-freezing liquid	Vehicles, 16-kVA diesel-electric generator	1
	Total	5.6

of the two power plants was a very troublesome task for maintenance.

In JARE-19 (1977/79), one of the two 65-kVA generators was replaced by a 110-kVA diesel-electric generator, which supplied all of the power for scientific and general uses.

In JARE-20 (1978/80), the remaining 65-kVA generator was also replaced by the same type 110-kVA diesel-electric generator, and one of them has supplied all of the necessary electric power of the station and other is kept in reserve.

During 1977/79, the waste heat recovery system was also rearranged by TAKEUCHI, one of the authors. By simplifying the binary power sources in the two separated engine rooms to a single source, firstly the fuel consumption was decreased remarkably as compared to that of binary sources and secondly, mechanics were freed from troublesome work.

Table 1 shows the development of logistics capacity at Syowa Station. Recently, the weight of fuels amounts to about 50–60% of the total cargo. The water consumption at Syowa Station is also shown in Table 1.

Table 3. Diesel-electric power generators used in JARE-1/20 (1956/81).

Station	Syowa				Mizuho	
Type	ZX-111 20 kVA	ZX-140 45 kVA	ZX-75 65 kVA	ZX-125 110 kVA	ZX-500B 12 kVA	ZX-20A 16 kVA
Engine room	JARE-1	JARE-7	JARE-9	JARE-9	trench	trench
Generator	Maker: Meidensha, Model: E-AF, Pole:4-poles, Phase: 3 phase, Cycle: 50 Hz, Power factor: 80%, Engine speed: 1500 rpm					
Voltage (V) AC	100	200	200	200	200	200
Current (A)	160	130	187	318	34.6	46.2
Max. output (kW)	16	36	52	88	9.6	12.8
Diesel engine	Maker: Isuzu, Stroke cycle: 4, Type: in-line, Cooling system: liquid cooling					
Model	DA-220	DA-120	DA-640T	73E-120	C221	C240
Combustion chamber	pre-comb.	pre-comb.	pre-comb.	direct inj.	voltex	voltex
Compression ratio	19.5	22	22	16.5	20	20
Cylinders	4	6	6	6	4	4
Bore (mm)	100	100	102	135	83	86
Stroke (mm)	130	130	130	140	102	102
Piston displacement volume (cc)	4084	6126	6373	12024	2207	2369
Output power PS/1500 rpm	33	65.5	82	140	21	25
Min. SFC (gr/PSH)	200	190	198	170	205	205
Turbocharging	none	none	turbo-charged	none	none	none
Starter (V/kW)	24/3	24/3.7	24/3.7	24/7.4	24/2.2	24/2.2
Generator for (V) charging battery (A)	24	24	24	24	24	24
Battery (V)	12	12	12	12	12	12
(Ah)	150×2	120×2	120×2	150×2	100×1	100×1

Table 2 shows an example of yearly fuel consumption. About 150 k $l$  of diesel fuel is consumed ordinarily by the diesel engines for electric generators, representing 56% of total fuel supply of 270 k $l$ .

Tables 3 and 4 show the electric power plants and their yearly mean and peak electric load at Syowa Station, which reaches 42–49 kW and 71–82 kW respectively at present.

Mizuho Station located at 70°41'53''S and 44°19'54''E inland isolated from Syowa Station by about 270 km, has four prefabricated huts and two trench engine rooms under the snow. In the trench engine rooms, two diesel-electric generators, 16 kVA and 12 kVA, are installed independently and one of them supplies all of the electric power. The coolant heat of the diesel engines, which has been also fully used for making cold and hot water by melting the snow, and the

Table 4. Diesel-electric power generators at Syowa and Mizuho Stations and the yearly mean and peak loads.

Year	Syowa Station				Mizuho Station (kVA)
	JARE-1 (kVA)	JARE-7 (kVA)	JARE-9 (kVA)	Yearly mean/peak load (kW)	
JARE-1 1956/58	20×2			2/4	
-2 1957/58	20×2			0	
-3 1958/60	20×2			5/7	
-4 1959/61	20×2			7/14	
-5 1960/62	20×2			9/14	
-6 1961/62	20×2			0	
-7 1965/67	20×2	45×2		27/43	
-8 1966/68	20×2	45×2		40/53	
-9 1967/69		45×2	65×1	42/87	
-10 1968/70		45×2	65×2	48/87	
-11 1969/71		45×2	65×2	50/82	1, 0.3
-12 1970/72		45×2	65×2	(21.2+29.5)/(26+48)*	12, 1
-13 1971/73		45×2	65×2	(22.5+26.3)/(29+52)*	12, 1
-14 1972/74		45×2	65×2	(22.5+26.2)/(36+53)*	12, 1
-15 1973/75		45×2	65×2	(21.2+24.8)/(33+53)*	12, 1
-16 1974/76		45×2	65×2	(22.2+28.8)/(31+58)*	12, 1
-17 1975/77		45×2	65×2	(23.3+28.8)/(34+64)*	12, 16
-18 1976/78		45×2	65×2	(20.2+27.1)/(28+55)*	12, 16
-19 1977/79		45×2	110×1	(48.9/82)**	16, 12
-20 1978/80			110×2	(42.1/71)**	16, 12
-21 1979/81			110×2		16, 12

\* (45+65 kVA)/(45+65 kVA).

\*\* (110 kVA/110 kVA).

hot water has also been used for heating a living room and for a bathtub.

The hot-water room-heating system ensures the safety of the wintering members, who are freed from the contamination of CO and CO<sub>2</sub> and the lack of oxygen which would be inevitable if the oil furnaces were used.

In the following articles, details of the waste heat recovering systems developed by the authors will be described.

## 2. A 45-kVA Diesel-Electric Power Generating Plant with Waste Heat Recovery System

A prefabricated power plant hut was built by JARE-7 in 1966. There were two sets of 45-kVA diesel-electric generators, two sets of exhaust-gas heat exchangers, two sets of shell-and-tube type horizontal coolant-to-water heat ex-

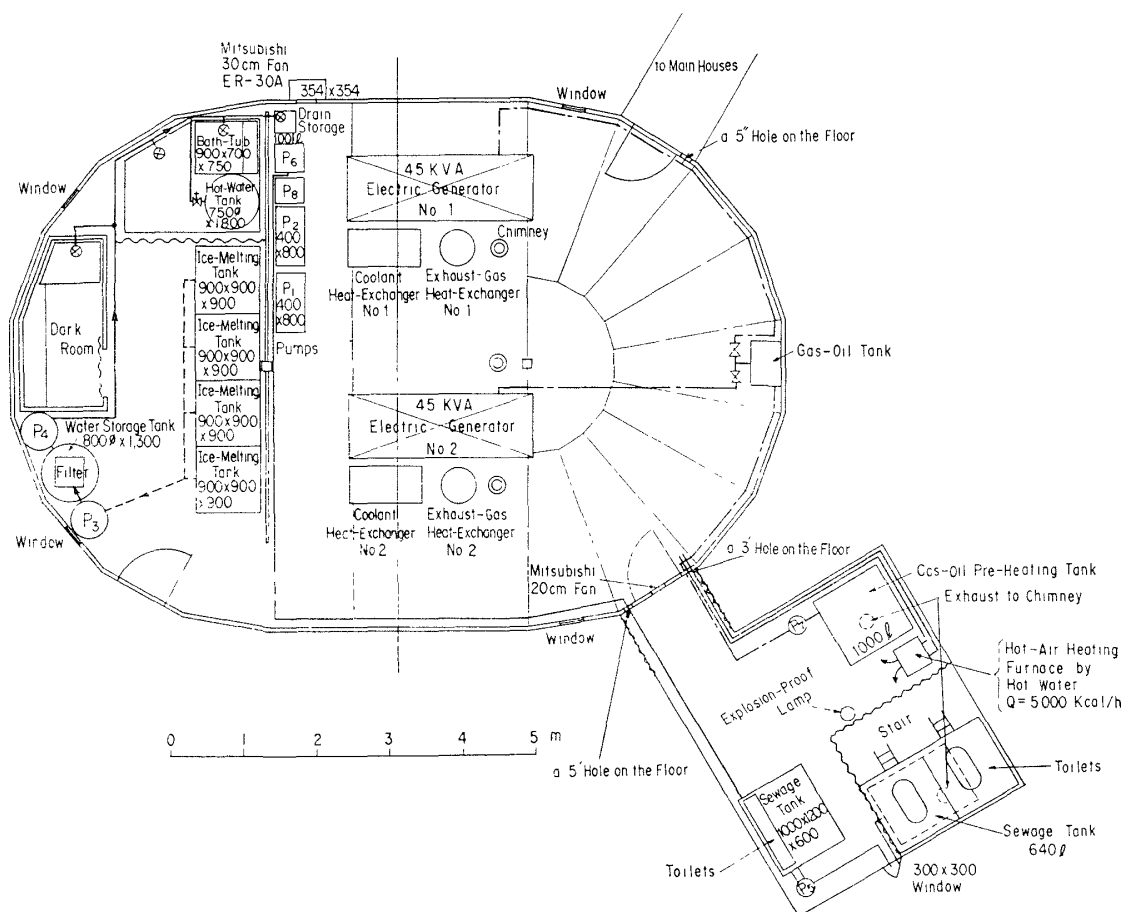


Fig. 3. JARE-7 engine room containing two sets of 45-kVA diesel-electric generators (Meidensha ZX-140 type, diesel engine Isuzu DA-120) and waste heat recovery systems for making cold and hot water, prepared for JARE-7 (1965/67).

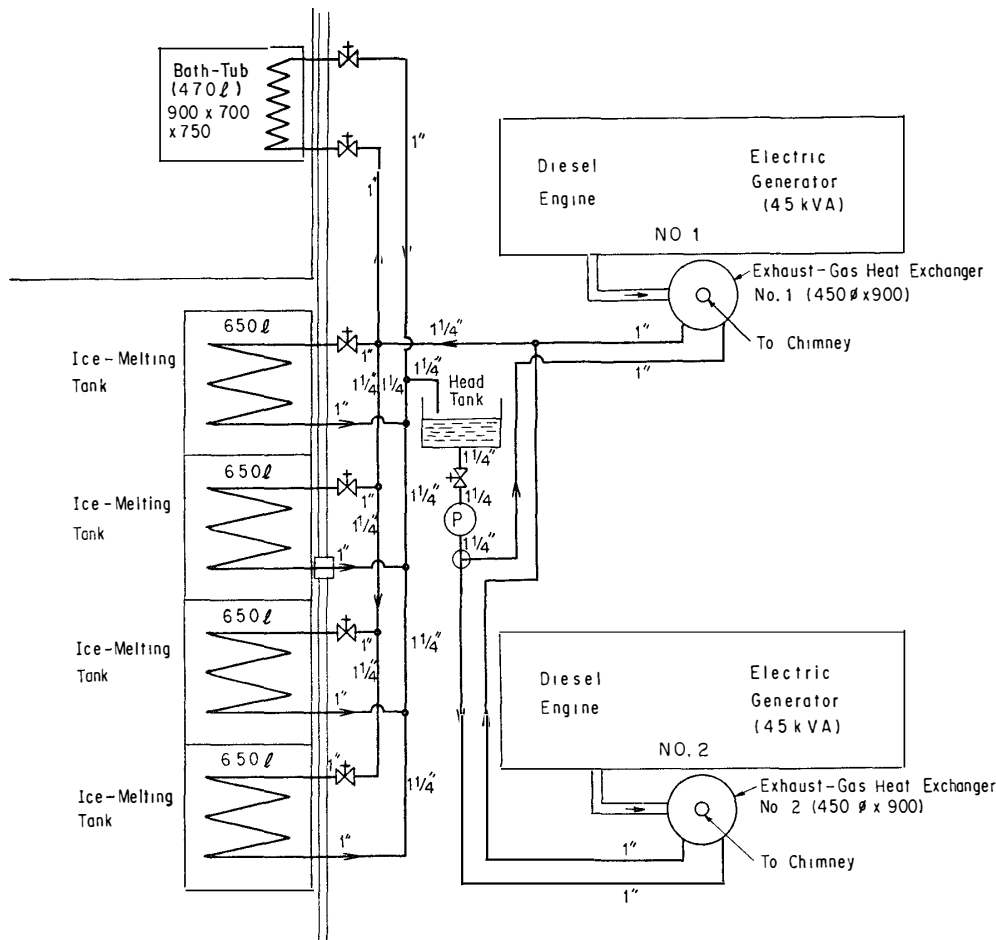
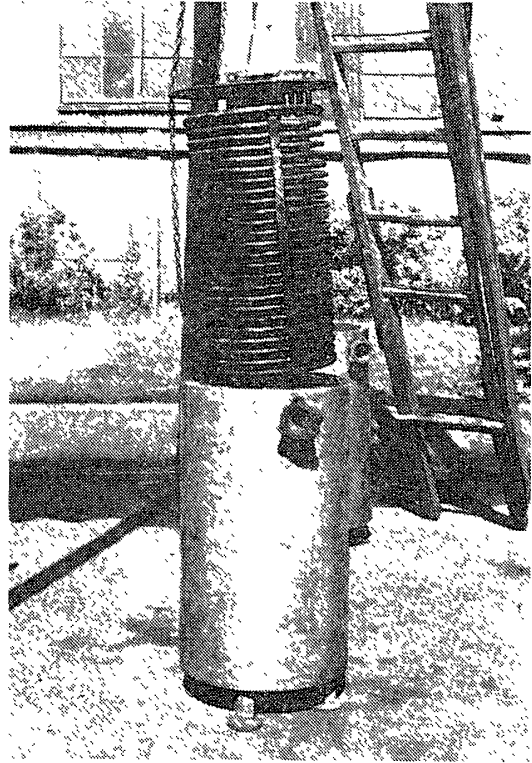


Fig. 4. Exhaust-gas heat recovery system in JARE-7 engine room.

changers for recovering the waste coolant heat of diesel engines, one hot-water storage stainless-steel tank (750 mm diam.  $\times$  1800 mm H, capacity 79 l), four ice-melting stainless-steel tanks (each measuring 900  $\times$  900  $\times$  900 mm, capacity 650 l), and one bathtub in this JARE-7 engine room (Figs. 3, 4).

### 2.1. Ice or snow-melting plant utilizing exhaust-gas energy of diesel engines

One of the two sets of the 45-kVA diesel-electric generators was run continuously until 1978. The greater part of the waste exhaust-gas energy of the diesel engines was recovered by the shell-and-coil type heat exchangers as shown in Figs. 5 and 6. Hot water of about 45°C was heated to 55–60°C by the exhaust of the diesel engines while flowing through the coils. The external diameter of stainless coil pipe was 18 mm, the total length of which was 94.3 m, and the total outer surface area was 5.33 m<sup>2</sup> (see Table 7). By this system,  $Q_r = 9000\text{--}18000$  kcal/h heat was recovered from the waste exhaust-gas energy, and 1–2 kl/day of cold water could be supplied by melting ice and snow.



*Fig. 5. Shell-and-coil type exhaust-gas heat exchanger prepared for JARE-7 (1965/67).*

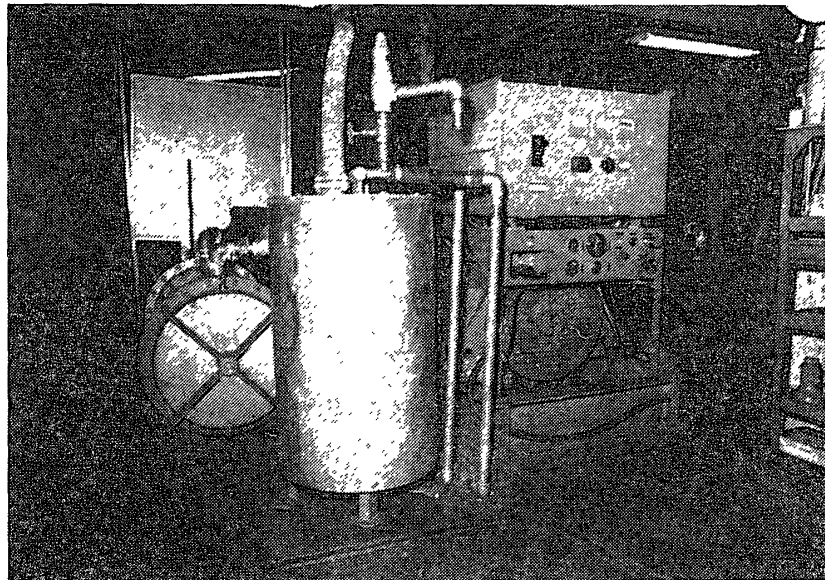


*Fig. 6. Inside view of JARE-7 engine room (45-kVA diesel-electric generator, shell-and-coil type exhaust-gas heat exchanger, and horizontal shell-and-tube type coolant-to-water heat exchanger to recover coolant heat of DA-120 diesel engine from right to left).*

## 2.2. System for making hot water with coolant of diesel engines

The coolant heat of diesel engines was utilized for making hot water of about 60–70°C. Two sets of horizontal stainless-steel shell-and-tube type heat exchangers were prepared for this purpose. As shown in Fig. 7 a new high temperature automatic thermo-valve, which opens at about 90°C, was installed at the inlet of an engine radiator, in addition to an ordinary low temperature automatic thermo-valve, which opens at about 65°C. The engine coolant flowing through the low temperature thermo-valve was bypassed to the shell side of a shell-and-tube type heat exchanger at the inlet of the high temperature thermo-valve. The engine coolant of 65–80°C transferred its heat to the low temperature water flowing through the inside of tubes and returned to the inlet of coolant pump of engine. Although the high temperature thermo-valve is closed normally, it opens when the coolant temperature rises abnormally, and some of the hot coolant from the engine is bypassed to the engine radiator to protect the engine from overheating.

A water pump  $P_1$  (1.5 kW, capacity 0.07 m<sup>3</sup>/min at  $H=24$  m H<sub>2</sub>O) shown in Fig. 8 recirculated the hot water between the hot-water storage tank and the shell-and-tube type heat exchangers. Another water pump,  $P_2$ , was used for recirculating the hot water between the hot-water storage tank and heating radiators provided at the inlet of heating furnaces for warming the fuel preheating room and the living and cooking quarters.

Hot water was also supplied to washstands in the living quarters. The water level of the hot-water tank was always kept at a constant level by charging automatically thereinto cold water from the cold-water tank.

## 2.3. Insulated hot and cold water feeding pipe

The hot and cold water made in the JARE-7 engine room was fed to the living quarters which were separated therefrom by about 160 m. For this purpose, two kinds of insulated piping units were developed by the authors. Fig. 9a shows one piping unit and its section. The piping unit was 140 mm in diameter and 4 m in length. A polyethylene outer pipe contained four aluminum pipes of 32-mm external diameter, and the space between them was filled with polyurethane foam insulator. The lower two aluminum pipes were used as feed and return pipes for hot water, and the remaining two as the feed and return pipes for cold water.

The other type of piping unit had three aluminum pipes as shown in Fig. 9b. The lower two pipes were used as feed and return pipes for hot water, and the remaining one was used for feeding cold water to messroom and living quarters. In each case, the heat loss from the two hot-water pipes prevented the freezing of cold water. Thus, we succeeded in supplying hot and cold water to messroom and living quarters (Fig. 10). The temperature drop of hot water at 45°C was

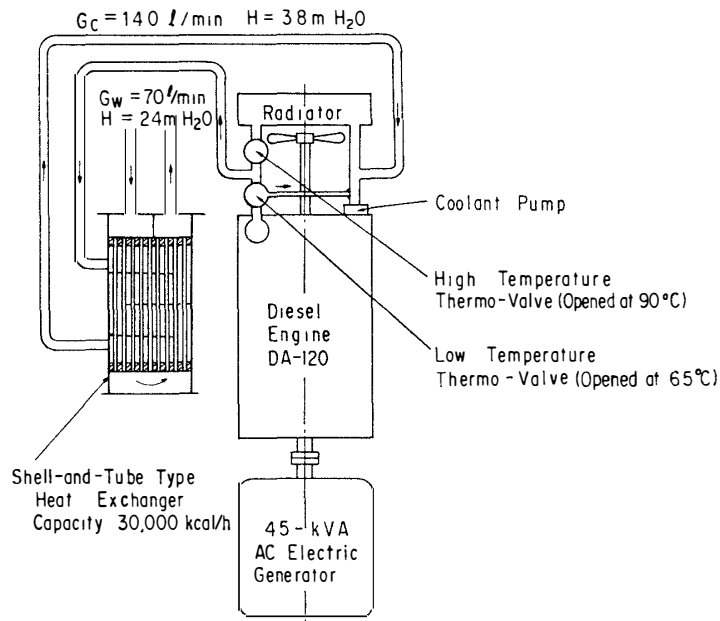


Fig. 7. Piping for coolant heat recovery system in JARE-7 engine room.

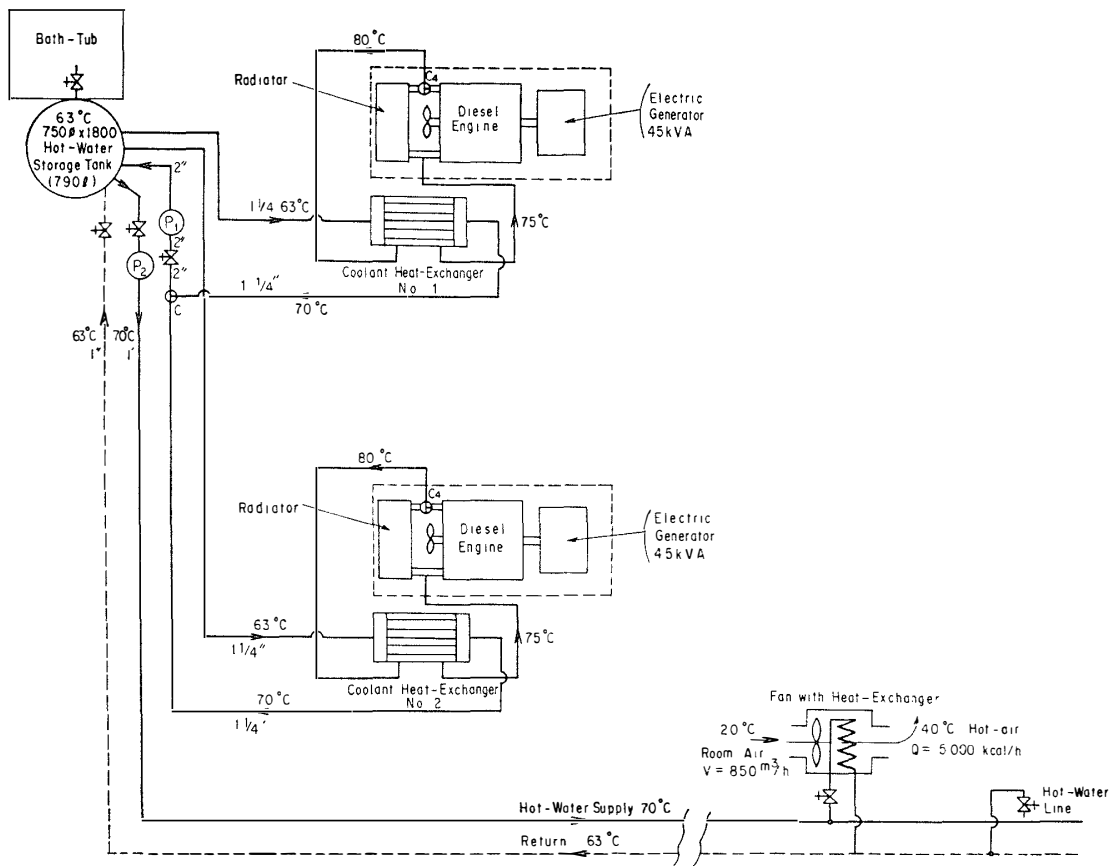
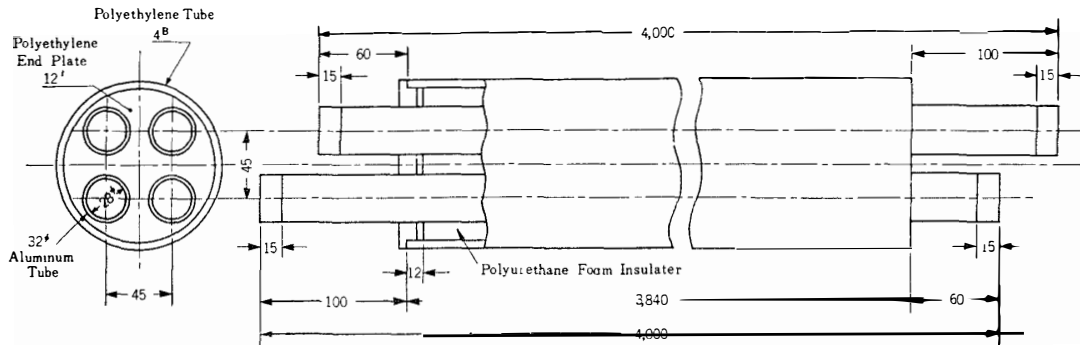
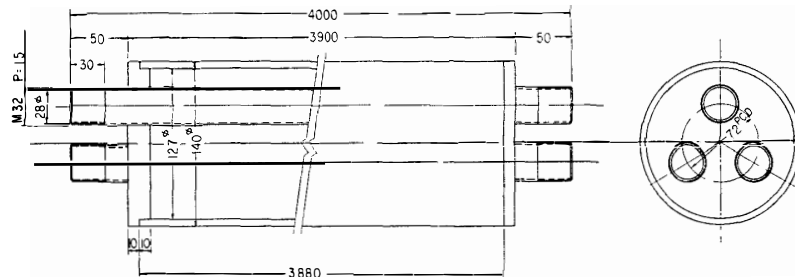


Fig. 8. Coolant heat recovery system in JARE-7 engine room.



(a) Four-tube type.



(b) Three-tube type.

Fig. 9. Insulated hot and cold water feeding pipes developed for JARE-7 (1965/67).



Fig. 10. Insulated hot and cold water feed pipes, feed pump with head-tank, and water filter using organic filter elements.

only 1.0–1.5°C during its flow through the insulated duct of 100-m length at a flow rate of 100–200 l/min at Syowa Station (SATO, 1967).

Experiments on the effectiveness of these piping units were done in a low-temperature testing room of the Research Institute of Transportation Technology, Tokyo, by the authors in August 1965. The data obtained and the results of theoretical analysis are shown in Appendix 1.

#### **2.4. Fuel preheating room and toilet**

As shown in Fig. 3, a fuel preheating room was built adjacent to the JARE-7 engine room. This room was warmed to about 10°C at floor level by hot air transferred by an axial fan from the engine room and by a heating furnace described in Subsection 2.2.

A diesel fuel tank (capacity 1 kl), toilets, and a sewage tank (capacity 75 l) were also installed in this room. The toilets were designed by Ebara Infilco Co., Ltd., and were similar to those of airplanes. The sewage from the bathtub and the toilets was mixed and pumped to a tide crack by a monoflex pump. The sewage was lifted vertically first to a roof level and then transported through an inclined 1.5B plastic pipeline of 80-m length. After the pumping was finished, the contents of the pipe were entirely drained off to protect it from freezing. The slope of inclination should be greater than 2°, and an air-cock should be installed at the foot of each end of the pipeline. This simple and most effective method for pumping water outdoors was developed by the members of JARE-7 (SATO, 1967). This pumping transportation of sewage made unnecessary the troublesome work of transporting it to tide crack by a vehicle with a vacuum tank.

#### **2.5. A 10-kl snow or ice-melting and cold-water storage tank installed outdoors**

To eliminate the laborious work of transporting and throwing snow or ice into the melting tank in the JARE-7 engine room, a 10-kl prefabricated outdoor tank was developed by the authors for JARE-8 in 1966. As shown in Figs. 11 and 12, eight steel pillars having U-grooves were placed vertically on the ground, and eight sidewall panels were inserted into the U-grooves to form a square bottomless tank support measuring  $4.06 \times 3.96 \times 1.00$  m. The steel panels for the sidewalls were filled with glass fiber as an insulator and were thoroughly water-proofed. The dimensions of each were  $1.0 \times 0.9 \times 0.078$  m. Furthermore, a water-proofed canvas sheet tank was extended inside the tank support and was fixed to the pillars by ropes. The pressure of water in the tank was sustained by the walls, pillars and four tension stays connecting the basic members of the tank support and not by the canvas itself. Another water-proof canvas sheet covered and insulated the tank from the cold atmosphere. Hot water was led to a stainless-steel tube type radiator submerged in the water and was recirculated to an

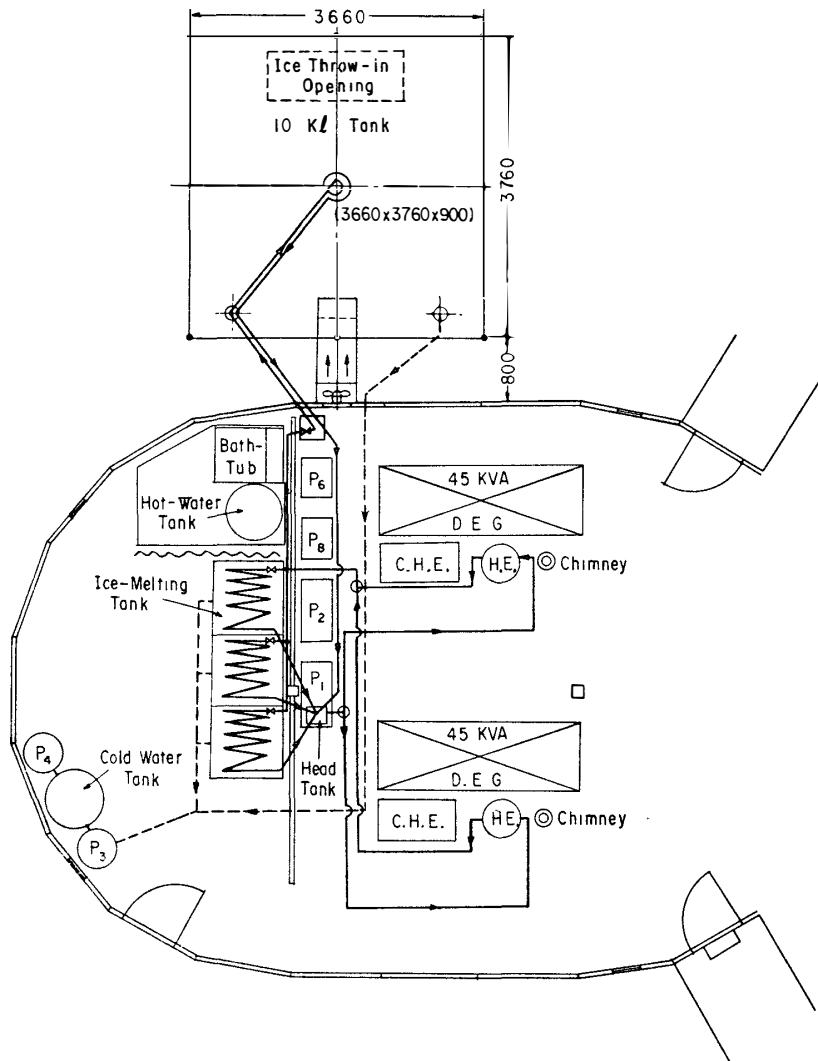


Fig. 11. Ten-kl outdoor ice-melting and cold water storage tank prepared for JARE-8 (1965/68).

exhaust-gas heat exchanger in the JARE-7 engine room.

This water making and storage system has been used successfully during the past 13 years. The water temperature in the tank was kept at 20–30°C even in winter. As the submerged heating radiator, a stainless-steel tube type radiator was most suitable because of its high resistance to hard ice, sand, dust and rust.

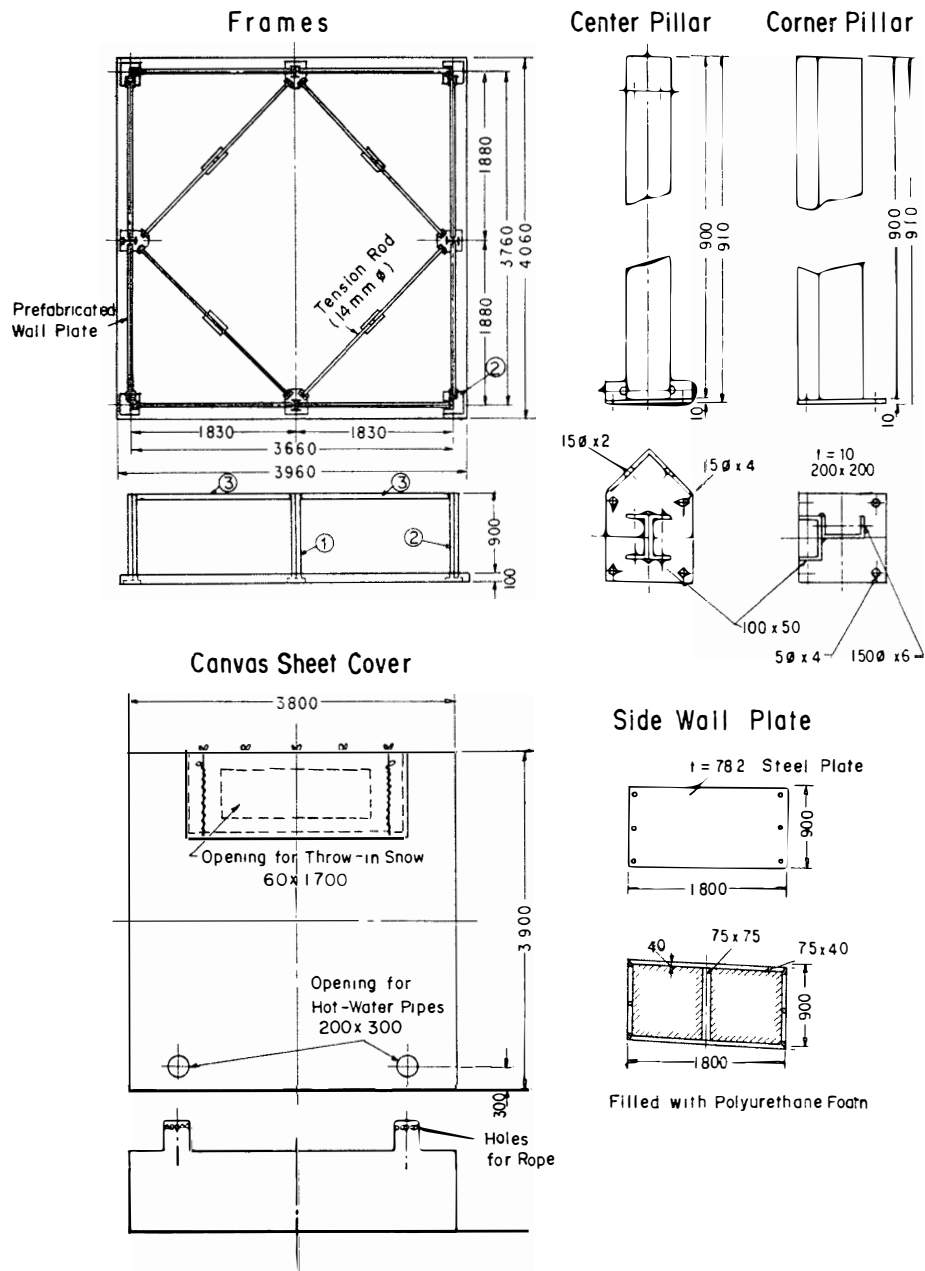


Fig. 12. Components of the 10-kl outdoor tank.

### 3. A 65-kVA Diesel-Electric Power Generating Plant with Waste Heat Recovery System

A new JARE-9 engine room was built in 1968. It contained a 65-kVA diesel-electric generator set and a coolant heat recovery system. As shown in Fig. 13 (TSUCHIYA, 1969), the engine coolant was led to a headtank and returned to the inlet of the water pump of the diesel engine. The hot water in the head-tank was pumped to a hot-water tank installed at a corner of the engine room

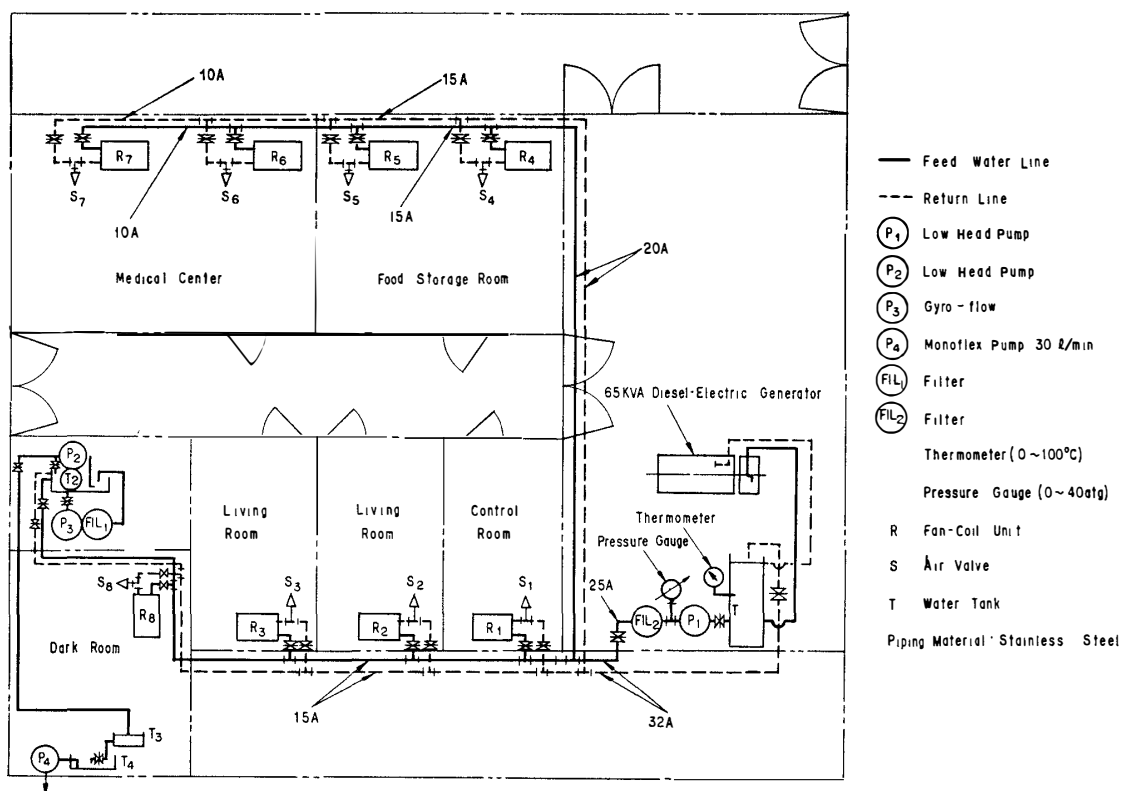


Fig. 13. JARE-9 engine room containing 65-kVA diesel-electric generator (Meidensha ZX-75 type diesel-electric generator) and coolant heat recovery system for making hot water used for heating of living rooms and other purposes.

and recirculated to the headtank.

The hot water reserved in the hot-water tank was circulated to eight fan-coil units through a stainless-steel pipeline and warmed six rooms of the living quarters. Another 65-kVA diesel-electric generator set was installed in the same engine room by JARE-10 (1968/70) as shown in Fig. 14 (ISHIWATA *et al.*, 1970).

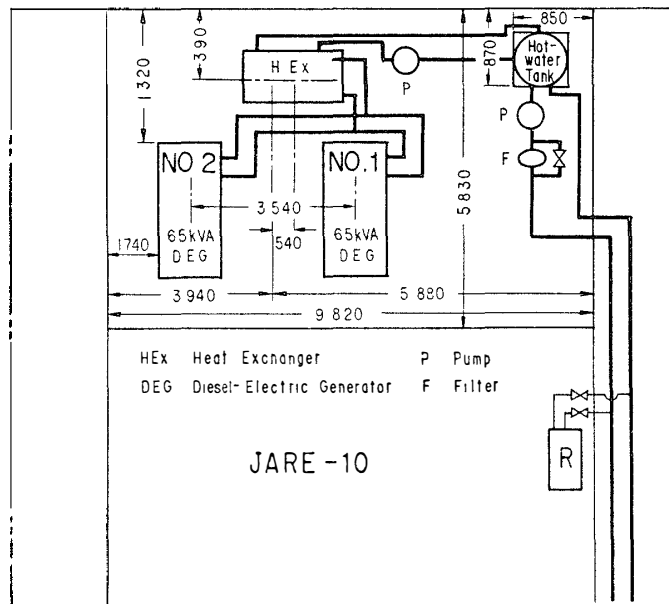


Fig. 14. JARE-9 engine room in JARE-10 (1968/70) containing two 65-kVA diesel-electric generators and rearranged coolant heat recovery system. Direct heating system by exhaust gas for JARE-9 was changed to indirect heating system through a horizontal shell-and-tube type water-to-water heat exchanger.

By this hot-water room-heating system utilizing the coolant heat of the 65-kVA diesel-electric generators, the heating load of the living quarters of the JARE-9 engine room, which was estimated as about 14000 kcal/h excluding the engine room itself, has been supplied satisfactorily from 1968 to 1977. The heating load of the engine room, which was also about 11300 kcal/h could be balanced by the heating loss due to the engine mechanical friction and the mechanical and electrical losses of the generators.

During JARE-10 (1968/70), the coolant heat recovering system was changed from the system of direct heating by engine coolant to an indirect heating system as shown in Fig. 14. A 130-k/ cylindrical water-storage outdoor tank made of corrugated steel plates and canvas sheets similar to the 10-k/ tank was built by JARE-11 (1969/71) (Fig. 15) near the JARE-9 engine room.

Shell-and-coil type exhaust-gas heat exchangers were installed in the same engine room as shown in Figs. 16 and 17, and the recovered heat was used for

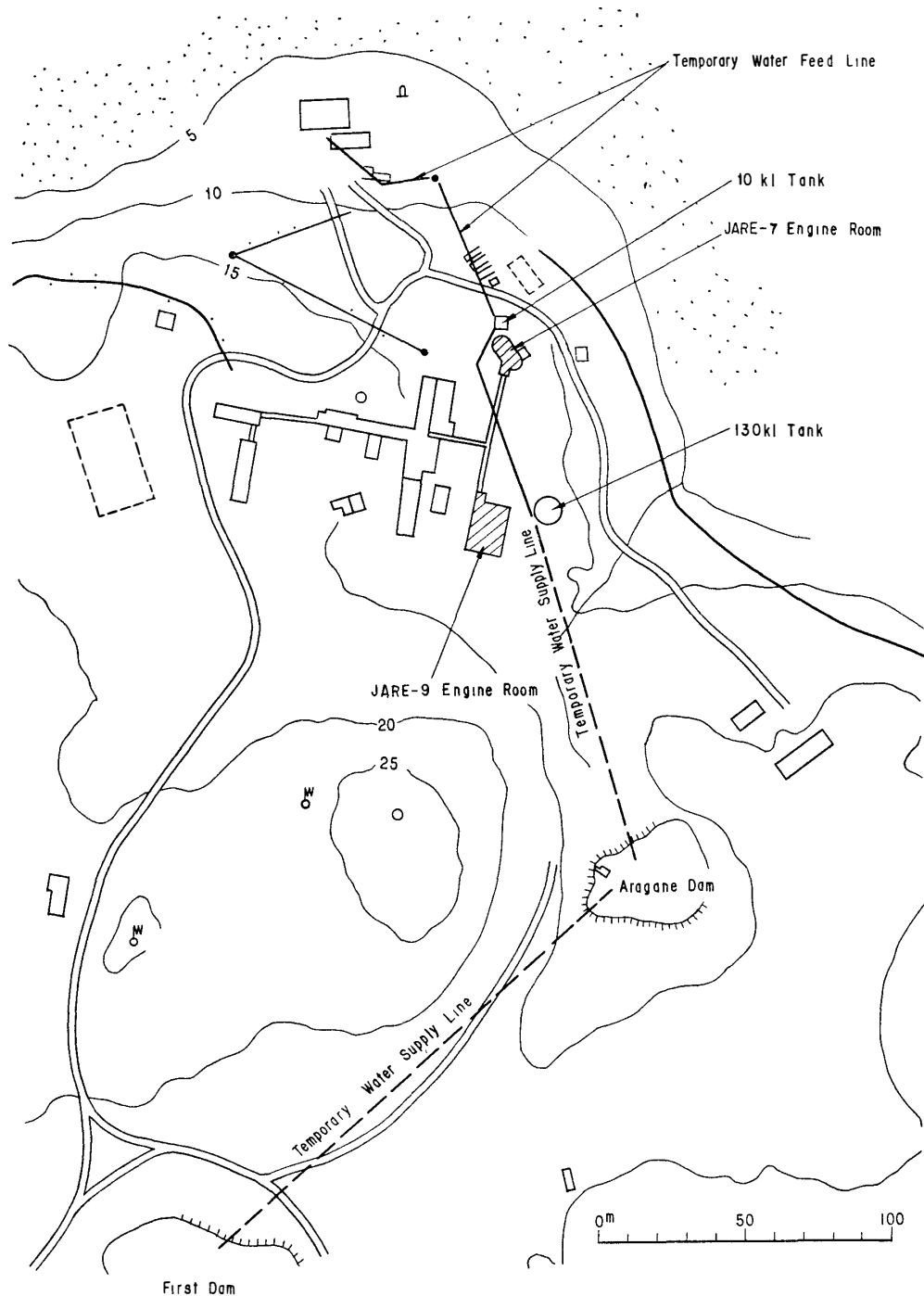


Fig. 15. Water supplying pipelines at Syowa Station during JARE-11 (1969/71).

heating the outdoor 130-k/l tank through an intermediate vertical water-to-water heat exchanger of shell-and-tube type. By this means, the temperature of the 130-k/l tank was kept between 6°C and 14°C throughout the year.

The water of the 130-k/l tank was pumped to the 10-k/l tank installed near the

JARE-7 engine room. The waste heat recovery system for the 45-kVA diesel-electric generators was not changed. The system shown in Fig. 16 was operated satisfactorily and saved much fuel.

In summer, pond water can be used. In winter, by putting into the pond a 2-kW electric heater, the bottom water could be prevented from freezing. To pump up the water, a fire pump and hoses were used to reduce the pumping time. However, the salt content increased gradually due to growth of the ice. Therefore, only the 10-k/ tank for melting snow or ice is used from March through November.

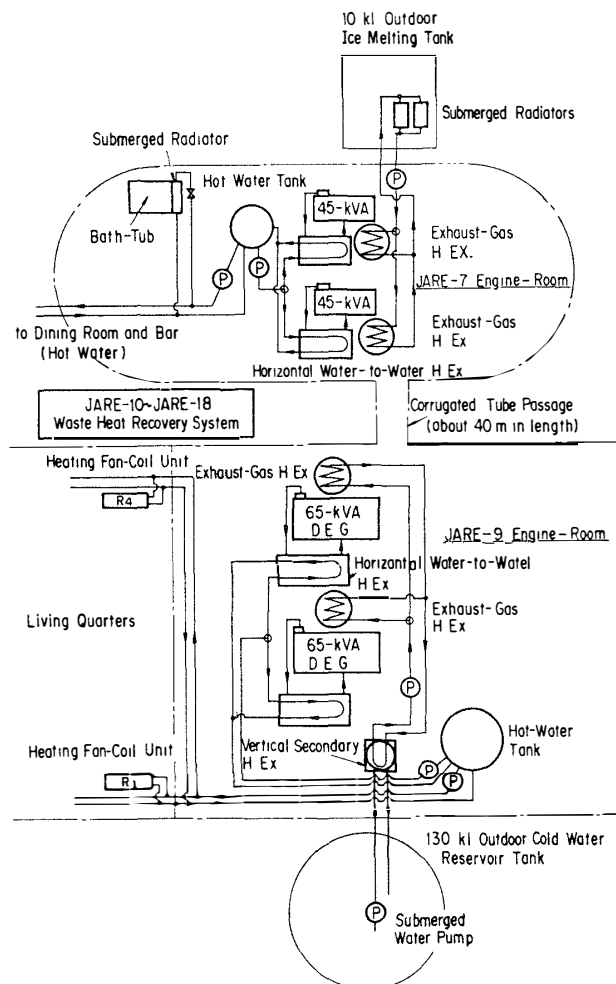
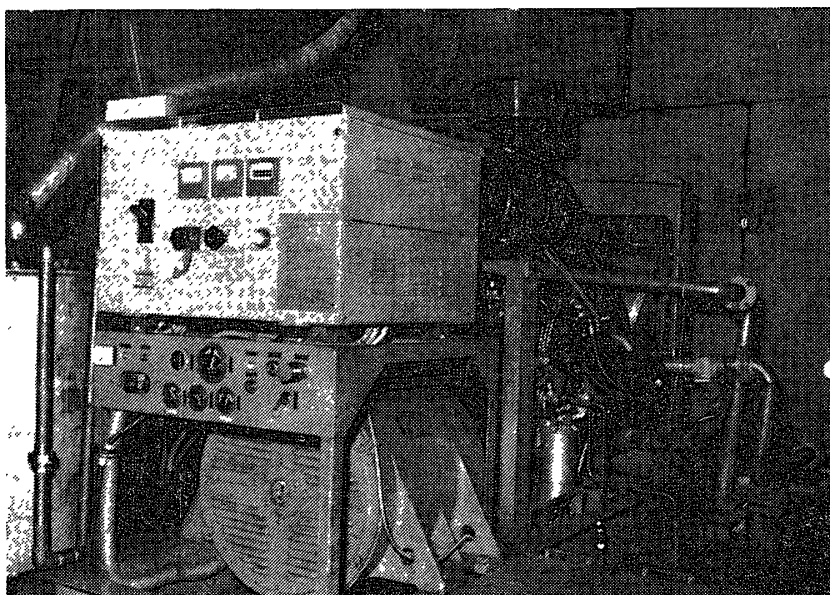


Fig. 16. Waste heat recovery systems in JARE-7 and JARE-9 engine rooms used by JARE-10/18 (1968/76).



*Fig. 17. Inside view of JARE-9 engine room containing 65-kVA diesel-electric generators. Piping for coolant heat recovering system is shown on the right side of the engine and a shell-and-coil type exhaust-gas heat exchanger for heating a 130-kl cold water outdoor tank is shown on the left side.*

#### 4. A 110-kVA Diesel-Electric Power Generating Plant with Waste Heat Recovery System

At the commencement of 110-kVA diesel-electric generator operation, the waste heat recovery system was changed from that shown in Fig. 16 to that in Fig. 18. Two photographs show the newly build system (Figs. 19 and 20). In

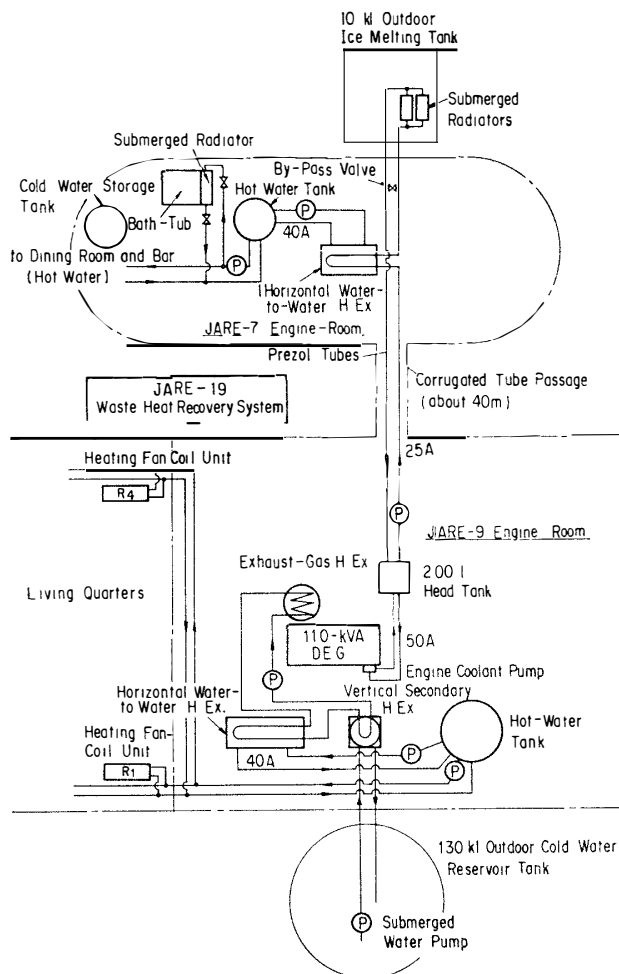
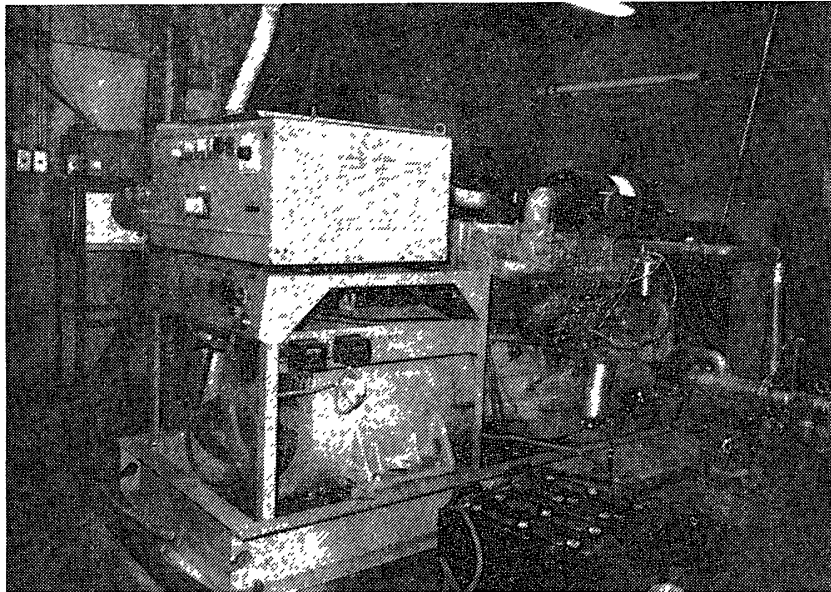
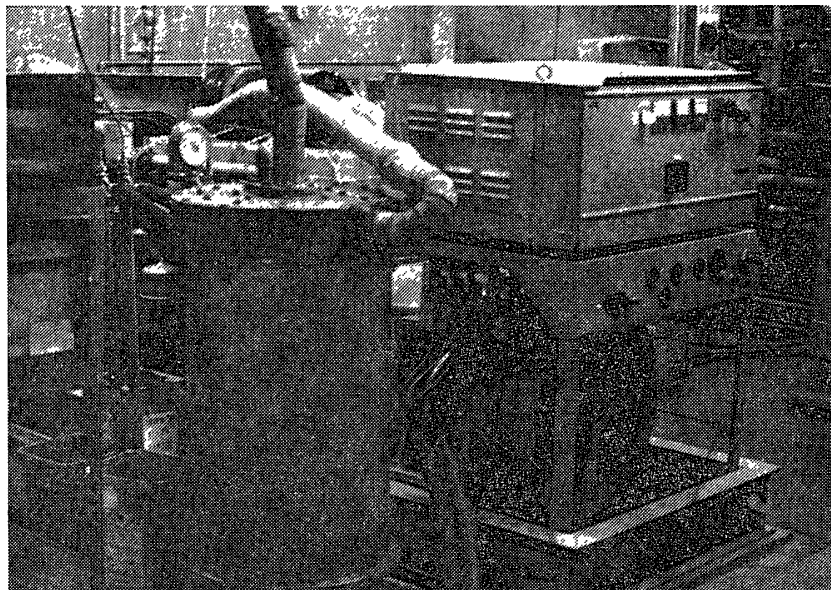


Fig. 18. JARE-9 engine room containing one 110-kVA diesel-electric generator and new heat recovering system combined with that of JARE-7 engine room in JARE-19 (1977/79).



*Fig. 19. 110-kVA diesel-electric generator for JARE-19 (1977/79) installed in the JARE-9 engine room. Right side view of engine and piping to and from the headtank for recovery of coolant heat are shown.*



*Fig. 20. Left side view of No. 1 110-kVA diesel-electric generator equipped with a fin-tube type exhaust-gas heat exchanger AL-F-1 prepared for JARE-19 (1977/79).*

the new system, coolant heat of the 110-kVA diesel engine was pumped to the JARE-7 engine room to provide heat to the horizontal coolant heat exchanger of shell-and-tube type and the 10-k $l$  snow-melting tank. The temperature of water in the 10-k $l$  tank was kept at 33–45°C. The water heated to 42–50°C by

the coolant heat exchanger was reserved in a hot-water tank in the JARE-7 engine room, and supplied to the living quarters and heated water in the bathtub through a submerged radiator.

On the other hand, the exhaust-gas energy of the 110-kVA diesel engines was used to heat water by means of an exhaust-gas heat exchanger. The hot water was recirculated through a horizontal water-to-water heat exchanger (shell-and-tube type) and a vertical water-to-water heat exchanger (shell-and-tube type) as shown in Fig. 18. The hot water heated by the former was reserved in a hot-water tank in the JARE-9 engine room and was used for heating rooms of the JARE-9 engine room. The hot water heated by the latter was used to prevent from freezing of water in the 130-k/ tank.

On the occasion of installation of another 110-kVA generator, the heat recovery system was changed from that of Fig. 18 to that of Fig. 21. Thus, the electric power source of Syowa Station was simplified from the double sources of 65-kVA and 45-kVA generators separated in two engine rooms to a single source from 110-kVA generators in the JARE-9 engine room. The simplified single

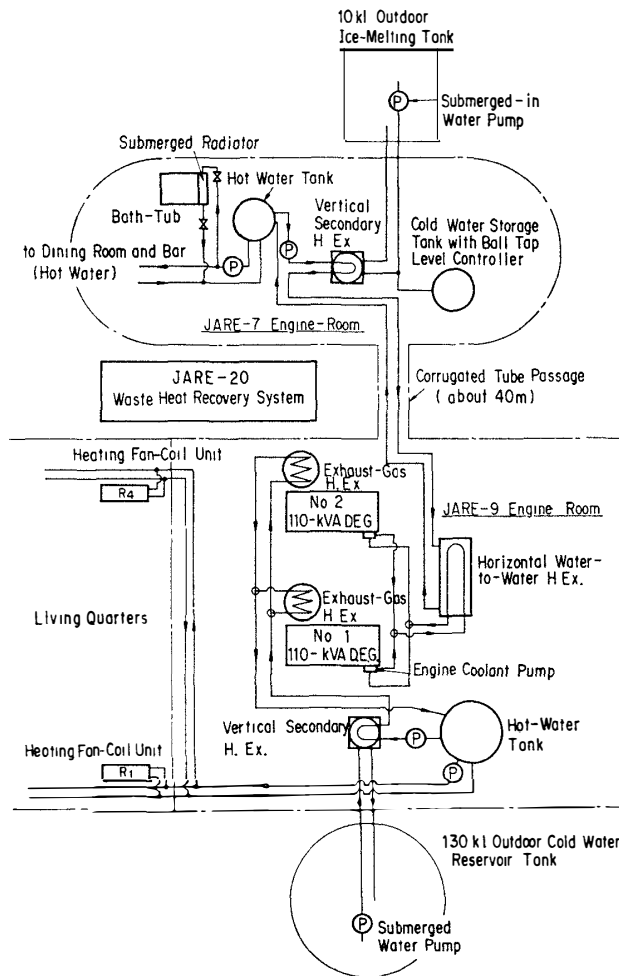


Fig. 21. JARE-9 engine room containing set of two 110-kVA diesel-electric generators and renewed waste heat recovering systems combined with that of JARE-7 engine room in 1979 (JARE-20).

source brought a considerable saving of fuel. In Fig. 22, the dotted lines show the monthly mean and peak loads of the 110-kVA generating system during the period from February 1978 to September 1979. The solid lines show those of the double sources as the mean values for JARE-16, -17 and -18. Both of them are nearly equal, but fuel consumption and specific fuel consumption (SFC) shown in Fig. 23 are very different. The fuel consumption represented by  $l/month$  and SFC expressed in  $l/kWh$  is remarkably decreased by using the single 110-kVA unit. The former decreased from 14.0–15.5  $l/month$  to 9.6–12.6  $l/month$  (68–81%) and the latter decreased from 0.382–0.432  $l/kWh$  to 0.282–0.356  $l/kWh$  (78–82%). The lowered fuel consumption is mainly due to the decreasing ratio of mechanical loss to output of a 110-kVA diesel engine compared with that of the 45-kVA and 65-kVA diesel engines and with the fact that the equivalence ratio at normal load of 110-kVA diesel engine coincides with its minimum SFC.

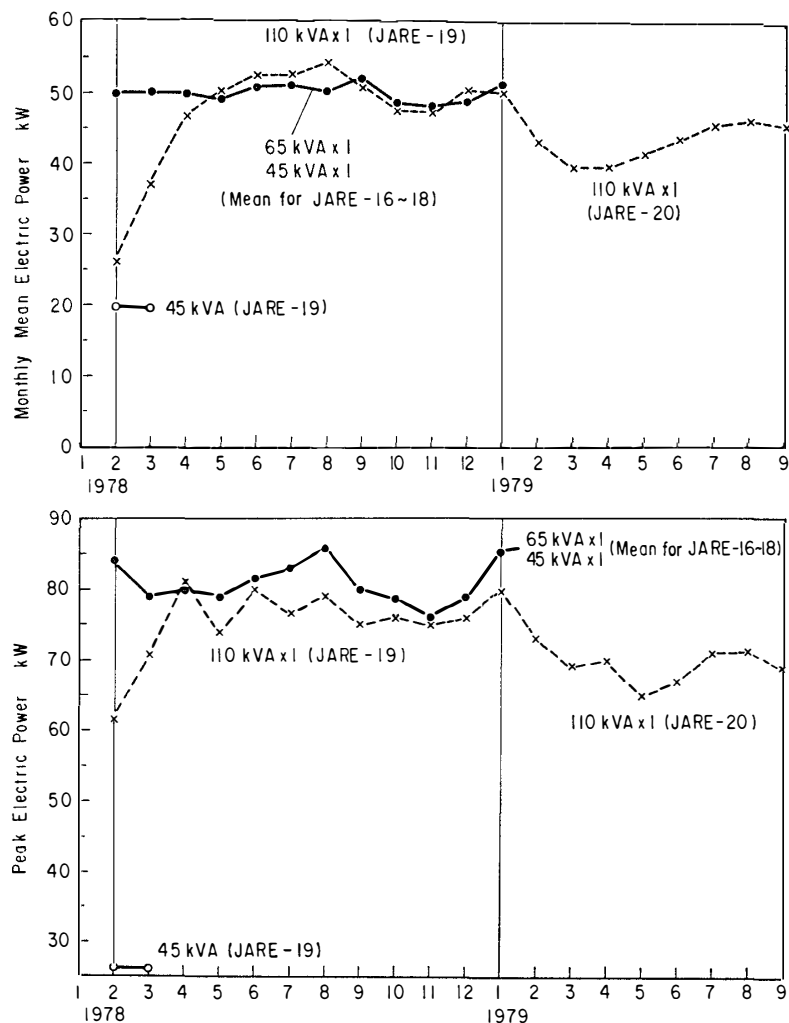


Fig. 22. Monthly mean and peak electric loads at Syowa Station from February 1978 to September 1979.

Energy Saving at Syowa and Mizuho Stations

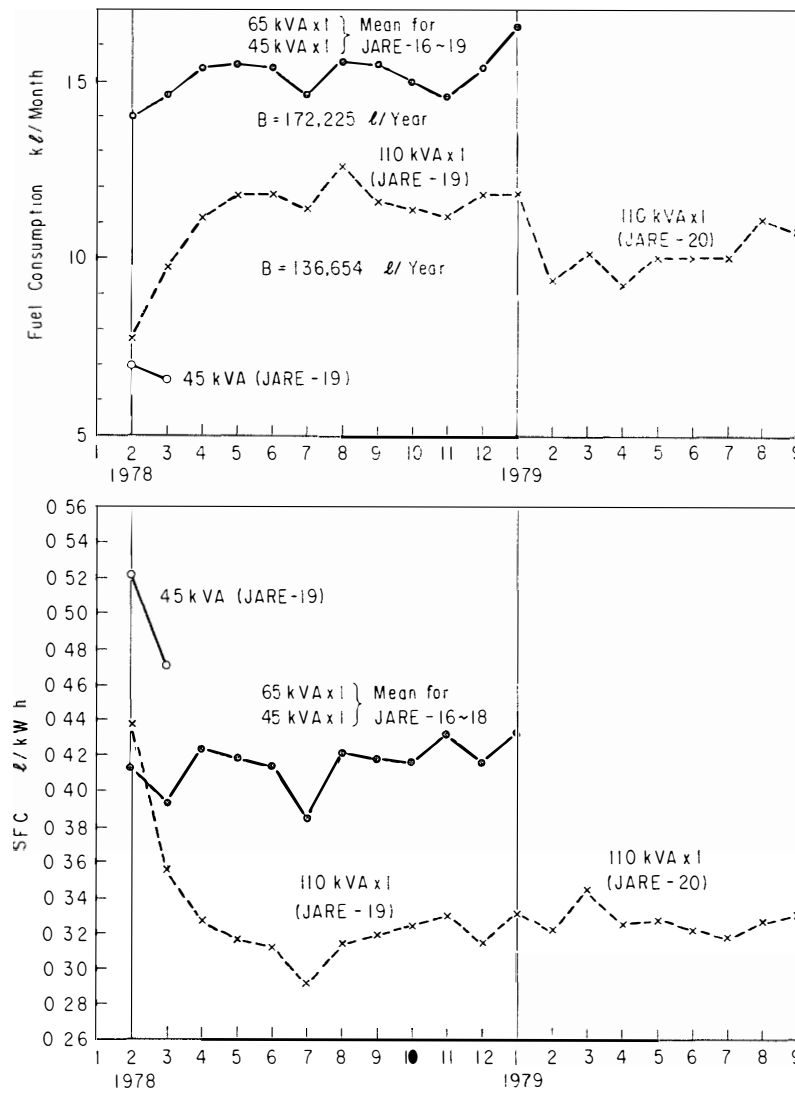


Fig. 23. Comparison of monthly mean SFC for 110-kVA diesel-electric generator and for two electric generators, that are one 45-kVA generator in JARE-7 engine room and one 65-kVA generator in JARE-9 engine room.

## 5. Estimation of Heat Balance of Diesel-Electric Generators

The following subscripts and symbols will be used herein.

Subscript;

- $g$ : exhaust gas of diesel engine,
- $a$ : air aspirated,
- $gd$ : dry exhaust gas without H<sub>2</sub>O (its unit weight is represented by kg\*),
- $w$ : steam,  $s$ : saturated state,  $ws$ : saturated steam,
- $aw$ : moisture contained in atmospheric air,
- $ad$ : dry air,
- $gw$ : moisture contained in exhaust gas.

Symbols;

- $h$ : enthalpy, kcal/kg,
- $h_{ga}$ : enthalpy of dry exhaust gas, kcal/kg\*,
- $h_w$ : enthalpy of superheated steam, kcal/kg,
- $h_w''$ : enthalpy of saturated steam (including the latent heat of evaporation. The zero point of  $h_w$  and  $h_w''$  is set for the saturated water at 0°C), kcal/kg,
- $H$ : calorific value of fuel, kcal/kg or enthalpy flow rate, kcal/h,
- $p$ : atmospheric pressure, mmHg abs.,
- $t$ : temperature, °C,
- $t_a$ : atmospheric air temperature, °C,
- $p_{sa}$ : saturated vapor pressure of steam for  $t_a$ , mmHg abs.,
- $\lambda_a$ : relative humidity,
- $x_a$ : absolute humidity of atmosphere, kg/kg\*,
- $G_a$ : weight flow rate of air aspirated by diesel engine, kg/h,
- $G_{ad}$ : weight flow rate of dry air contained in  $G_a$ , kg\*/h
- $G_{aw}$ : weight flow rate of moisture contained in  $G_a$ , kg/h,
- $G_g$ : weight flow rate of exhaust gas, kg/h,
- $G_{gd}$ : weight flow rate of dry exhaust gas contained in  $G_g$ , kg\*/h,
- $G_{gw}$ : weight flow rate of steam contained in  $G_g$ , kg/h,

- $x_a$ : absolute humidity of air, kg/kg\*,  
 $x_s$ : saturated absolute humidity of exhaust gas, kg/kg\*,  
 $R_{gd}$ : gas constant for dry exhaust gas, kgm/kg\*K,  
 $R_w$ : gas constant for steam ( $R_w = 47.05$  kgm/kgK),  
 $G_{ws}$ : weight flow rate of saturated steam in exhaust gas, kg/h,  
 $L_{min}$ : stoichiometric air-fuel ratio,  $L_{min} = 14.2$  for gas oil,  
 $\phi$ : equivalence ratio of exhaust gas,  
 $G_f$ : weight flow rate of fuel supplied to engine, kg/h,  
 $B$ : volume flow rate of fuel supplied to engine, l/h,  
 $Q$ : heat flow rate, kcal/h.

The flow rates of dry air and steam contained in atmospheric air aspirated by a diesel engine are given by

$$G_{ad} = G_a / (1 + x_a) \text{ kg}^*/\text{h}, \quad (1)$$

$$G_{aw} = x_a G_{ad} = x_a G_a / (1 + x_a) \text{ kg/h}, \quad (2)$$

$$x_a = 0.622 \lambda_a p_{sa} / (p - \lambda_a p_{sa}) \text{ kg/kg}^*. \quad (3)$$

If the fuel supply  $G_f$  and air flow rate  $G_a$  are measured, the flow rate of the exhaust gas can be given by

$$G_g = G_{ad} + G_f \text{ kg/h}, \quad (4)$$

$$G_a = G_{ad} + G_{aw} \text{ kg/h}, \quad (5)$$

and

$$G_g = G_{gd} + G_{gw} \text{ kg/h}. \quad (6)$$

When the fuel  $G_f$  is burned in the engine cylinder with the supply of air  $G_a$ , containing dry air  $G_{ad}$ , the equivalence ratio of combustion gas is given by

$$\phi = L_{min} G_f / G_{ad}. \quad (7)$$

The flow rate of the dry exhaust gas can be calculated by

$$G_{gd} = G_g / (1 + 0.0806 \phi) \text{ kg}^*/\text{h}, \quad (8)$$

and the steam content of  $G_g$  is

$$G_{gw} = 0.0806 \phi G_{gd} \text{ kg/h}. \quad (9)$$

The total content of steam in the exhaust gas becomes

$$G_w = G_{aw} + G_{gw} \text{ kg/h}. \quad (10)$$

The higher calorific value of the fuel containing the latent heat of steam condensation is represented by  $H_o$  and its lower calorific value by  $H_u$ , and the values for gas oil are given as

$$H_o = 10837 \text{ kcal/kg}, \quad H_u = 10162 \text{ kcal/kg}.$$

The heat supplied to an engine by the fuel is

$$Q_f = H_o G_f \text{ kcal/h.} \quad (11)$$

The temperatures of the exhaust gas are defined as

- $t_{ei}$ : temperature at the inlet of a turbocharger, °C,
- $t_{eo}$ : temperature at the outlet of a turbocharger, °C,
- $t_{g1}$ : temperature at the inlet of a heat exchanger, °C,
- $t_{g2}$ : temperature at the outlet of a heat exchanger, °C.

If condensation of steam contained in the exhaust gas does not occur, the enthalpy flow rate for these four temperatures can be calculated by

$$H_{ei} = (h_{gd})_{ei} G_{gd} + (h_w)_{ei} G_w \text{ kcal/h,} \quad (12)$$

$$H_{eo} = (h_{gd})_{eo} G_{gd} + (h_w)_{eo} G_w \text{ kcal/h,} \quad (13)$$

$$H_{g1} = (h_{gd})_{g1} G_{gd} + (h_w)_{g1} G_w \text{ kcal/h,} \quad (14)$$

$$H_{g2} = (h_{gd})_{g2} G_{gd} + (h_w)_{g2} G_w \text{ kcal/h.} \quad (15)$$

The heat drop in a turbocharger is

$$Q_T = H_{ei} - H_{eo} \text{ kcal/h,} \quad (16)$$

and the heat flow rate contained in exhaust gas is  $Q_r = H_{g1}$  and the available heat recovered by an exhaust-gas heat exchanger is

$$Q_R = H_{g1} - H_{g2} \text{ kcal/h.} \quad (17)$$

If some part of the steam contained in the exhaust gas condenses in the exhaust-gas heat exchanger, eq. (15) should be replaced by

$$H_{g2} = (h_{gd})_{g2} G_{gd} + (h_w'')_{g2} G_{ws} \text{ kcal/h,} \quad (15')$$

where the saturated steam flow rate can be calculated by

$$G_{ws} = (x_s)_{g2} G_{gd} \text{ kg/h,} \quad (18)$$

$$(x_s)_{g2} = (R_{gd}/R_w) [p_s/(p-p_s)]_{g2} \text{ kg/kg}^*, \quad (19)$$

$$R_{gd} = 29.27 - 0.93\phi \text{ kgm/kg}^*\text{K,} \quad (20)$$

$$(x_s)_{g2} = (0.622 - 0.0198\phi) [p_s/(p-p_s)]_{g2} \text{ kg/kg}^*. \quad (19')$$

The total flow rate of the outlet gas from the heat exchanger in this case is decreased to

$$G_{out} = G_{gd} + G_{ws} \text{ kg/h,} \quad (21)$$

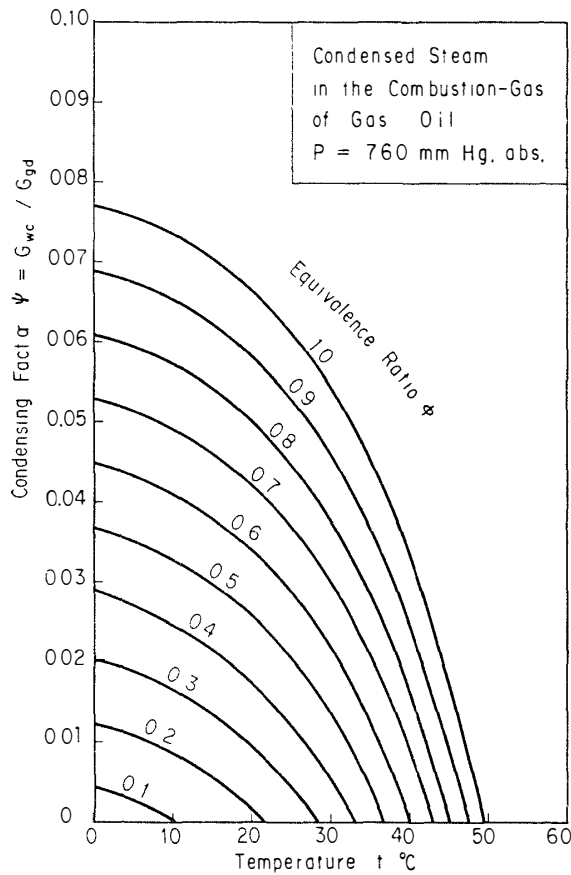


Fig. 24. Condensation factor  $\psi$ , the weight ratio of condensed water to 1 kg\* of dry combustion gas of gas oil at any temperature  $t$  and equivalence ratio  $\phi$ .

Table 5. Enthalpy of dry combustion gas of gas oil,  $h_{gd}$  kcal/kg\* ( $C=0.8584$ ,  $H=0.1269$ ,  $N=0.0147$ ,  $L_{min}=14.2$ , Equivalence ratio  $\phi=L_{min}G_f/G_{ad}$ ).

$t$ °C	$\phi=0$	0.1	0.2	0.3	0.4	0.5	0.6	0.7	0.8	0.9	1.0
0	0	0	0	0	0	0	0	0	0	0	0
50	12.02	12.02	12.00	11.97	11.95	11.94	11.92	11.90	11.89	11.87	11.85
100	24.08	24.07	24.05	24.01	23.98	23.96	23.93	23.91	23.89	23.86	23.83
150	36.20	36.19	36.17	36.13	36.10	36.08	36.05	36.03	36.02	35.98	35.95
200	48.40	48.40	48.39	48.36	48.33	48.32	48.30	48.28	48.28	48.25	48.22
250	60.71	60.72	60.72	60.70	60.69	60.69	60.68	60.67	60.69	60.67	60.64
300	73.14	73.17	73.18	73.18	73.18	73.20	73.21	73.21	73.25	73.25	73.23
350	85.70	85.75	85.78	85.80	85.82	85.86	85.89	85.91	85.97	85.99	85.99
400	98.40	98.47	98.53	98.57	98.61	98.67	98.73	98.77	98.85	98.90	98.92
450	111.24	111.34	111.42	111.49	111.55	111.64	111.73	111.79	111.90	111.97	112.02
500	124.22	124.35	124.46	124.56	124.65	124.76	124.88	124.97	125.11	125.21	125.29
550	137.34	137.50	137.64	137.78	137.90	138.04	138.19	138.31	138.48	138.61	138.72
600	150.60	150.79	150.97	151.14	151.29	151.47	151.65	151.80	152.01	152.17	152.31
650	163.99	164.22	164.43	164.64	164.82	165.04	165.25	165.44	165.68	165.88	166.06
700	177.51	177.77	178.02	178.27	178.49	178.74	178.99	179.22	179.49	179.73	179.95

and the condensed steam in the heat exchanger is

$$G_{wc} = G_w - G_{ws} = (G_{aw} + G_{gw}) - G_{ws} \text{ kg/h.} \quad (22)$$

If the steam content in the air,  $G_{aw}$ , is negligible compared with  $G_{gw}$ ,

$$G_{wc} = G_{gw} - G_{ws} = \psi G_{gd} \text{ kg/h,} \quad (23)$$

$$\psi = G_{wc}/G_{gd} = 0.0806\phi - (0.622 - 0.0198\phi) [p_s/(p - p_s)]_{g2}. \quad (24)$$

As a standard state,  $p = 760$  mmHg abs. and  $t_{g2} = 0^\circ\text{C}$ , and  $p_s = 4.6$  mmHg abs. are adopted. Then eq. (24) becomes

$$\psi_0 = 0.0807\phi - 0.00381. \quad (25)$$

The calculated condensing factor  $\psi$  from eq. (24) is shown in Fig. 24. It shows that the allowable lowest temperature in an exhaust-gas heat exchanger should be kept higher than  $50^\circ\text{C}$  for avoiding condensation of steam and corrosion of heating surfaces.

The maximum recovery efficiency of a heat exchanger can be estimated from eqs. (14) and (17),

$$\eta_{\text{rec}} = Q_R/H_{g1} = 1 - (H_{g2}/H_{g1}). \quad (26)$$

In these calculations,  $h_{gd}$  is shown in Table 5 as a function of temperature and equivalence ratio  $\phi$ , although the effect of the latter is not very great. The enthalpies of steam  $h_w$  and  $h_w''$  should be read from a steam table (JSME, 1968).

As an example,

$$p = 773.0 \text{ mmHg abs., } t = 11.0^\circ\text{C, } \lambda_a = 0.77, \quad p_s = 9.8 \text{ mmHg abs.,}$$

$$x_a = 0.00613 \text{ kg/kg*},$$

$$G_a = 289.8 \text{ kg/h, } \quad G_f = 9.04 \text{ kg/h,}$$

$$G_{ad} = G_a/(1 + x_a) = 289.8/1.00613 = 288.0 \text{ kg*/h,}$$

$$G_{aw} = G_a - G_{ad} = 289.8 - 288.0 = 1.8 \text{ kg/h,}$$

$$\phi = L_{\text{min}} G_f/G_{ad} = 14.2(9.04)/288.0 = 0.446,$$

$$G_g = G_{ad} + G_f = 288.0 + 9.04 = 297.0 \text{ kg/h,}$$

$$G_{gd} = G_g/(1 + 0.0806\phi) = 297.0/(1 + 0.0806 \times 0.446) \\ = 297.0/1.0359 = 286.7 \text{ kg*/h,}$$

$$G_{gw} = G_g - G_{gd} = 297.0 - 286.7 = 10.3 \text{ kg/h,}$$

$$G_w = G_{aw} + G_{gw} = 1.8 + 10.3 = 12.1 \text{ kg/h,}$$

$$Q_f = H_o G_f = (10837)(9.04) = 98000 \text{ kcal/h,}$$

$$t_{ei} = 375^\circ\text{C, } h_{gd} = 92.25 \text{ kcal/kg*}, \quad h_w = 770.7 \text{ kcal/kg,}$$

$$t_{eo} = 345^\circ\text{C, } h_{gd} = 84.58 \text{ kcal/kg*}, \quad h_w = 756.1 \text{ kcal/kg,}$$

$$\begin{aligned}
 t_{g1} &= 335^\circ\text{C}, & h_{gd} &= 82.04 \text{ kcal/kg}^*, & h_w &= 751.2 \text{ kcal/kg}, \\
 t_{g2} &= 85^\circ\text{C}, & h_{gd} &= 20.36 \text{ kcal/kg}^*, & h_w'' &= 633.4 \text{ kcal/kg}, \\
 R_{gd} &= 29.27 - 0.93\phi = 29.27 - 0.93(0.446) = 29.27 - 0.41 = 28.86 \text{ kgm/kg}^*\text{K} \\
 \text{at } t_{g2} &= 85^\circ\text{C}, & p_s &= 433.6 \text{ mmHg abs.}, & p_s/(p-p_s) &= 433.6/(773.0-433.6) = 1.278, \\
 (x_s)_{g2} &= (28.86/47.05)(1.278) = 0.784 \text{ kg/kg}^*, \\
 G_{ws} &= (x_s)_{g2} G_{gd} = 0.784(286.7) = 224.8 \text{ kg/h}.
 \end{aligned}$$

$G_{ws}$  is greater than  $G_w = 12.1 \text{ kg/h}$ , so that no condensing occurs. The enthalpy of the exhaust gas can be calculated as follows from eqs. (12), (13), (14) and (15):

$$\begin{aligned}
 t_{ei} &= 375^\circ\text{C}, & H_{ei} &= (92.25)(286.7) + (770.7)(12.1) \\
 & & &= 26450 + 9320 = 35770 \text{ kcal/h}, \\
 t_{eo} &= 345^\circ\text{C}, & H_{eo} &= (84.58)(286.7) + (756.1)(12.1) \\
 & & &= 24250 + 9150 = 33400 \text{ kcal/h}, \\
 t_{g1} &= 335^\circ\text{C}, & H_{g1} &= (82.04)(286.7) + (751.2)(12.1) \\
 & & &= 23520 + 9090 = 32610 \text{ kcal/h},
 \end{aligned}$$

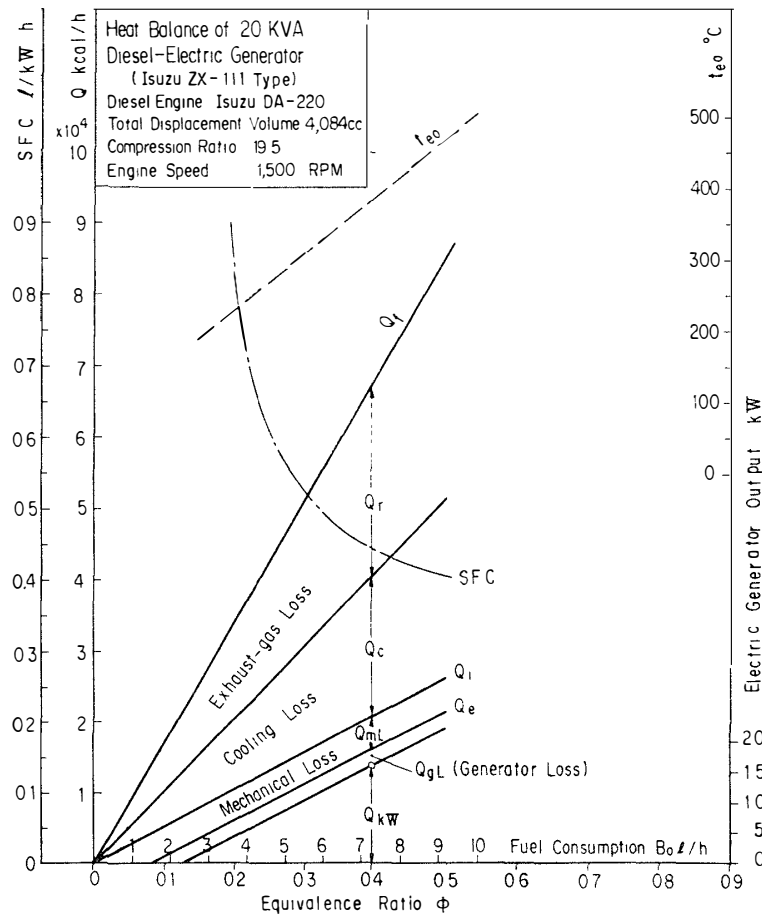


Fig. 25. Heat balance of 20-kVA diesel-electric generator prepared for JARE-1 (1956/58). Meidensha ZX-111 type, diesel engine: DA-220, total piston displacement volume 4084 cc, compression ratio 19.5, 33PS/1500 rpm.

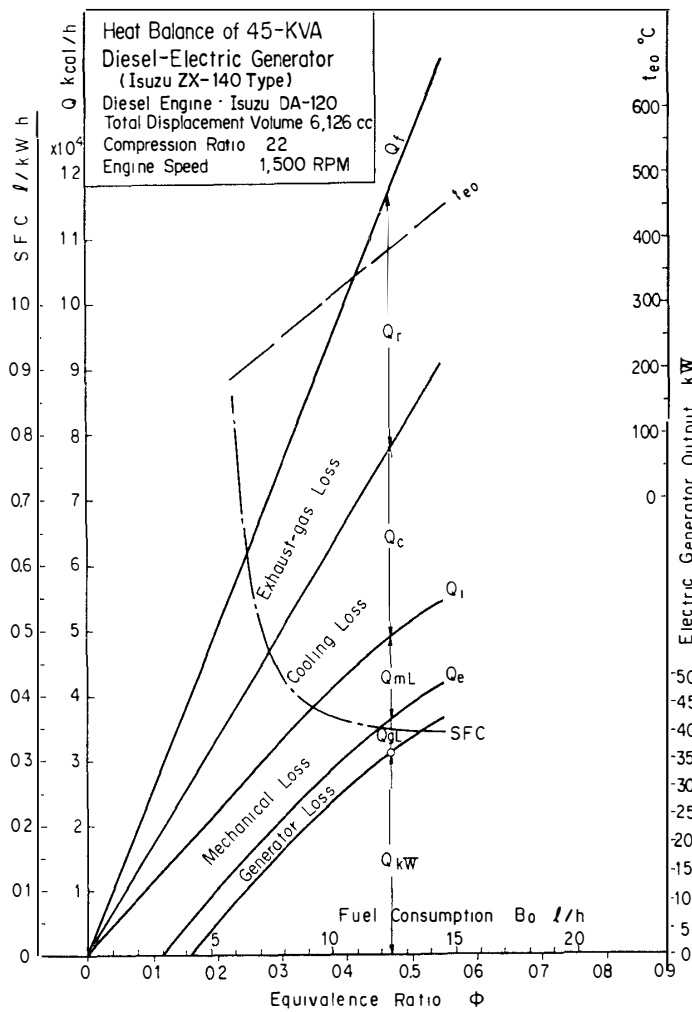


Fig. 26. Heat balance of 45-kVA diesel-electric generator used for JARE-7/9. Meidensha ZX-140 type, diesel engine: Isuzu DA-120, total piston displacement volume 6126 cc, compression ratio 22, 65.5PS/1500 rpm.

$$t_{g2} = 85^\circ\text{C}, \quad H_{g2} = (20.36)(286.7) + (633.4)(12.1) = 5840 + 7660 = 13500 \text{ kcal/h.}$$

The energy absorbed by the turbocharger

$$Q_T = H_{ei} - H_{eo} = 35770 - 33400 = 2370 \text{ kcal/h (2.76 kW)},$$

and the energy recovered by the exhaust-gas heat exchanger

$$Q_R = H_{g1} - H_{g2} = 32610 - 13500 = 19100 \text{ kcal/h.}$$

The recovery efficiency

$$\eta_{rec} = Q_R / H_{g1} = 19100 / 32610 = 0.586.$$

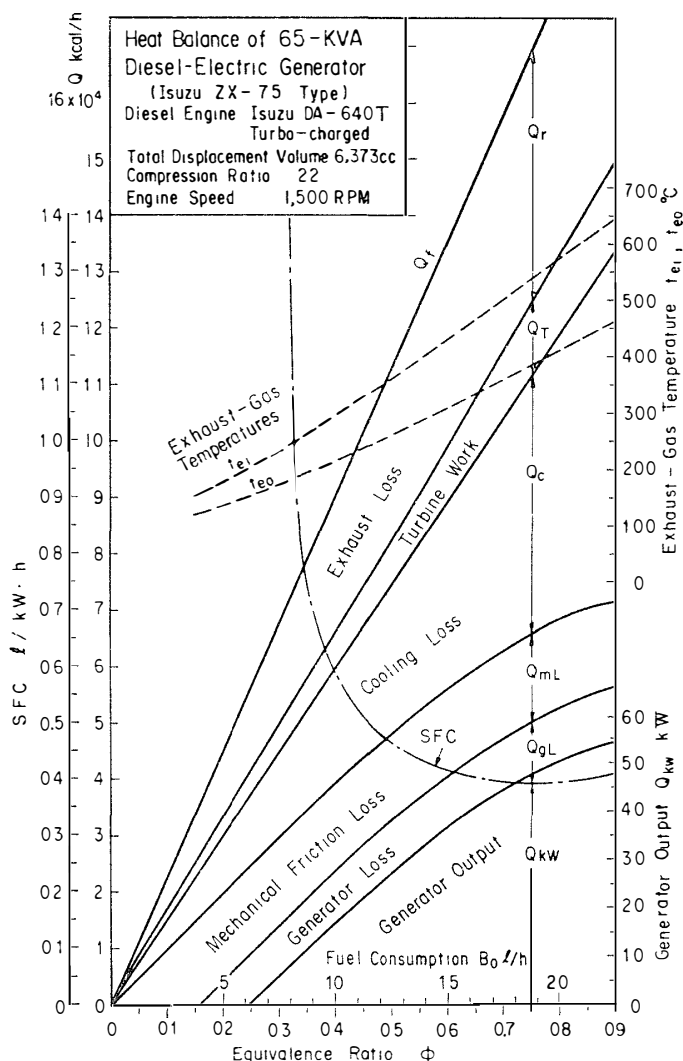


Fig. 27. Heat balance of 65-kVA diesel-electric generator used for JARE-9/19. Meidensha ZX-75 type, diesel engine: Isuzu DA-640T, total piston displacement volume 6373 cc, compression ratio 22, 82PS/1500 rpm.

If the heat supplied by the fuel,  $Q_f$  calculated by eq. (11), heat  $(Q_f - Q_r)$ , and heat  $(Q_f - Q_r - Q_c)$  are plotted against the equivalence ratio  $\phi$  as shown in Figs. 25, 26, 27 and 28, these three curves pass through the origin. When the output voltage kV, output current A in ampere and power factor  $\cos \Phi$  are given, the output power of the electric generator  $Q_{kW}$  can be calculated by

$$Q_{kW} = 860 \text{ kVA} \cos \Phi = 860 \text{ kW} \text{ kcal/h}, \quad (27)$$

where the power factor  $\cos \Phi$  is 80% and the generator loss  $Q_{gL}$  is estimated to be about 17% of  $Q_{kW}$ , so that the power necessary for driving the generator, that is, power equal to the brake output of the diesel engine, can be estimated by

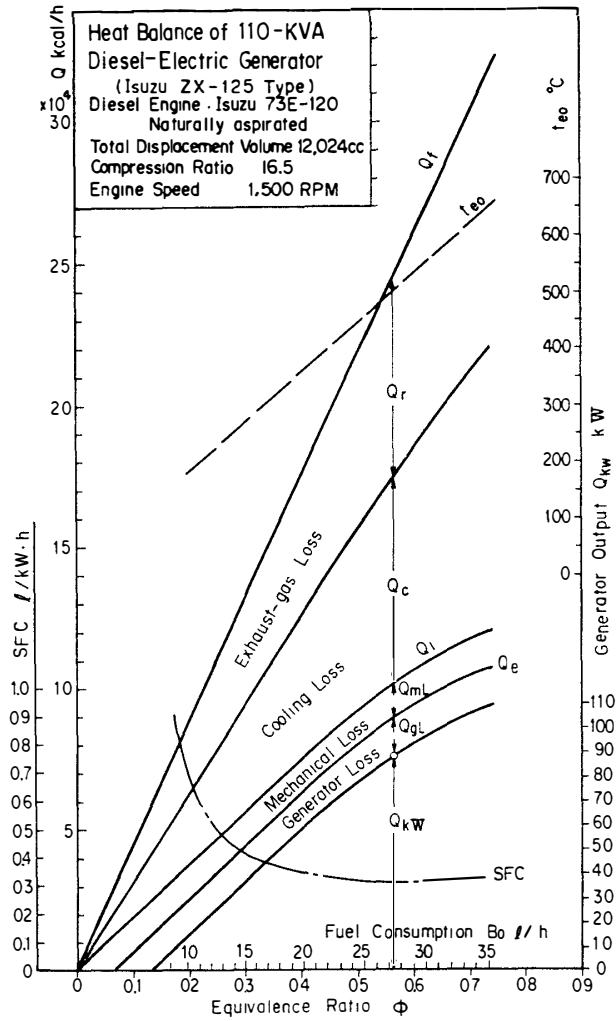


Fig. 28. Heat balance of 110-kVA diesel-electric generator prepared for JARE-19. Meidensha XZ-125 type, diesel engine: Isuzu 73E-120, total piston displacement volume 12024 cc, compression ratio 16.5, 140PS/1500 rpm.

$$Q_e = Q_{kW} + Q_{gL} = 1.17 Q_{kW} \text{ kcal/h.} \quad (28)$$

As shown in these figures, the curve  $Q_e$  does not pass through the origin but cuts the abscissa axis at a point below the origin. The negative value of  $Q$  at the origin indicates the mechanical loss  $Q_{mL}$  of the diesel engine in kcal/h.

Hence the indicated output of the diesel engine can be obtained by

$$Q_i = Q_e + Q_{mL} = Q_{kW} + Q_{gL} + Q_{mL} \text{ kcal/h.} \quad (29)$$

The curve  $Q_i$  should also pass through the origin as shown in these figures, and the cooling loss of the diesel engine can be approximately given by

$$Q_c = Q_f - Q_r - Q_T - Q_i = Q_f - Q_r - Q_T - Q_{kW} - (Q_{mL} + Q_{gL}) \text{ kcal/h.} \quad (30)$$

Table 6. The heat balance of diesel-electric generators prepared for JARE.

a. 20-kVA diesel electric generator (Isuzu ZX-111 type, diesel engine DA-220).

Run No.	Generator output (kVA) (kW)		$\phi$	$t_{g1}$ (°C)	$Q_f$	$Q_{kW}$	$Q_r$	$Q_c$	$Q_{mL}$	$Q_{gL}$	$G_a$ (kg/h)	SFC (l/kWh)
1	20	16	0.390	380	66430	13760	25530	20400	4400	2340	223	0.446
2	15	12	0.326	327	55490	10320	21550	16880	4400	2340	223	0.498
3	10	8	0.258	274	43890	6880	17630	12640	4400	2340	223	0.590
4	6.8	5.44	0.220	243	37500	4678	15320	10760	4400	2340	223	0.741
5	5	4	0.195	221	33160	3440	13760	9220	4400	2340	223	0.892

b. 45-kVA diesel-electric generator (Isuzu ZX-140 type, diesel engine DA-120).

Run No.	Generator output (kVA) (kW)		$\phi$	$t_{g1}$ (°C)	$Q_f$	$Q_{kW}$	$Q_r$	$Q_c$	$Q_{mL}$	$Q_{gL}$	$G_a$ (kg/h)	SFC (l/kWh)
1	45	36	0.473	381	117600	30960	39190	29690	12500	5260	326	0.347
2	40	32	0.431	350	107300	27520	35580	26440	12500	5260	326	0.356
3	35	28	0.386	320	95910	24080	32130	21940	12500	5260	326	0.364
4	30	24	0.348	288	86590	20640	28660	19530	12500	5260	326	0.383
5	25	20	0.314	253	78030	17200	24920	18150	12500	5260	326	0.415
6	20	16	0.287	220	71520	13760	21720	18280	12500	5260	326	0.475
7	15	12	0.257	190	63940	10320	18750	17110	12500	5260	326	0.567
8	10	8	0.238	158	59280	6880	15750	18890	12500	5260	326	0.787

c. 65 kVA diesel-electric generator (Isuzu ZX-75 type, diesel engine DA-640-T).

Run No.	Generator output (kVA) (kW)		$\phi$	$t_{ei}$ (°C)	$t_{eo}$ (°C)	$Q_f$	$Q_{kW}$	$Q_r$	$Q_c$	$Q_T$	$Q_{mL}$	$Q_{gL}$	$G_a$ (kg/h)	SFC (l/kWh)
1	65	52	0.805	585	400	185300	44720	44100	56990	16590	15300	7600	301	0.392
2	60	48	0.745	535	367	170000	41280	40060	50830	14930	15300	7600	300	0.389
3	55	44	0.685	485	335	156000	37840	36080	46360	12820	15300	7600	299	0.389
4	50	40	0.640	450	310	145000	34400	33000	42900	11800	15300	7600	298	0.399
5	45	36	0.590	410	285	133000	30960	28910	39950	10280	15300	7600	296	0.407
6	40	32	0.550	380	265	125000	27520	27730	37460	9390	15300	7600	296	0.427
7	35	28	0.507	345	240	114000	24080	24940	33660	8420	15300	7600	295	0.446
8	30	24	0.465	315	220	105000	20640	22700	31240	7530	15300	7600	296	0.481
9	25	20	0.427	290	200	96800	17200	20580	29070	7050	15300	7600	297	0.532
10	20	16	0.390	260	185	88600	13760	18890	27220	5830	15300	7600	298	0.608
11	15	12	0.350	235	165	80100	10320	16810	24660	5415	15300	7600	300	0.733
12	10	8	0.313	215	150	71800	6880	15160	21860	5005	15300	7600	301	0.987

$t_{ei}$ : inlet gas temperature of an exhaust-gas turbine, °C,  $t_{eo}$ : outlet gas temperature of the exhaust-gas turbine, °C,  $Q_T$ : output power of the exhaust-gas turbine, kcal/h.

d. 110 kVA diesel-electric generator (Isuzu ZX-125 type, diesel engine 73E-120).

Run No.	Generator output (kVA) (kW)		$\phi$	$t_{g1}$ (°C)	$Q_f$	$Q_{kW}$	$Q_r$	$Q_c$	$Q_{mL}$	$Q_{gL}$	$G_a$	SFC
							(kcal/h)				(kg/h)	(l/kWh)
1	110	88	0.565	500	248000	75680	91800	55000	12500	13000	575	0.312
2	105	84	0.540	475	237000	72240	87200	52100	12500	13000	577	0.314
3	100	80	0.515	455	228000	68800	83100	49500	12500	13000	579	0.316
4	95	76	0.495	437	219000	65360	79700	48400	12500	13000	580	0.320
5	90	72	0.472	417	209000	61920	75500	46100	12500	13000	581	0.322
6	85	68	0.450	397	199000	58480	71600	43400	12500	13000	582	0.326
7	80	64	0.428	380	191000	55040	68500	42000	12500	13000	584	0.331
8	75	60	0.408	360	182000	51600	64600	40300	12500	13000	585	0.337
9	70	56	0.388	342	173000	48160	61200	38200	12500	13000	586	0.344
10	65	52	0.369	325	166000	44720	57900	37900	12500	13000	587	0.353
11	60	48	0.353	313	158000	41280	55700	35500	12500	13000	588	0.365
12	55	44	0.333	295	150000	37840	52300	34400	12500	13000	589	0.377
13	50	40	0.318	284	143000	34400	50200	32900	12500	13000	590	0.397
14	45	36	0.300	265	135000	30960	46800	31700	12500	13000	591	0.417
15	40	32	0.282	250	128000	27520	44000	31000	12500	13000	593	0.444
16	35	28	0.262	234	119000	24080	40900	28600	12500	13000	594	0.470
17	30	24	0.243	218	111000	20640	37900	26900	12500	13000	595	0.511
18	25	20	0.225	200	102000	17200	34800	24500	12500	13000	596	0.567
19	20	16	0.206	185	93800	13760	32000	22600	12500	13000	597	0.650

$\phi$ : equivalence ratio,  $\phi=1/n$ ,  $n$ : excess-air factor,  $t_{g1}$ : inlet gas temperature of an exhaust-gas heat exchanger, °C,  $Q_f$ : heat supplied by fuel, kcal/h,  $Q_{kW}$ : output power of generator, kcal/h,  $Q_r$ : exhaust-gas heat energy, kcal/h,  $Q_c$ : coolant heat energy, kcal/h,  $Q_{mL}$ : mechanical friction loss of engine, kcal/h,  $Q_{gL}$ : generator loss, kcal/h,  $G_a$ : weight flow rate of air aspirated by engine, kg/h, SFC: specific fuel consumption, l/kWh.

In the case where the equivalence ratio  $\phi$  is greater than 0.5, the value of  $Q_c$  obtained by this method may be slightly greater than its true value because it includes some heat loss due to incomplete combustion of fuel indicated by generation of carbon soot in this region.

Tables 6a, b, c and d show the heat balances for four kinds of diesel-electric generators installed at Syowa Station during JARE-1 and JARE-21.

The specific fuel consumption (SFC) shown in these figures was calculated by

$$\text{SFC} = B/\text{kW} \quad \text{l/kWh}, \quad (31)$$

and the power plant efficiency can be calculated by

$$\eta_o = 860/[(\text{SFC})\rho_f H_o], \quad (32)$$

where  $\rho_f$  is the specific density of the fuel, which is 0.84 for gas oil. The SFC, which shows its minimum value at an equivalence ratio higher than 0.6, increases with decreasing equivalence ratio, and reaches infinity at an equivalence ratio satisfying the following condition:

$$Q_i = Q_{mL} + Q_{gL}, \quad Q_{kW} = 0. \quad (33)$$

For decreasing the SFC of a diesel-electric generator plant, it is most important to select a diesel engine having a small mechanical loss  $Q_{mL}$  and an electric generator having a small generator loss  $Q_{gL}$  and, moreover, to select a normal running state to correspond to the equivalence ratio giving a minimum SFC.

The yearly mean SFC of the 110-kVA diesel-electric generator plant observed in JARE-20 was only 0.328 l/kWh, and the power plant efficiency was 28.8%, but the greater part of the waste heat of the engine was recovered and used for making cold water by melting ice or snow, and for heating hot water for room-heating and bathtub uses at both Syowa and Mizuho Stations in Antarctica.

## 6. Exhaust-Gas Heat Exchangers

Several types of exhaust gas to water heat exchangers as described below were developed by the authors.

### 6.1. Shell-and-coil type exhaust-gas heat exchangers

During about twenty years from JARE-1 to JARE-18 (1956/76), the shell-and-coil heat exchangers were used for recovering the waste heat from exhaust gas of diesel engines coupled to electric generators. Their main design data are shown in Table 7 and their features are shown in Figs. 2, 5, 6, 29, 30 and 31. The heat exchanger is composed of a cylindrical stainless shell, a top cover plate with water inlet and outlet headers connected to three or four coils, and a center duct. The hot exhaust gas of a diesel engine flows tangentially into the shell at a point near the top end thereof and swirls downward around the coils. When it reaches the bottom end of the shell, it turns up through the center duct to a chimney. On the one hand, cold water pressurized by a pump is led to the inlet header on the top cover plate and is divided and fed to each coil. While the water is flowing through the coil tubes, it absorbs the waste exhaust-gas energy and is led to an outlet header on the top cover plate. The heat exchangers used were very compact and effective and could absorb about 60% of the waste exhaust-gas energy as shown in Table A-4 in Appendix, but some difficulties were experienced as described below.

#### (a) *Acid corrosion of coils*

When the heat exchanger was used for heating cold water of the ice-melting tank directly, the outlet gas temperature was occasionally decreased to about 50–55°C, and the combustion gas contacted very cold coil surfaces, so that some of the water vapor contained in the combustion gas condensed on the coil surfaces. The gas-oil fuel contains about 0.4% sulphur, and its combustion gas contains about 0.025% of SO<sub>2</sub>, about 3% of which changes to SO<sub>3</sub>. The SO<sub>3</sub> component combines with the condensed water to form H<sub>2</sub>SO<sub>4</sub>. The corrosion effect of H<sub>2</sub>SO<sub>4</sub> on stainless steel is very significant. It causes severe pitting corrosion

Table 7. Shell-and-coil type exhaust-gas heat exchanger for JARE.

Items	JARE-1 (1956/58)	JARE-2 (1957/59)	JARE-7/15 (1965/75)	JARE-16/18 (1974/78)	Remarks
Capacity (kcal/h)	10000	12000	18000	15000	
Type	vertical	horizontal	vertical	vertical	
Shell					
Materials			SUS-27	SUS-27	J.I.S. designation
Inner diam. (mm)	297	297	420	420	
Outer diam. (mm)	300	300	423	423	
Total height (mm)	705+(100)	805	804+(100)	638+[175]+(100)	[ ]: coil support height,
Center duct	with	without	with	with	( ): leg height
Inner diam. (mm)	158	—	158	158	
Outer diam. (mm)	160	—	160	160	
Water jacket	with	with	without	without	
Outer diam. (mm)	350	322	—	—	
Height (mm)	555	500	—	—	
Heat insulator					
Material	R.W.	R.W.	R.W.	R.W.	R.W.: rockwool
Coils					
Materials	Al coated steel	Al coated steel	SUS-28, SUS-32 M-5, S-TEN-1 Al coated S-TEN-1	SUS-32 NTK-30A	
Inner diam. (mm)	17	17	14	14	
Outer diam. (mm)	22	22	18	18	
Inner coil					
Coil diam. (mm)	200	139	200	200	
Pitch (mm)	30	30	30	30	
Number of turns	15	23	25	20	
2nd coil					
Coil diam. (mm)	260	198	260	260	
Pitch (mm)	30	30	30	30	
Number of turns	16	23	25	20	
3rd coil					
Coil diam. (mm)	—	257	320	320	
Pitch (mm)	—	30	30	30	
Number of turns	—	24	25	20	
4th coils					
Coil diam. (mm)	—	—	380	380	
Pitch (mm)	—	—	30	30	
Number of turns	—	—	25	20	
Total coil length (m)	23.5	45.8	94.3	75.5	
Total outer surface area of coils (m <sup>2</sup> )	1.62	3.17	5.33	4.27	
Water jacket surface area (m <sup>2</sup> )	0.52	0.50	0	0	
Total heating area $F_o$ (m <sup>2</sup> )	2.14	3.67	5.33	4.27	
Overall coefficient of heat transmission $K_{tm}$ (kcal/m <sup>2</sup> h°C)	—	—	19.5	19.5	
Electric generators (kVA)	20	20	45/65	45/65	



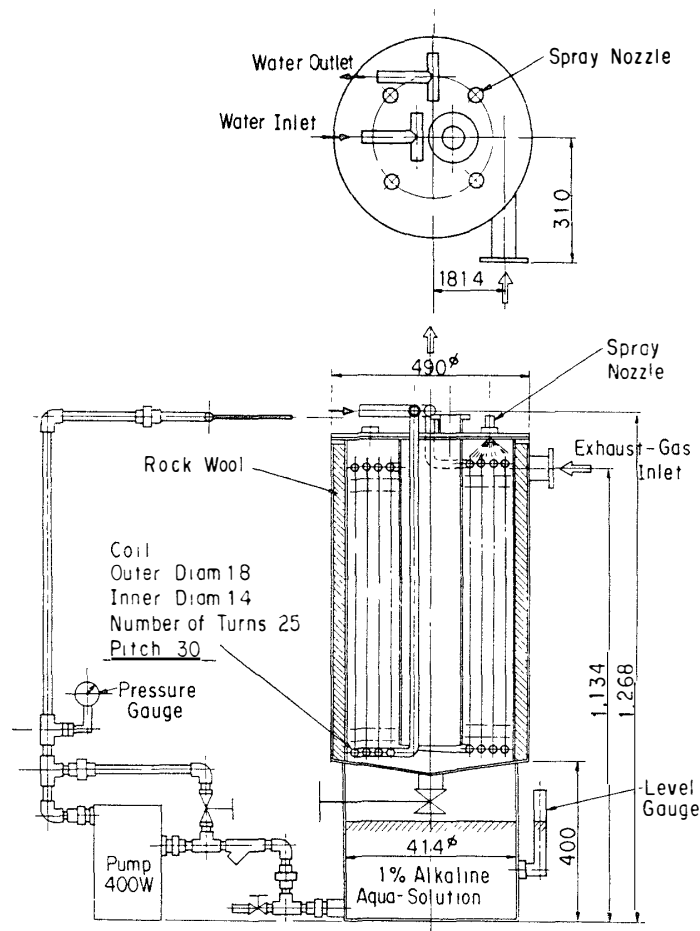


Fig. 30. Shell-and-coil type exhaust-gas heat exchanger provided with alkaline aqua-solution spraying nozzles (JARE-16/18).

aqua solution, such as 1% of CaOH. Fig. 30 shows the system, which was prepared for JARE-16/18 (1974/78). The exhaust-gas heat exchanger was mounted on an alkaline solution reservoir tank. The solution was pumped up by a small pump, and the pressurized solution was injected through four low-pressure spray nozzles installed on the top cover plate. By spraying the solution over the four coils in the shell from time to time, acid corrosion could be prevented somewhat, and at the same time, the soot adhering to the coil surface could be dissolved into the solution.

(b) *Decrease of heat transfer with time due to soot accumulation on coil surface*

As is well known, another important problem relating to exhaust-gas heat exchangers used for diesel engines is the decrease of heat transfer with time caused by increased heat resistance due to an adhering soot layer on exchanger heating surfaces.

Figs. 33 and 34 show the results of observation in the JARE-7 engine room

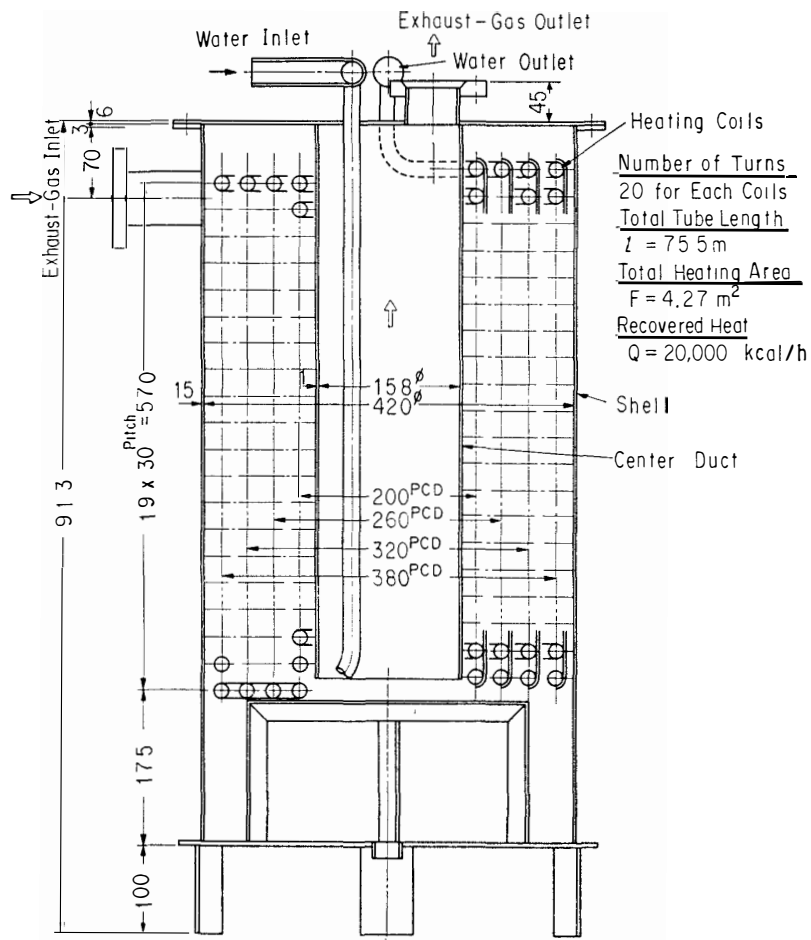


Fig. 31. Shell-and-coil type exhaust-gas heat exchanger with a bottom chamber for collecting soot (JARE-16|18).



Fig. 32. Severe acid corrosion of stainless-steel coils by exhaust gas of diesel engine (Materials, SUS-316 and SUS-304).

Table 8. Materials used for heating coils of exhaust-gas heat exchangers.

JIS Standard	C	Si	P	Mn	S	Ni	Cr	Mo	Sb	Cu
SUS-304L (SUS-28)	<0.02	<1.00	<0.04	<2.00	<0.03	9-13	18-20	—	—	—
SUS-316 (SUS-32)	<0.08	<1.00	<0.04	<2.00	<0.03	10-14	16-18	2-3	—	—
SUS-316L (SUS-33)	<0.03	<1.00	<0.04	<2.00	<0.03	12-15	16-18	2-3	—	—
NIK 30-A (NAS-305)	<0.06	<1.00	<0.03	<2.00	<0.02	28-31	19-21	2-3	—	2.75- 3.75
M-5	<0.06					15-17	17-19	4.5-6	—	—
S-TEN-1	0.09	0.35	0.019	0.42	0.022	—	—	—	0.098	0.34

- Note: 1) SUS-304L: Severe acid corrosion was observed.  
 2) SUS-316, SUS-316L: Some acid corrosion was observed, but less than SUS-304L.  
 3) NIK 30-A: called Carpenter-20; can resist acid corrosion.  
 4) M-5: can resist acid corrosion.  
 5) S-TEN-1: was developed by Shin Nihon Seitetsu Co., Ltd.; does not contain Ni and Cr but can resist acid corrosion. Alumered S-TEN-1 was used as coil material, but internal surface of coil cannot be alumered.

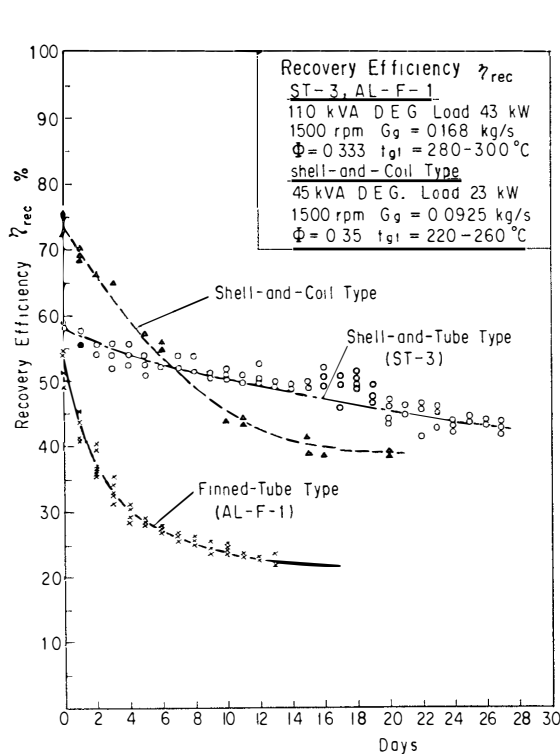


Fig. 33. Decreasing recovery efficiency  $\eta_{rec}$  of exhaust-gas heat exchanger due to soot layer adhering to heating surfaces.

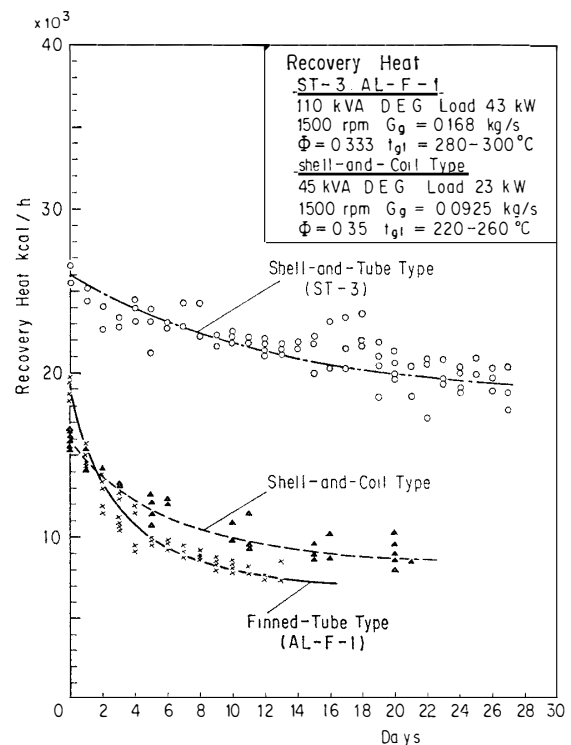


Fig. 34. Decreasing recovered heat  $Q_R$  by exhaust-gas heat exchangers due to soot layer adhering to heating surfaces.

(JARE-14, 1973) and in the JARE-9 engine room (JARE-19, 1978) by TAKEUCHI, one of the authors. In these experiments, the inlet gas temperature  $t_{g1}$  of the heat exchanger and the outlet temperature  $t_{g2}$  were recorded electrically over a period of 20 to 30 days.

The heat  $Q_R$  recovered by an exhaust-gas heat exchanger is expressed by eq. (17) and is nearly proportional to the temperature difference  $(t_{g1} - t_{g2})$  and to the gas flow rate  $G_g$ . The recovery efficiency  $\eta_{rec}$  defined by eq. (26) can also be calculated. As shown in Fig. 33, the recovery efficiency of the shell-and-coil type is about 73% at the start but decreases to 40% after three weeks because of soot adhering to coil surfaces, so that it is necessary to clean off the soot from time to time.

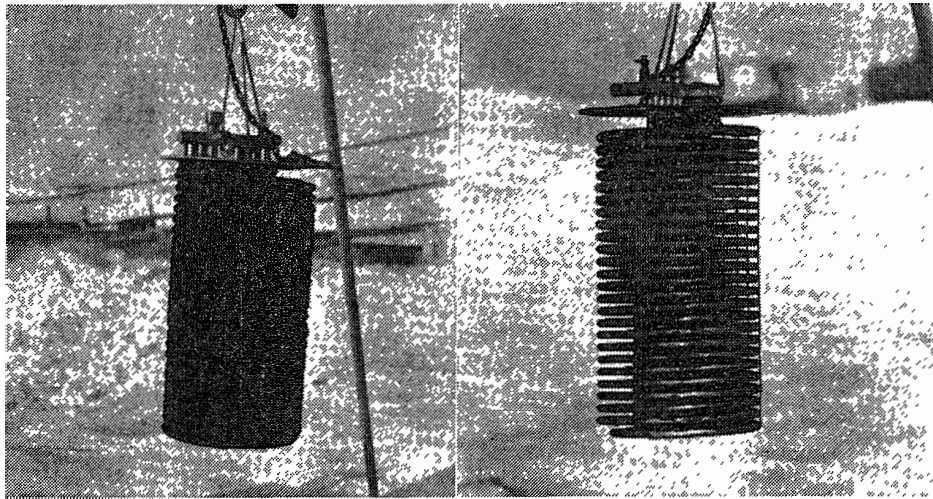


Fig. 35. Cleaning of soot adhering to heating coil of exhaust-gas heat exchanger by blizzard (TAKEUCHI, JARE-14). Left: before cleaning, right: after cleaning in blizzard.

As shown in Fig. 35, TAKEUCHI succeeded in removing the soot adhering to the coil by hanging it in a storm wind. This is a very interesting method, but care must be taken to cause all of the water remaining in the coil to be drained off completely by pressurized air, because frozen water in the coil will rupture the coil tube.

In the shell-and-coil type heat exchanger, the engine exhaust gas flows tangentially into the shell at its top part and flows down around the coils to its bottom, then rising through the center duct connected to a chimney by a flexible pipe. Hence, the heat exchanger itself can be considered as a cyclone separator, and the separated soot is accumulated at the bottom of the shell and chokes the gas flow to the center duct. Fig. 31 shows an improved type having a bottom space to avoid the choking of gas flow by the accumulated soot.

Table 9. Vertical shell-and-tube type exhaust-gas heat exchangers for JARE.

Items	JARE-19 (1977/79)	JARE-20 (1978/80)	JARE-21 (1979/81)	
Type	ST-1	ST-2	ST-3	
Capacity (kcal/h)	15000/25000	15000/25000	25000	
Shell				
Material	SUS-304	SUS-304	SUS-304	
Inner diam. (mm)	500	500	540	
Outer diam. (mm)	504	504	546	
Height (mm)				
Upper gas chamber	120	120	150	
Shell	800	800	800	
Lower gas chamber	150 (SUS-304)	150 (SUS-304)	120 (FC-25)	
Legs	100 (SUS-304)	100 (SUS-304)	115 (FC-25)	
Total	1179	1179	1179	
Heat insulator				
Material	rock wool	without	without	
Cooling of upper gas chamber	uncooled	uncooled	cooled by water outer diam. of water jacket 616 mm (205 mm from top)	
Tube plate				
Material	SUS-304	SUS-304	SUS-304	
Diam.×thickness (mm)	500×6t	500×6t	upper 538×10t lower 630×10t	
Tubes				
Material	SUS-304	SUS-304TB	SUS-316TB-A	
Inner diam. (mm)	23	23	21.4 22.4	
Outer diam. (mm)	25.4	25.4	25.4 25.4	
Tube length (mm)	800	800	800 800	
Number of tubes	112	112	112 112	
Outer surface area (m <sup>2</sup> )	7.15	7.15	7.15 7.15	
Inner surface area (m <sup>2</sup> )	6.47	6.47	6.02 6.31	
Working fluid				
Shell side	water	water	water	
Area $A_w$ (m <sup>2</sup> )	0.0698	0.0698	0.0861 0.0861	
Tube side	gas	gas	gas	
Area $A_g$ (m <sup>2</sup> )	0.0233	0.0233	0.02014 0.02207	
Velocity (m/s)	7.04	7.04	8.15 7.44	
( $V_g=0.164$ m <sup>3</sup> /s)				
Overall coefficient of heat transmission $K_{lm}$ (kcal/m <sup>2</sup> h°C)	28.2	28.2	35.1	
Recovery efficiency $\eta_{rec}$	0.57	0.74	0.72	
Temperature efficiency $\Phi_g$ (gas side)	0.90	0.91	0.86	



water flows through the shell side (JARE-19, 1977/79). The heating capacity was increased to 21000–25000 kcal/h as shown in Fig. 34 and Table A-5 in Appendix and was sufficient for recovering the waste heat of the 110-kVA diesel-electric generator in the JARE-9 engine room. The prototype ST-1 (JARE-19) and ST-2 (JARE-20, 1978/1980) were made entirely of stainless steel SUS-304 pipes and sheets welded together. Inlet gas chambers were not cooled by water, but the shell under the top tube plate was contacted by water directly, so that excess thermal stress and failure occurred on the shell surfaces just below the top tube plate as shown in Fig. 37.

For removing the excess thermal stress on the shell surfaces, the upper inlet gas chamber was also water-cooled in an improved type ST-3 (JARE-21, 1979/81) as shown in Figs. 36 and 38. In this type, the shell is made of SUS-304 stainless-steel sheets, and the heating tubes are made of SUS-316L or TB-A and are 800 mm in length. The bottom box was cast from FC-25 and had an opening with a cover plate for occasionally scraping out the accumulated soot. In the

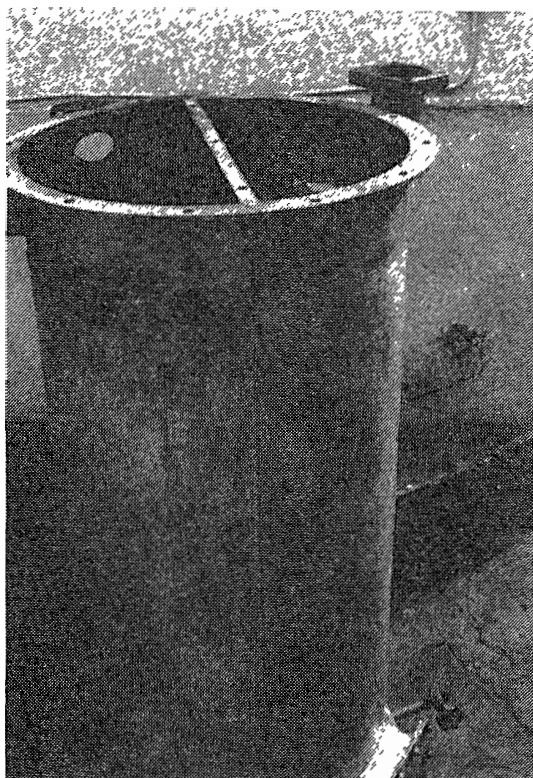


*Fig. 37. Repaired thermal crack occurring on the boundary of water jacket and uncooled shell surface heated by inlet high temperature exhaust-gas jet in ST-2 prepared for JARE-20 (1978/80).*

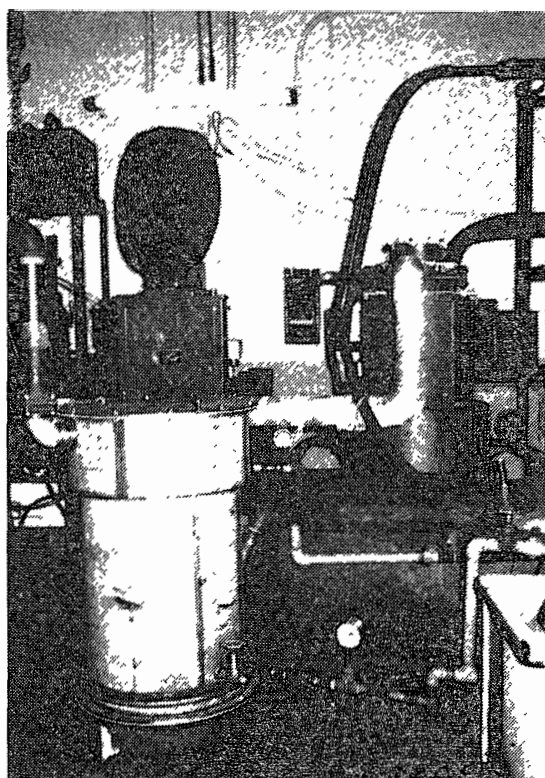


*Fig. 38. ST-3 shell-and-tube type exhaust-gas heat exchanger being tested in Engine Laboratory of Nihon University, Tokyo (6 October 1979).*

ST-3 type, the soot adhering on the inner surfaces of vertical heating tubes can be scraped off easily without touching any part of the water system by removing only the top cover plate. The theoretical and experimental analyses of the ST-3 type are shown in Appendix 2. The fouling effect of soot is less than that in the shell-and-coil type as shown in Figs. 33 and 34.

### 6.3. Vertical fin-tube type exhaust-gas heat exchangers

A vertical fin-tube type heat exchanger AL-F-1 as shown in Table 10 and Fig. 39 was developed by the authors for JARE-19. It is composed of an aluminum cylinder with 36 longitudinal axial fins, a water-cooled shell, and a center tube made of SUS-304. The engine exhaust gas flows down through the axial fins to the bottom and turns up through the center tube connected to a chimney.

Cold water conducted to an inlet at the bottom of the heat exchanger rises up through an annular passage formed between the center tube and the inner surface of the finned cylinder to its outlet and is conducted again to the bottom of outer water jacket of shell by a pipe.

The estimated fin efficiency is about 98.6%, so that the total fin area can be considered as the same as a direct heating area.

The maximum heating capacity of the AL-F-1 is about 18000 kcal/h at the start as shown in Fig. 34, but decreases to about 7000 kcal/h after two weeks due to soot fouling. Generally, the heating capacity of an exhaust-gas heat exchanger  $Q_R$  is represented by

$$Q_R = K_{am} F(t_{gm} - t_{wm}) = K_{lm} F \Delta t_{lm} \text{ kcal/h,} \quad (34)$$

where

- $t_{gm}$ : mean gas temperature, °C,
- $t_{wm}$ : mean water temperature, °C,
- $\Delta t_{lm}$ : logarithmic mean temperature difference, °C,

$$\Delta t_{lm} = (\Delta t_1 - \Delta t_2) / \ln(\Delta t_1 / \Delta t_2) \quad (\text{counterflow}), \quad (35)$$

$$\Delta t_1 = t_{g1} - t_{w2}, \quad \Delta t_2 = t_{g2} - t_{w1},$$

- $t_{g1}$ : inlet gas temperature, °C,       $t_{g2}$ : outlet gas temperature, °C,
- $t_{w1}$ : inlet water temperature, °C,       $t_{w2}$ : outlet water temperature, °C,
- $K_{am}$ : overall coefficient of heat transmission for arithmetic mean temperature difference, kcal/m<sup>2</sup>h°C,
- $K_{lm}$ : overall coefficient of heat transmission for logarithmic mean temperature difference, kcal/m<sup>2</sup>h°C,
- $F$ : a standard heating area, here, the area of the gas side being taken as  $F$ , m<sup>2</sup>.

Table 10. Vertical fin-tube type exhaust-gas heat exchangers prepared for JARE.

Items	AL-F-1 JARE-19 (1977/79)	AL-F-2 JARE-21 (1979/81)	AL-F-3 JARE-22 (1980/82)
Type	built-up	integrally cast	built-up
Capacity $Q_R$ (kcal/h)	18000	18000	24000
Total heating area $F_o$ (m <sup>2</sup> )	5.704	5.971	6.754
Overall coefficient of heat transmission			
$K_{lm}$ (kcal/m <sup>2</sup> h°C)	25.6	26.3	28.5
$K_{lm}F_o$ (kcal/h°C)	146	157	192
Shell			
Material	SUS-304	AC4A-T6	SUS-304
Inner diam.×thickness	400×2t	418×8t	444.4×6.4t
Outer diam.×thickness	500×2t	554×10t	556×3t
Vertical length	794	800	800
Heating surface area (gas side) $F_s$ (m <sup>2</sup> )	0.998	3.050	1.116
Coefficient of heat transfer (kcal/m <sup>2</sup> h°C)			
Water side $\alpha_{w1}$	135	112	223
Gas side $\alpha_g$	10.0	11.6	28.8
Overall coefficient of heat transmission			
$K_s$ (kcal/m <sup>2</sup> h°C)	9.31	10.5	25.5
$K_sF_s$ (kcal/h°C)	9.29	32.0	29.5
Fin tube			
Material	AC4A-T6	AC4A-T6	AC4A-T6
Tip radius of fin (mm)	199	209	222
Hub radius of fin (mm)	125	129	125
Thickness of fin at tip (mm)	8	10	7
Thickness of fin at hub (mm)	13	10	13
Height of fin (mm)	74	80	97
Number of fins	36	36	36
Vertical length of fin (mm)	764	800	800
Vertical length of tube (mm)	794	800	800
Total fin area $F_f$ (m <sup>2</sup> )	4.071	2.304	5.587
Fin efficiency $\eta_f$	0.986	0.993	0.93
Hub area of fin $F_h$ (m <sup>2</sup> )	0.242	0.361	0.254
Tip area of fin $F_t$ (m <sup>2</sup> )	0.220	0.762	0.202
Equivalent directly heating area $F_{fd}$ (m <sup>2</sup> )	4.473	2.695	5.638
Coefficient of heat transfer (kcal/m <sup>2</sup> h°C)			
Water side $\alpha_{w2}$	215	189	308
Gas side $\alpha_g$	10.0	11.6	28.8
Overall coefficient of heat transmission			
$K_f$ (kcal/m <sup>2</sup> h°C)	9.65	10.9	26.3
$K_fF_{fd}$ (kcal/h°C)	42.8	29.4	148.3

Items	AL-F-1 JARE-19 (1977/79)	AL-F-2 JARE-21 (1979/81)	AL-F-3 JARE-22 (1980/82)
Center tube			
Material	SUS-304	A-6063	(AC4A-T6)
Inner diam.×thickness (mm)	93.6×4t	90×5t	230
Outer diam. (mm)	101.6	100	
Vertical length (mm)	794	800	763
Heating surface area $F_T$ (m <sup>2</sup> )	0.233	0.226	center partition
Coefficient of heat transfer (kcal/m <sup>2</sup> h°C)			plate SUS-304
Water side $\alpha_{w2}$	215	189	(169B×760H×3t)
Gas side $\alpha_{gT}$	37.5	53.7	
Overall coefficient of heat transmission			
$K_T$ (kcal/m <sup>2</sup> h°C)	31.9	41.8	
$K_T F_T$ (kcal/h°C)	7.44	9.45	

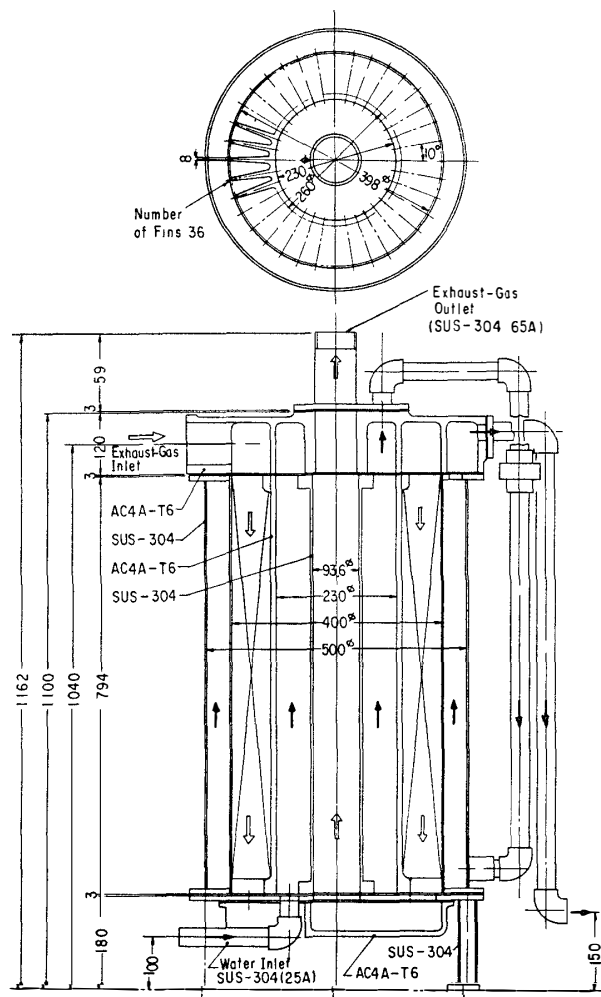


Fig. 39. Fin-tube type exhaust-gas heat exchanger AL-F-1 prepared for JARE-19 (1977/79).

The overall coefficient of heat transmission through a wall depends mainly on the heat transfer coefficient of the gas side,  $\alpha_g$ , because the heat transfer coefficient of the water side,  $\alpha_w$ , is much greater than  $\alpha_g$ . Hence, for increasing  $K_{lm}$  or  $K_{am}$ , the heat transfer coefficient of the gas side,  $\alpha_g$  should be increased, and the latter is proportional to the gas velocity. Accordingly, for increasing  $Q_R$  with the same

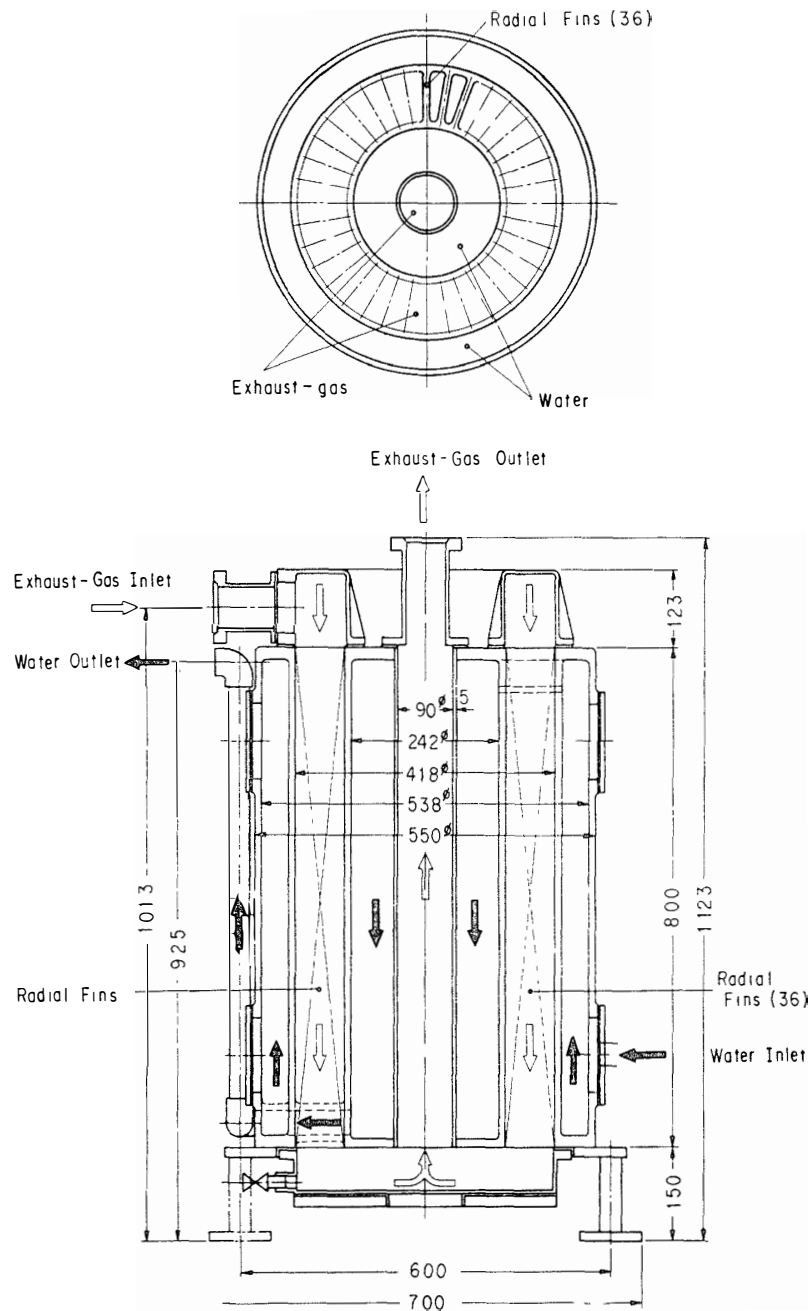


Fig. 40. Integrally cast fin-tube type exhaust-gas heat exchanger AL-F-2 prepared for JARE-21 (1979/81).

heating surface area  $F$ , the gas velocity in the heat exchanger should be kept as high as possible.

The merits of the fin-tube type exhaust-gas heat exchanger are as follows:

(a) Aluminum fins are kept at high temperature and protected from acid corrosion, whereby durability will be improved compared with that of shell-and-coil or shell-and-tube types.

(b) The soot adhering to its heating surfaces can be scraped off easily by removing the top cover only.

(c) The cost will be lower than that of the ST-3 type because of the simplicity of manufacturing.

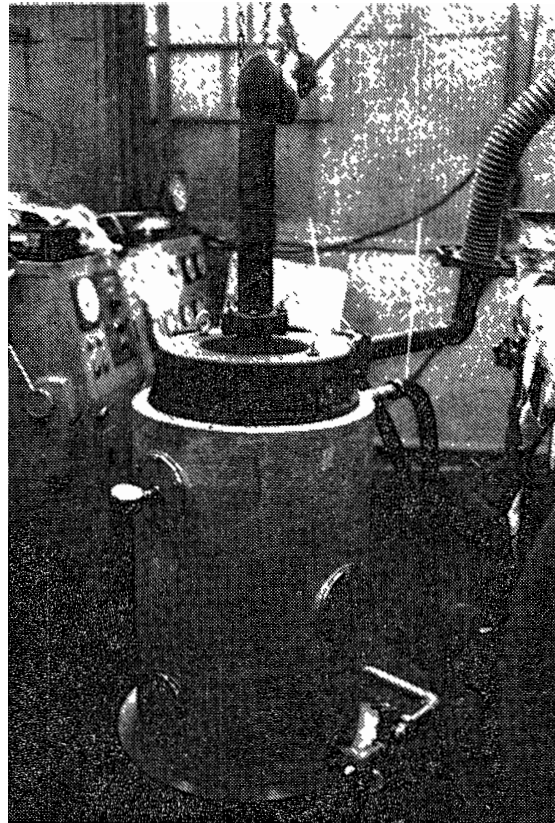


*Fig. 41. Integrally cast aluminum fin-tube type exhaust-gas heat exchanger AL-F-2 prepared for JARE-21 (1979/81).*

In the AL-F-1, the water piping system had to be removed to remove soot. To overcome this defect, the AL-F-2 type as shown in Figs. 40 and 41 was manufactured for JARE-21. It is composed of three parts, *i.e.*, an uncooled top cover with gas inlet and outlet made of FC-25, an integrally cast aluminum center body with axial fins and a water jacket, and a bottom cover made of SUS-304. However, the AL-F-2 has two demerits, one of which is the difficulty of integrally casting the body. The other is that rapid cooling of the heated center body must be

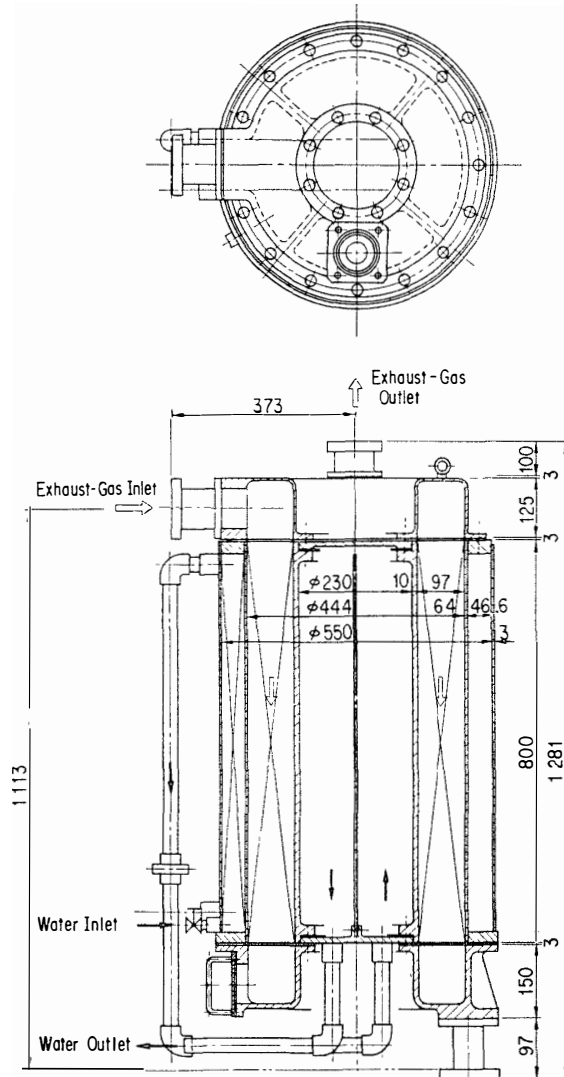


Fig. 42. Fin-tube type exhaust-gas heat exchanger AL-F-3 prepared for JARE-22 (1980/82).

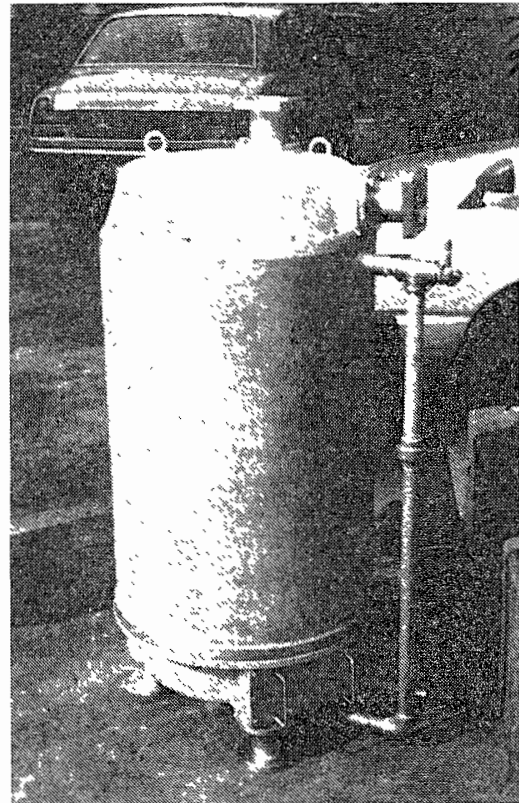


Fig. 43. Fin-tube type exhaust-gas heat exchanger AL-F-3 prepared for JARE-22.

strictly avoided to prevent mechanical failure due to excessive thermal stress.

For JARE-22 (1980/82), AL-F-3 was prepared. This is an improved type of AL-F-1 as shown in Figs. 42 and 43. The exhaust-gas velocity in this new type is 9.66 m/s and  $K_{lm}$  was increased to 28.5 kcal/m<sup>2</sup>h°C compared with 4.28 m/s and 25.6 kcal/m<sup>2</sup>h°C in the AL-F-1. Moreover, soot scraping can be done without touching the water system.

## 7. Experimental Analysis of Exhaust-Gas Heat Exchangers

As described above, the authors developed three kinds of heat exchangers for recovering the waste heat of diesel engines. These heat exchangers were tested in the Engine Laboratory of Nihon University, Tokyo, before they were shipped to Antarctica. A turbocharged high-speed diesel engine, Isuzu-640T, coupled to an electric eddy-current dynamometer was used as the exhaust-gas source. The engine is of the same type as that used for the 65-kVA diesel-electric power generator at Syowa Station (see Table 3). The heat balance of this engine is shown in Fig. 27 and Table 6c.

The experimental equipment is shown in Fig. 44. The exhaust gas of the diesel engine is introduced into an exhaust-gas heat exchanger being tested, and the outlet gas is sucked in by a Nash pump and delivered into the atmosphere through a chimney. As a heating load, a bathtub filled with water was used, and

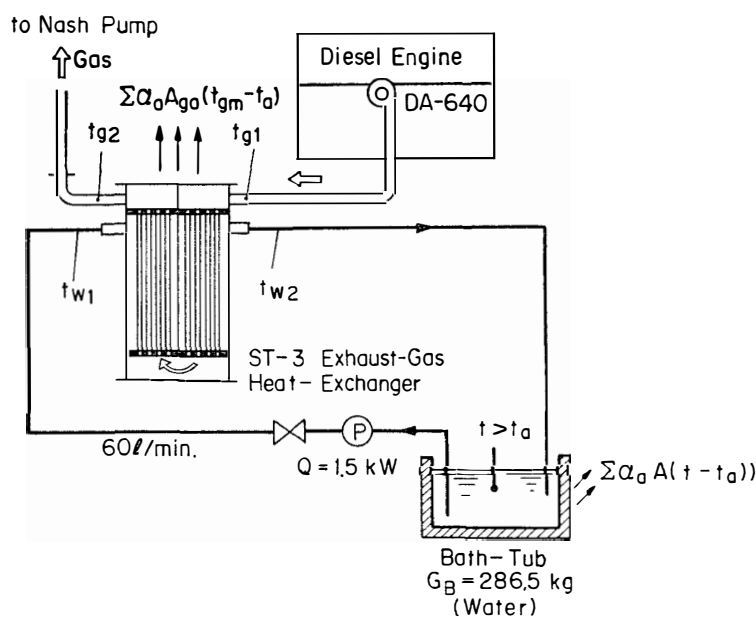


Fig. 44. Experimental equipment for testing exhaust-gas heat exchangers in Engine Laboratory of Nihon University, Tokyo.

a water pump recirculated the hot water between the water side of the heat exchanger and the bathtub.

As an example, the test on a shell-and-tube type ST-3 heat exchanger will be described below.

- $G_g$ : weight flow of exhaust gas, kg/h,
- $c_{pgm}$ : mean specific heat at constant pressure of exhaust gas, kcal/kg°C,
- $t_{gm}$ : mean gas temperature  $t_{gm} = (t_{g1} + t_{g2})/2$ , °C,
- $t_a$ : atmospheric air temperature, °C,
- $A_{ga}$ : cooling surface area of heat exchanger, contacting exhaust gas at one side and atmosphere at the other side, m<sup>2</sup>,
- $\alpha_g$ : heat transfer coefficient of gas side, kcal/m<sup>2</sup>h°C,
- $\alpha_w$ : heat transfer coefficient of water side, kcal/m<sup>2</sup>h°C,
- $\alpha_a$ : heat transfer coefficient of air side due to natural convection, kcal/m<sup>2</sup>h°C,
- $R_g$ : thermal resistance of gas side boundary layer, m<sup>2</sup>h°C/kcal,
- $R_c$ : thermal resistance of soot layer, m<sup>2</sup>h°C/kcal,
- $R_w$ : thermal resistance of water side boundary layer, m<sup>2</sup>h°C/kcal,
- $R_m$ : thermal resistance of metal wall, m<sup>2</sup>h°C/kcal,
- $\lambda_c$ : thermal conductivity of soot, kcal/mh°C,
- $\lambda_m$ : thermal conductivity of metal wall, kcal/mh°C,
- $F_i$ : internal surface area of tubes, m<sup>2</sup>,
- $F_o$ : external surface area of tubes, m<sup>2</sup>,
- $l$ : length of one tube, m,
- $z$ : number of tubes in one path area,
- $d_i$ : internal diameter of tube, m,
- $d_o$ : external diameter of tube, m,
- $D_s$ : inner diameter of shell, m,
- $\delta_c$ : thickness of soot layer, m,
- $\delta_m$ : thickness of metal wall, m,
- $c_M$ : specific heat of heated material, kcal/kg°C,
- $G_M$ : weight of heated material, kg,
- $G_B$ : total weight of water contained in bathtub, kg,
- $\Phi_g$ : temperature efficiency of gas side,
- $c_w$ : specific heat of water,  $c_w = 1.0$  kcal/kg°C,
- $t$ : mean water temperature in bathtub, °C,
- $\tau$ : time, h,
- $\eta_{rec}$ : recovery efficiency.

After starting the engine, measurements were made every 5 minutes until the mean water temperature of the bathtub became substantially constant. The following

four methods for estimating the heating capacity of the heat exchanger  $Q_R$ , overall coefficient of heat transmission  $K_{lm}$  or  $K_{am}$ , recovery efficiency  $\eta_{rec}$ , and temperature efficiency  $\Phi_g$  can be recommended.

(a)  $Q_{R1}$  obtained by measurement of exhaust-gas temperatures  $t_{g1}$  and  $t_{g2}$

The heat transferred from hot exhaust gas to water in the heat exchanger can be calculated by

$$Q_{R1} = G_g c_{pgm} (t_{g1} - t_{g2}) - \sum \alpha_a A_{ga} (t_{gm} - t_a) \text{ kcal/h,} \quad (36)$$

$$G_g = G_a + G_f \text{ kg/h,} \quad (37)$$

where  $G_g$  denotes the total exhaust gas containing steam, and  $c_{pgm}$  is its mean specific heat at constant pressure for mean gas temperature  $t_{gm}$ . The first term of eq. (36) represents the apparent total enthalpy drop, and the second term indicates the heat loss from the hot parts of the shell, contacting hot gas on its inside and room air on its outer side, respectively. The cooling surface area  $A_{ga}$  and the heat transfer coefficient  $\alpha_a$  should be estimated theoretically.

As an example, for ST-3 (Fig. 36)  $t_{gm} = 207^\circ\text{C}$ ,  $t_a = 19^\circ\text{C}$ , for top cover plate  $A_{ga} = 0.229 \text{ m}^2$ ,  $\alpha_a = 5.75 \text{ kcal/m}^2\text{h}^\circ\text{C}$ ,

$$\alpha_a A_{ga} = 1.32 \text{ kcal/h}^\circ\text{C}$$

for bottom box  $A_{ga} = 0.229 \text{ m}^2$ ,  $\alpha_a = 2.00 \text{ kcal/m}^2\text{h}^\circ\text{C}$ ,  $\alpha_a A_{ga} = 0.46 \text{ kcal/h}^\circ\text{C}$ ,

$$\sum \alpha_a A_{ga} (t_{gm} - t_a) = 1.78(207 - 19) = 335 \text{ kcal/h.}$$

The results of experiments are shown in Table A-5 in Appendix. The heating capacity  $Q_{R1}$  obtained by this method will be most accurate, because the temperature difference ( $t_{g1} - t_{g2}$ ) is very great, although the weight flow rate of the air and fuel should be measured experimentally.

In the case of counter flow, the overall coefficient of heat transmission  $K_{lm}$  and  $K_{am}$  can be obtained from eqs. (34) and (35) by putting

$$F = F_i = 2z(\pi d_i l) = 2(56)[\pi(0.0214)(0.800)] = 6.02 \text{ m}^2,$$

$$\begin{aligned} 1/K_{lm} &= \sum R = R_g + R_c + R_m + R_w \\ &= (1/\alpha_g)(F_i/F_c) + (\delta_c/\lambda_c) + (\delta_m/\lambda_m) + (1/\alpha_w)(F_i/F_o) \text{ m}^2\text{h}^\circ\text{C/kcal,} \end{aligned} \quad (38)$$

where  $F_c$  is the internal surface area of the soot layer. At the start,  $F_c = F_i$  and  $\delta_c = 0$ , because the internal surface of the tubes is clean.

The arithmetic temperature difference  $\Delta t_{am}$  is represented by

$$\Delta t_{am} = t_{gm} - t_{am} = (t_{g1} + t_{g2})/2 - (t_{w1} + t_{w2})/2 = (\Delta t_1 + \Delta t_2)/2 \text{ }^\circ\text{C.} \quad (39)$$

Generally, the arithmetic mean temperature difference  $\Delta t_{am}$  is greater than the logarithmic mean temperature difference  $\Delta t_{lm}$ , so that the overall coefficient of heat transmission  $K_{am}$  is less than  $K_{lm}$ .

The recovery efficiency  $\eta_{rec}$  of the heat exchanger can be calculated by eq. (26), and the temperature efficiency  $\Phi_g$  of the heat exchanger is defined as

$$\Phi_g = (t_{g1} - t_{g2}) / (t_{g1} - t_{w1}). \quad (40)$$

The outlet gas temperature  $t_{g2}$  and outlet water temperature  $t_{w2}$  can be calculated by expressing the inlet gas temperature  $t_{g1}$  and the inlet water temperature  $t_{w1}$  as follows:

$$t_{g2} = t_{g1} - \Phi_g (t_{g1} - t_{w1}) \text{ } ^\circ\text{C}, \quad (41)$$

$$t_{w2} = t_{w1} + (c_{pgm} G_g / c_w G_w) \Phi_g (t_{g1} - t_{w1}) \text{ } ^\circ\text{C}. \quad (42)$$

The mean value of  $K_{lm}$ ,  $\eta_{rec}$ , and  $\Phi_g$  for ST-3 are obtained by experiment as shown in Table A-6 in Appendix.

$$K_{lm} = 35.1 \text{ kcal/m}^2\text{h}^\circ\text{C}, \quad \eta_{rec} = 0.715, \quad \text{and} \quad \Phi_g = 0.860.$$

(b) *Heating capacity  $Q_{R2}$  obtained from measurement of inlet and outlet water temperatures*

The heat transferred from the hot exhaust gas to the water will also be estimated by

$$Q_{R2} = c_w G_w (t_{w2} - t_{w1}) + \sum \alpha_a A_{wa} (t_{wm} - t_a) \text{ kcal/h}. \quad (43)$$

The last term of eq. (43) shows the heat loss from the hot surface area of the shell contacting water on its inner side and atmospheric air on its outer side by natural convection. The heating capacity obtained by this method occasionally entails some errors due to the difficulty of measuring the small temperature difference  $(t_{w2} - t_{w1})$ .

(c) *Heating capacity  $Q_{R3}$  obtained from measurement of water temperature rise in a bathtub as heating load*

A new method of obtaining the heating capacity of a heat exchanger was devised by AWANO, one of the authors. It depends on the measuring of mean water temperature rise of a bathtub with time. The principle is as follows:

For a small time interval  $d\tau$ , the following heat equilibrium equation should be valid:

$$\begin{aligned} (Q_{R3} + Q_p) d\tau &= [K_{am} F_i (t_{gm} - t) + Q_p] d\tau \\ &= (c_w G_w + \sum c_M G_M) dt + \sum \alpha_a A (t - t_a) d\tau, \end{aligned} \quad (44)$$

where

- $Q_p$ : pump work supplied, kcal/h,  
 $G_w$ : total weight of water contained in the bathtub, heat exchanger, pump, and pipe lines, kg,  
 $t_0$ : initial temperature of water in the bathtub, °C,  
 $t_{gm}$ : mean gas temperature, which is kept nearly constant but rises slightly with time, °C,  
 $t$ : instantaneous mean temperature of water, °C,  
 $\sum c_M G_M$ : total sum of heat capacities of materials to be heated by water, such as shell, tubes, piping, pump, and bathtub, kcal/°C,  
 $A$ : cooling surface area of shell, piping, pump, and bathtub, which contact water on the inside and atmospheric air on the outside, m<sup>2</sup>,  
 $\tau$ : time, h.

From eq. (44), we get

$$\frac{dt}{d\tau} = a - bt, \quad (45)$$

where

$$a = (K_{am} F_i t_{gm} + \sum \alpha_a A t_a + Q_p) / (c_w G_w + \sum c_M G_M) \text{ } ^\circ\text{C/h}, \quad (46)$$

$$b = (K_{am} F_i + \sum \alpha_a A) / (c_w G_w + \sum c_M G_M) \text{ } 1/\text{h}. \quad (47)$$

By integrating eq. (45), the instantaneous mean water temperature  $t$  in the bathtub can be represented by

$$t = (a/b) - [(a/b) - t_0] e^{-b\tau} \text{ } ^\circ\text{C}. \quad (48)$$

For determining the constant term  $(a/b)$  in eq. (48), the following approximation is very useful. From eqs. (46) and (47), the constant term  $(a/b)$  can be estimated by neglecting the heat-loss terms  $\sum \alpha_a A t_a$  and  $\sum \alpha_a A$  and pump work  $Q_p$  as follows:

$$(a/b) \doteq K_{am} F_i t_{gm} / (K_{am} F_i) = t_{gm} \text{ } ^\circ\text{C}, \quad (49)$$

and from eq. (48),

$$e^{-b\tau} = (t_{gm} - t) / (t_{gm} - t_0). \quad (50)$$

The mean value of  $b$  can be determined from eq. (50) by experiment, and the overall coefficient of heat transmission  $K_{am}$  can be determined from eq. (47) by

$$K_{am} = [b(c_w G_w + \sum c_M G_M) - \sum \alpha_a A] / F_i \doteq b(c_w G_w) / F_i \text{ } \text{kcal/m}^2\text{h}^\circ\text{C}. \quad (50)$$



- $c_I$ : specific heat of ice, kcal/kg°C,  
 $t_{Bf}$ : final temperature of water in the bathtub, °C,  
 $t_{Bm}$ : mean temperature of water,  $t_{Bm} = (t_{B0} + t_{Bf})/2$ , °C  
 $t_a$ : atmospheric temperature, °C,  
 $G_w$ : total weight of water contained in the water system, *i. e.*, heat exchanger, water piping, pump, and a bathtub, kg,  
 $G_I$ : weight of ice block, kg,  
 $t_I$ : initial temperature of ice, °C.

The equation of heat balance can be written as follows:

$$[Q_{R4} + Q_p + \sum \alpha_a A (t_a - t_{Bm})] \tau_m = G_I (-c_I t_I + r + c_w t_{Bf}) + c_w G_w (t_{Bf} - t_{B0}). \quad (53)$$

Hence, the transferred heat will be

$$Q_{R4} = K_{am} (t_{gm} - t_{Bm}) F_i = [G_I (-c_I t_I + r + c_w t_{Bf}) + c_w G_w (t_{Bf} - t_{B0})] / \tau_m - [Q_p + \sum \alpha_a A (t_a - t_{Bm})] \text{ kcal/h.} \quad (54)$$

The last term of eq. (54), which is pump work and the transferred heat from atmosphere to water, may be ignored as a first approximation, whereby the overall coefficient  $K_{am}$  can be calculated by

$$K_{am} = [G_I (-c_I t_I + r + c_w t_{Bf}) + c_w G_w (t_{Bf} - t_{B0})] / [\tau_m (t_{gm} - t_{Bm}) F_i] \text{ kcal/m}^2 \text{h}^\circ \text{C.} \quad (55)$$

As an example, in Table A-5 in Appendix 3 for the heat exchanger ST-2,

$$\begin{aligned}
 G_w &= 257 \text{ kg}, & G_I &= 42.8 \text{ kg}, & t_I &= 0^\circ \text{C}, \\
 t_{B0} &= 20^\circ \text{C}, & t_{Bf} &= 20^\circ \text{C}, & t_a &= 18^\circ \text{C}, \\
 \tau_m &= 0.2388 \text{ h}, & t_{g1} &= 300^\circ \text{C}, & t_{g2} &= 39^\circ \text{C}, \\
 t_{gm} &= 170^\circ \text{C}, & t_{Bm} &= 20^\circ \text{C}, & F_i &= 6.47 \text{ m}^2.
 \end{aligned}$$

From eq. (55),

$$\begin{aligned}
 K_{am} &= [42.8(80 + 1 \times 20) + (1)(257)(20 - 20)] / [0.2388(170 - 20)(6.47)] \\
 &= [4280 + 0] / [0.2388(150)(6.47)] = 18.5 \text{ kcal/m}^2 \text{h}^\circ \text{C}, \\
 Q_{R4} &= K_{am} F_i (t_{gm} - t) = (18.5)(6.47)(170 - t) \\
 &= 119.7(170 - t) = 20350 - 120t \text{ kcal/h.} \quad (56)
 \end{aligned}$$

In eq. (56),  $t$  denotes the hot-water temperature in the bathtub at any time  $\tau$ .

In Appendix 2, the theoretical calculations on the design of a shell-and-tube type exhaust-gas heat exchanger ST-3 are explained.

In Appendix 3, the experimental data on the exhaust-gas heat exchangers, such as shell-and-coil type, shell-and-tube type, and vertical fin-tube type, are described.

## 8. Bubble Type Exhaust-Gas Heat Exchanger

### 8.1. Two-stage bubble type heat exchanger for making hot water and melting ice

As a result of many experiences during the last twenty years on the exhaust-gas heat exchangers for recovering exhaust-gas energy from diesel engines, the following two difficulties were recognized:

- (a) Acid corrosion of heating surfaces
- (b) Decrease of heat transfer with time due to the soot fouling of heating surfaces.

To overcome these difficulties, the authors developed a new bubble type exhaust-gas heat exchanger for JARE-18 (1976/78). In this heat exchanger, the engine exhaust gas is blown into the bottom of a body of water in a heating tank through many small holes. As the bubbles rise through the water, the heat of the bubbles is transferred to the surrounding water through the bubble surfaces. In other words, the bubble surface itself makes the heating surface, and the temperature of the bubble surface will be nearly equal to the water temperature because the heat transfer coefficient of water boundary layer is very great. Accordingly, the heat transfer from each bubble to water depends mainly on thermal conduction in the bubble. The necessary minimum depth of water required for fully transferring the heat in a bubble to the water decreases with decreasing diameter of the bubble.

In Figs. 45 and 46, a diagrammatic sectional view of the new heat exchanger and its external view are shown. In Fig. 45, the engine exhaust flows down through a center tube surrounded by a water jacket and is blown into the water of the lower heating tank through three perforated plates. The delivery gas from the lower heating tank is led to the surrounding space of an upper heating tank and is blown again into the water of the upper heating tank where its remaining heat is transferred to the water.

The gas from the upper heating tank is exhausted into the air through three collecting pipes and a flexible tube connecting them to a chimney. The cold water is fed to a float chamber in order to keep a constant water level  $H_U$  in the upper heating tank. To the side of the lower heating tank, a hot-water reservoir tank was installed, in which a pair of electrodes for detecting the water level  $H_L$

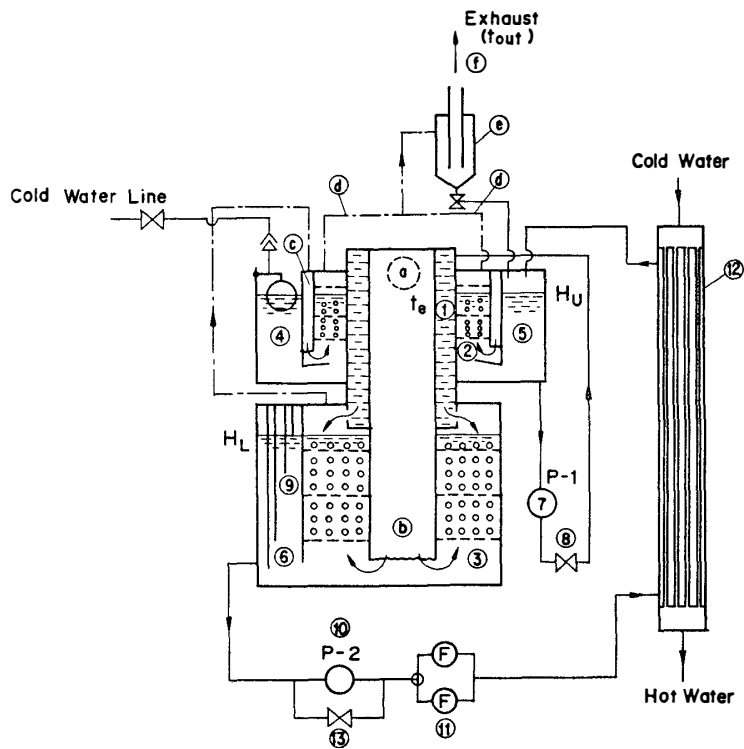


Fig. 45. Bubble type exhaust-gas heat exchanger BE-1 prepared for JARE-18 (1976/78).

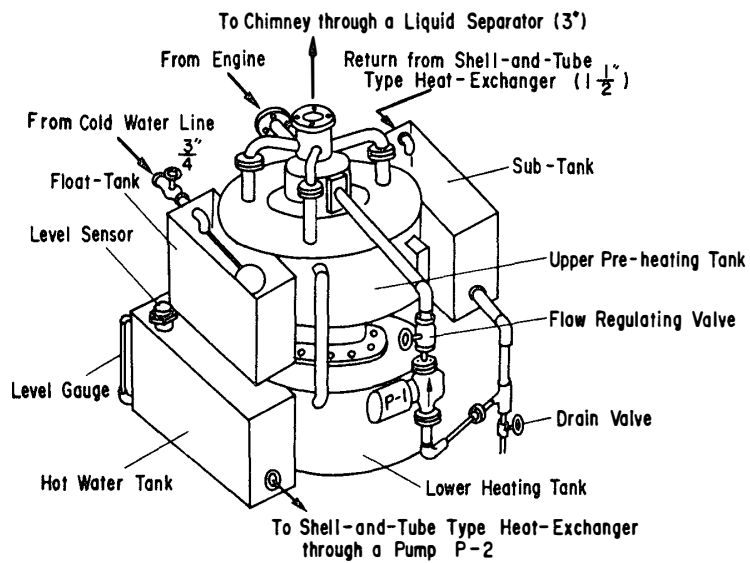


Fig. 46. Bubble type exhaust-gas heat exchanger BE-1 prepared for JARE-18.

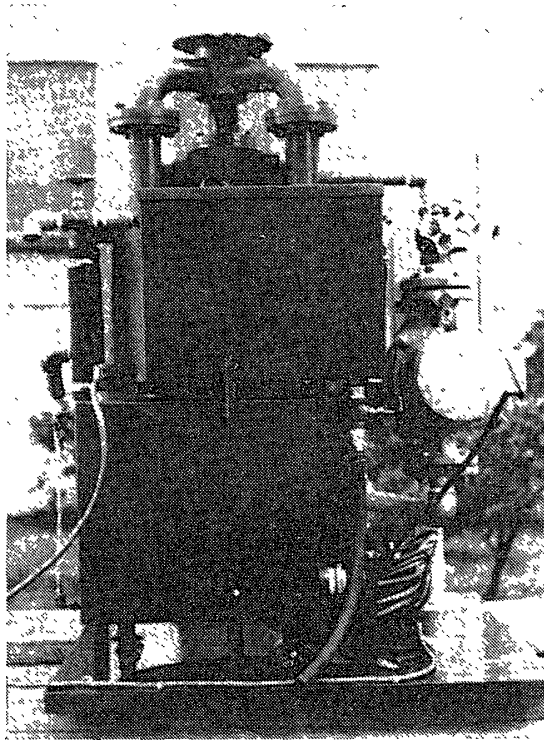


Fig. 47. Bubble type exhaust-gas heat exchanger BE-1 prepared for JARE-18.

and another pair to activate an alarm buzzer indicating an allowable minimum water level of the lower heating tank were installed. The water level of the lower heating tank  $H_L$  can be kept constant by on-off control of a motored pump P-1, which transfers the water from the upper heating tank to the lower heating tank.

The hot water in the reservoir tank is recirculated by another water pump P-2 to heating loads, such as fan-coil units for heating rooms, radiators submerged in hot-water tanks, the bathtub filled with water, or the ice-melting tank.

## 8.2. Experimental analysis of the bubble type heat exchanger

The same notations described in Section 5 will be also used here for analyzing the thermal performance of the new bubble type exhaust-gas-to-water heat exchanger.

The wet intake-air aspirated by a diesel engine  $G_a$  is composed of dry air  $G_{ad}$  and moisture  $G_{aw}$  as shown in eqs. (1) and (2). Fuel gas oil of  $G_f$  is injected into the engine cylinder and burnt with dry air  $G_{ad}$  with an equivalence ratio  $\phi$  as calculated by eq. (7). The exhaust gas from the diesel engine is composed of dry exhaust gas  $G_{gd}$  and steam  $G_w$ , which is given as the sum of steam  $G_{gw}$  and  $G_{aw}$ . The weight flow rate  $G_{gw}$  represents the water vapor produced by the combustion of dry air  $G_{ad}$  and fuel  $G_f$ , which contains  $H$  as a component.

When the bubbles of the engine exhaust rise up through the water in the heating tank, the bubble gases will be saturated by steam having a partial pressure  $p_s$  corresponding to the water temperature through which the bubbles finally rise. The saturated steam  $G_{ws}$  can be calculated by eqs. (18) and (19), and the total gas flow  $G_{out}$  can be obtained by eq. (21).

If the outlet gas temperature  $t_{out}$  is low, some of the water vapor contained in the engine exhaust  $G_w$  will be condensed as the gas flows through the water, and the condensed water vapor  $G_{wc}$  can be calculated by eqs. (22) or (23). On the contrary, however, if the temperature  $t_{out}$  is higher than about 32–38°C, some part of the water in the heating tank will evaporate until the partial pressure of water vapor reaches  $p_s$  corresponding to water temperature of the upper tank. In this case, the evaporated water in the heating tank can be estimated by

$$G_{we} = G_{ws} - G_w = G_{ws} - (G_{aw} + G_{gw}) \text{ kg/h,} \quad (57)$$

and the outlet heat from the chimney can be calculated by

$$Q_{out} = (h_{gd})_{out} G_{gd} + (h'') G_{ws} \text{ kcal/h.} \quad (58)$$

The available maximum energy,  $Q_A$  recovered from the energy of the engine exhaust  $Q_e = H_{g1}$  calculated by eq. (14) becomes

$$Q_A = Q_e - Q_{out} \text{ kcal/h} \quad (59)$$

$$= Q_B + Q_H + Q_{Loss} \text{ kcal/h,} \quad (60)$$

where

$Q_B$ : heat absorbed by hot-water tank, bathtub, or ice-melting tank,

$Q_H$ : heat required for heating the water contained in the heating tank, pipelines, and radiator,

$Q_{Loss}$ : heat loss from heating tank, pipelines, and bathtub.

The maximum recovery efficiency of the heat exchanger is

$$(\eta_{rec})_{max} = Q_A / Q_e. \quad (61)$$

Two experiments on the new bubble type exhaust-gas heat exchanger were conducted by the authors in the Engine Laboratory of Nihon University, Tokyo.

Figs. 48 and 49 show the flow diagrams of water for No. 1 and No. 2 experiments respectively. In No. 1 experiment, the upper heating tank (HU) and the lower heating tank (HL) of the heat exchanger were connected in series. A recirculating water pump P-2 with a flow rate of 6840 kg/h fed the hot water of the heat exchanger to a radiator submerged in a bathtub containing 200 kg of water. The rise of the water temperature in the bathtub was measured and was

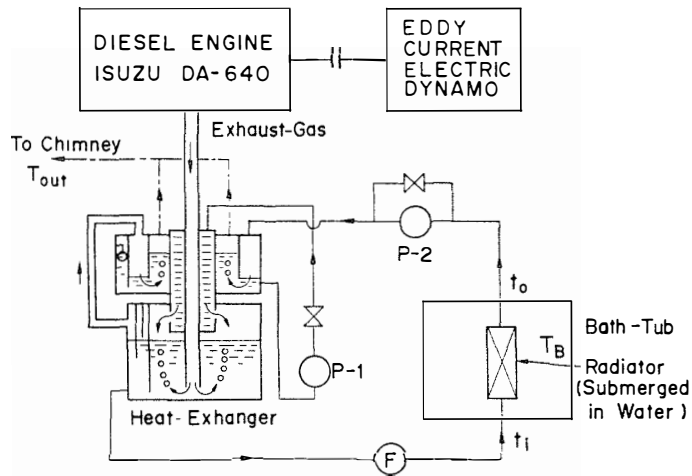


Fig. 48. Flow diagram of water for experiment No. 1 on a BE-1 bubble type exhaust-gas heat exchanger.

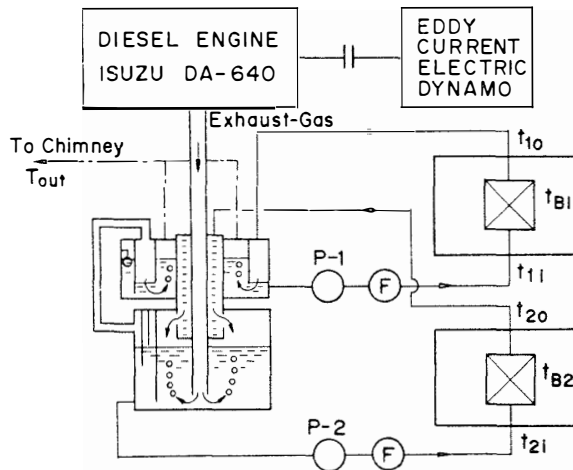


Fig. 49. Flow diagram of water for experiment No. 2 on a BE-1 bubble type exhaust-gas heat exchanger.

$t_{B0} = 11.5^{\circ}\text{C}$  at the start of heating and increased gradually with time  $\tau(h)$ , reaching  $t_B = 55.4^{\circ}\text{C}$  after one hour. The temperature of the bathtub water at any time  $\tau$  can be represented as in eq. (48),

$$t_B = (a/b) - [(a/b) - t_{B0}]e^{-b\tau} \quad ^{\circ}\text{C}, \quad (62)$$

where

$$a = \frac{K_R F_R t_{Rm} + \sum \alpha_a A t_a}{c_w G_B + \sum c_M G_M} \quad ^{\circ}\text{C/h}, \quad (63)$$

$$b = \frac{K_R F_R + \sum \alpha_a A}{c_w G_B + \sum c_M G_M} \quad 1/h, \quad (64)$$

$$a/b = (K_R F_R t_{Rm} + \sum \alpha_a A t_a) / (K_R F_R + \sum \alpha_a A) \div t_{Rm}, \quad (65)$$

- $K_R$ : overall coefficient of heat transmission of radiator, kcal/m<sup>2</sup>h°C,
- $F_R$ : heating surface area of radiator, m<sup>2</sup>,
- $t_{Rm}$ : mean water temperature in radiator, °C,
- $G_B$ : weight of water in the bathtub,  $G_B = 200$  kg,
- $c_w$ : specific heat of water, 1 kcal/kg°C.

The other notations are the same as in eq. (44).

For No. 1 experiment,

$$t_B = t_{Rm} - (t_{Rm} - t_{B0})e^{-b\tau} = 79 - (79 - 11.5)e^{-0.98\tau} \text{ } ^\circ\text{C}. \quad (66)$$

From eq. (64),

$$K_R F_R \div b c_w G_B = (0.98)(1)(200) = 196 \text{ kcal/h}^\circ\text{C},$$

so that

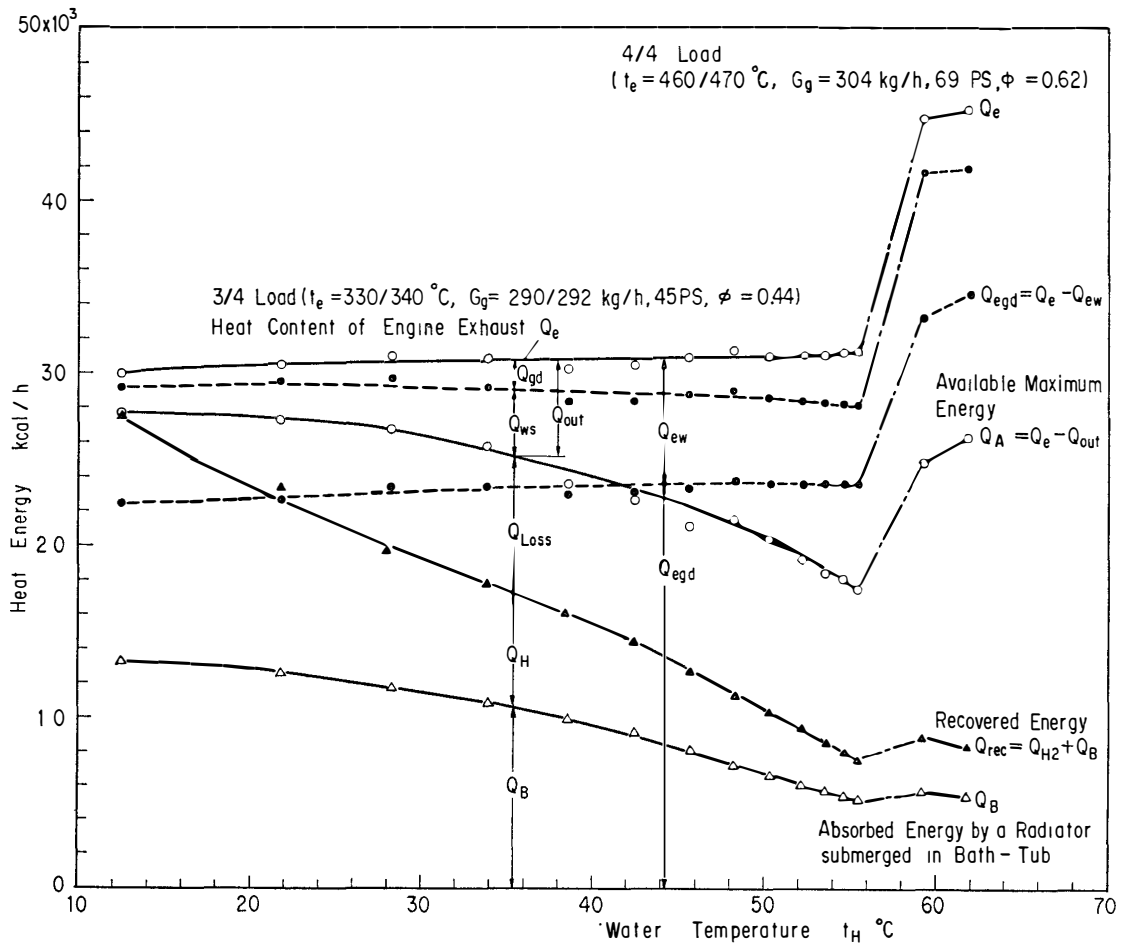


Fig. 50. Results of experiment No. 1 on a BE-1 bubble type exhaust-gas heat exchanger.

$$Q_B = K_R F_R (t_{Rm} - t_B) = 196(79 - t_B) = 15480 - 196t_B \text{ kcal/h.} \quad (67)$$

In the same way, from the measured temperature of water in the heating tank  $t_H$ , which is heated by bubble gas with temperature  $t_{Hb}$  and the heating surface area  $F_{Hb}$

$$t_H = t_{Hb} - (t_{Hb} - t_{H0})e^{-br} = 59.5 - (59.5 - 12.6)e^{-2.30r} \text{ }^\circ\text{C,} \quad (68)$$

$$K_{Hb} F_{Hb} \div b c_w G_H = (2.30)(1)(118) = 271 \text{ kcal/h}^\circ\text{C,}$$

$$Q_H = K_{Hb} F_{Hb} (t_{Hb} - t_H) = 271(59.5 - t_H) = 16125 - 271t_H \text{ kcal/h,} \quad (69)$$

where  $G_H$  is the weight of the water contained in the heating tank ( $G_H = 118 \text{ kg}$ ) and its initial temperature  $t_{H0} = 12.6^\circ\text{C}$ . The maximum recovery efficiency  $(\eta_{rec})_{max}$  is 0.923–0.562 for this system and 27600–17500 kcal/h can be recovered by this system. The results of No. 1 experiment are shown in Fig. 50.

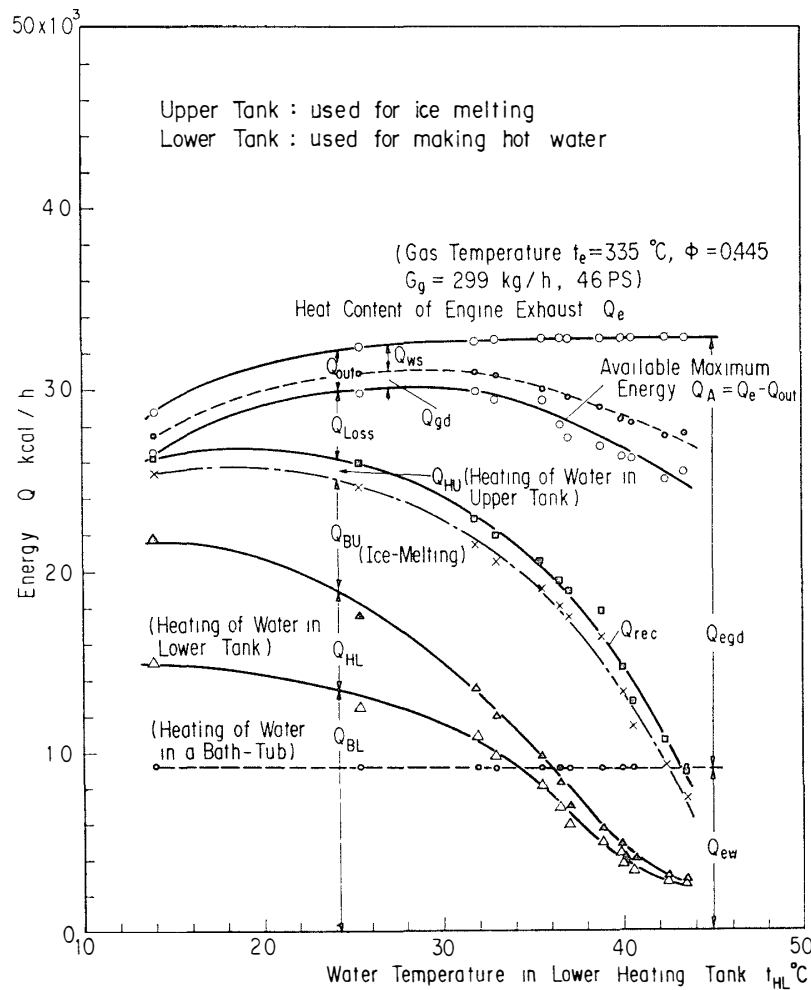


Fig. 51. Results of experiment No. 2 on a BE-1 bubble type exhaust-gas heat exchanger.

In No. 2 experiment, the upper heating tank (HU) system was used for making cold water by melting an ice block of  $G_I = 51.3$  kg floating on the water of  $G_w = 148.7$  kg at  $8.0^\circ\text{C}$ . On the other hand, the lower heating tank (HL) system was used for making hot water by heating the water  $G_B = 210.9$  kg in a bathtub.

In the upper heating tank system, a recirculating pump P-1 fed the hot water from the upper heating tank to a radiator submerged in the ice-melting tank at a rate of 6430 kg/h. After one hour, the water temperature increased from  $8.0^\circ\text{C}$  to  $24.9^\circ\text{C}$  and the ice block was completely melted.

The heat absorbed during one hour was as follows:

$$\begin{aligned} Q_{BU} &= c_w G_w (t_{w2} - t_{w1}) + G_I (80 + t_{w2}) \\ &= (1)(148.7)(24.9 - 8.0) + 51.3(80 + 24.9) = 2513 + 5381 = 7894 \text{ kcal/h.} \end{aligned}$$

During one hour, the water contained in the upper heating tank was also heated from  $10.5^\circ\text{C}$  to  $30.5^\circ\text{C}$ . The weight was  $G_{HU} = 56.3$  kg, so that

$$Q_{HU} = c_w G_{HU} (t_{HU2} - t_{HU1}) = (1)(56.3)(30.5 - 10.5) = 1126 \text{ kcal/h.}$$

Hence,

$$Q_{BU} + Q_{HU} = 7894 + 1126 = 9020 \text{ kcal/h.}$$

On the other hand, in the lower heating tank system, the temperature of the hot water in the other bathtub was represented by

$$t_{BL} = t_{Rm} - (t_{Rm} - t_{BL0})e^{-b\tau} = 46.4 - (46.4 - 7.7)e^{-1.83\tau} = 46.4 - 38.7e^{-1.83\tau} \text{ } ^\circ\text{C,}$$

$$K_R F_R = b c_w G_B = (1.83)(1)(210.9) = 386 \text{ kcal/h}^\circ\text{C,}$$

$$Q_{BL} = K_R F_R (t_{Rm} - t_{BL}) = 386(46.4 - t_{BL}) = 17910 - 386t_{BL} \text{ kcal/h.}$$

At the same time, the water contained in the lower heating tank of  $G_{HL} = 61.5$  kg was heated from  $t_{HL0} = 8.5^\circ\text{C}$  to  $41.6^\circ\text{C}$  after one hour.

$$t_{HL} = t_{Hb} - (t_{Hb} - t_{H0})e^{-b\tau} = 41.6 - (41.6 - 8.5)e^{-3.5\tau} = 41.6 - 33.1e^{-3.5\tau} \text{ } ^\circ\text{C,}$$

$$K_{Hb} F_{Hb} = b c_w G_{HL} = (3.5)(1)(61.5) = 215 \text{ kcal/h}^\circ\text{C,}$$

$$Q_{Hb} = K_{Hb} F_{Hb} (t_{Hb} - t_{HL}) = 215(41.6 - t_{HL}) = 8944 - 215t_{HL} \text{ kcal/h.}$$

In the lower heating tank system,  $Q_{BL} + Q_{Hb}$  can be absorbed. The available maximum recovery efficiency  $(\eta_{rec})_{max} = 0.906 - 0.773$ , which is better than in experiment No. 1 because the temperature  $t_{HU}$  is lower than that of experiment No. 1. The experimental results are shown in Fig. 51.

## 9. Heat Exchangers for Recovering Coolant Heat of Diesel Engines

### 9.1. Horizontal shell-and-tube type heat exchangers

For JARE-7 (1965/67), the authors developed a horizontal shell-and-tube type heat exchanger for recovering coolant waste heat from diesel engines driving 45-kVA electric generators. General views are shown in Fig. 52, and the design data are given in Table 11. Two sets of the coolant-to-water heat exchangers

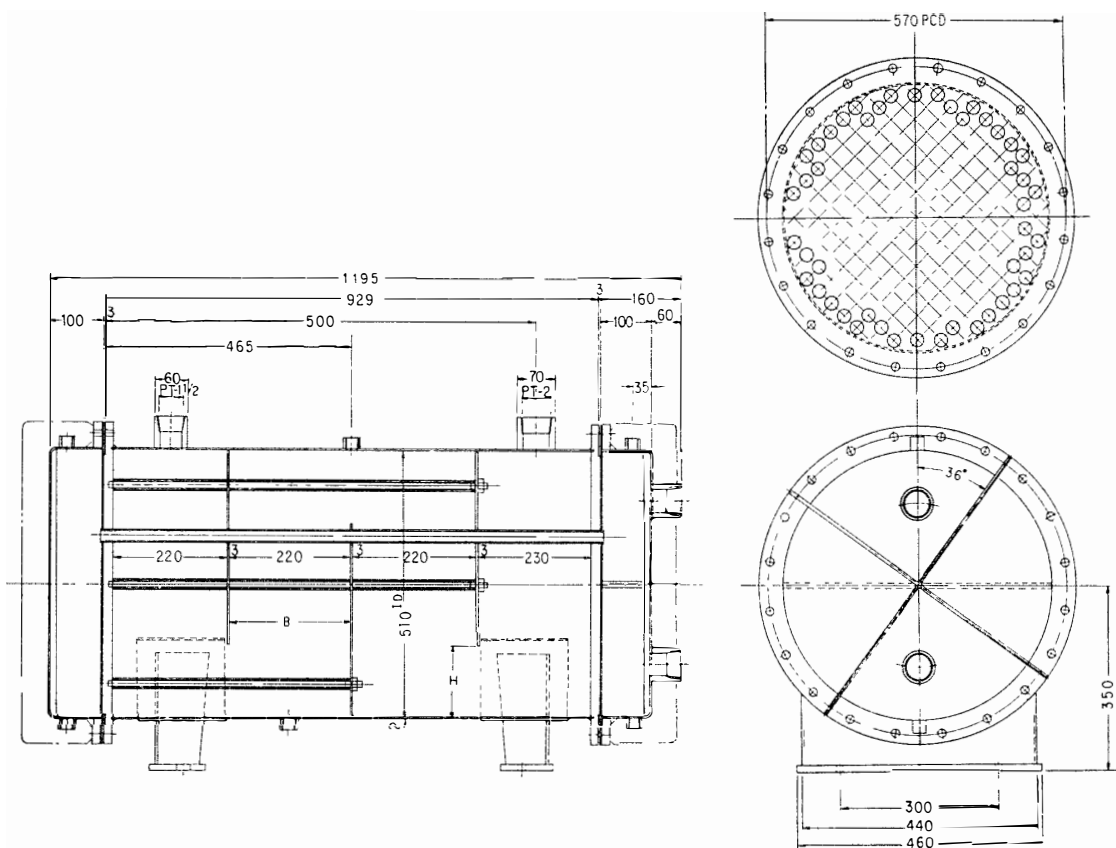


Fig. 52. Horizontal shell-and-tube type heat exchanger prepared for JARE-7 (1965/67) to recover coolant heat of diesel engine.

Table 11. Shell-and-tube type coolant heat recovery heat exchangers and secondary heat exchanger prepared for JARE.

Items	JARE-7 (1965/67)	JARE-10 (1968/70)	JARE-13 (1971/73)- JARE-20 (1978/80)
Capacity $Q_c$ (kcal/h) Type Purpose	50000 horizontal coolant heat recovery (45 kVA)	60000 horizontal coolant heat recovery (65 kVA)	45000 vertical secondary heat exchanger
Shell side			
Shell			
Material	SUS-28	SUS-32	SUS-28TPA
Outer diam. (mm)	515	506	165.2 (6B)
Inner diam. (mm)	510	500	158.4
Total length (mm)	1255	1836	1179
Center height (mm)	350	350	—
Liquid ( $t_{o1}$ , $t_{o2}$ °C)	coolant (80, 74)	cold water (65, 70)	cold water (12, 16)
Tube plate			
Material	SUS-28	SUS-32	SUS-28
Outer diam. (mm)	610	655	265
Thickness (mm)	18	22	22
Pipe arrangement	square	triangle	triangle
Pitch $P_t$ (mm)	32	34	23
Number of tubes $Z$	164	146	26
Baffle plate			
Number $N$	3	7	5
Thickness	3	3	3
Distance	220×3+230	179×7+176	160×5+173
Equivalent diam. of tube space $D_e$ (mm)	27.2	26	14.4
Effective flow area $a_s$ (m <sup>2</sup> )	0.02482	0.02396	0.00539
Flow rate (l/min)	160	200	200
(kg/h)	9600	12000	12000
Flow velocity $w_o$ (m/s)	0.1035	0.1426	0.618
Reynolds number $Re$	7163	8897	7119
Baffle-cut ratio $A/D_s$	0.278	0.263	0.242
Nusselt number $Nu$	58.1	69.5	95.8
Heat transfer coefficient $\alpha_o$ (kcal/m <sup>2</sup> h°C)	1227	1526	3380
Temperature efficiency $\Phi_o$	0.404	0.328	0.0556
Pipe diameter	2B	2B	1B
Tube side			
Material	SUS-28TPS	SUS-32TPS	SUS-28TB
Outer diam. $d_o$ (mm)	25	25	18



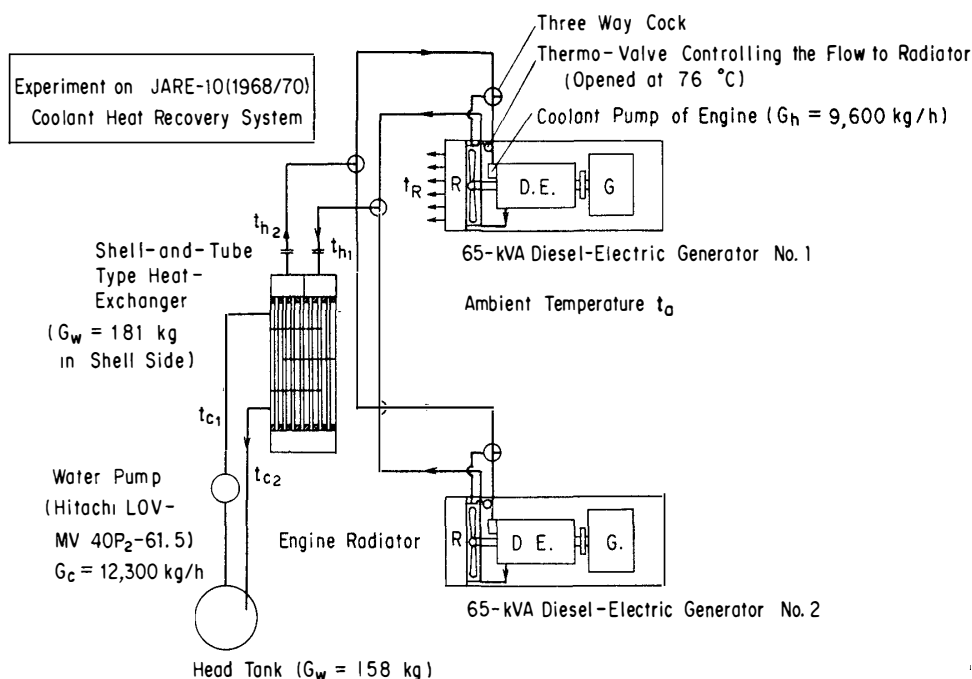


Fig. 54. Experiment on the horizontal shell-and-tube type heat exchanger prepared for JARE-10 (1968/70) to recover coolant heat of diesel engine. Experiment was carried out at Nakajima Denki Co., Ltd. in November 1968. The results are shown in Table 12.

JARE-7 engine room. The hot water was fed to the living quarters and to a bathtub.

For JARE-10 (1968/70), the same type horizontal heat exchanger, but with slightly larger heating capacity, was manufactured and installed in the JARE-9 engine room and was used for absorbing the coolant heat of a diesel engine driving a 65-kVA electric generator (Figs. 53, 54; Table 12). The hot water was stored in another hot-water tank installed in the JARE-9 engine room and used for room-heating in the living quarters of the JARE-9 engine room (Fig. 16).

For JARE-19 (1977/79), engine power was increased for driving the 110-kVA electric generator, and the waste heat recovering system was also rearranged from that shown in Fig. 16 to that in Fig. 18.

The engine coolant of the 110-kVA engine was recirculated through a head-tank installed near the engine, and the coolant in the headtank was fed to a horizontal heat exchanger installed in the JARE-7 engine room, which was separated from the JARE-9 engine room by about 40 m, and also to a radiator submerged in a 10 k/ snow melting tank installed outdoors and returned again to the head-tank. The hot water heated by the horizontal heat exchanger was stored in the hot-water tank of the JARE-7 engine room and supplied to a bathtub and the living quarters.

Another horizontal heat exchanger was used as a secondary heat exchanger in

Table 12. Results of experiments on the performance of horizontal shell-and-tube coolant-to-water heat exchanger for recovering coolant energy of diesel engine prepared for JARE-10 (1968/70).

Run No.	Time	Condition	V	I (A)	kVA	kW	$t_{g1}$	$t_{h1}$	$t_{h2}$	$\Delta t_h$	$t_{c1}$	$t_{c2}$	$\Delta t_c$	$t_R$	$t_a$	$\Delta t_R$	$Q_R$ (kcal/h)	
1	10 00	Engine starts	200	0	2	1.6	—	—	—	—	—	—	—	13.8	11.0	2.8	3500	
2	10 10	Without H. Ex., water pump off	200	75	15	12	170	74.0	—	—	—	—	—	15.5	—	—	—	
3	10 15	With H.Ex., W.P. off	200	100	20	16	235	78.5	—	—	—	—	—	29.5	13.5	16.0	20000	
4	10 20		200	125	25	20	292	78.5	—	—	—	—	—	34.6	13.2	21.4	26800	
5	10 25		200	150	30	24	341	79.0	—	—	—	—	—	37.6	14.1	23.5	29400	
6	10 31		200	150	30	24	348	78.0	—	—	—	—	—	18.0	13.8	4.2	5260	
7	10 41		200	150	30	24	348	78.0	—	—	—	—	—	18.2	15.1	3.1	3900	
8	10 55		200	150	30	24	351	78.8	63.0	15.8	—	—	—	19.8	16.1	3.7	4600	
9	11 03		Thermo-valve to radiator opened	200	150	30	24	353	81.8	76.0	5.8	—	—	—	20.0	17.0	3.0	3800
10	11 08		200	150	30	24	353	82.3	78.0	4.3	—	—	—	34.1	16.8	17.3	21700	
11	11 12		With H.Ex., W.P. in	200	150	30	24	—	—	—	—	—	—	—	—	—	—	—
12	11 18		200	150	30	24	333	78.0	59.5	18.5	61	63	2	19.7	16.5	3.2	4000	
13	11 23	200	150	30	24	349	79.5	66.2	13.3	66	68	2	20.7	17.5	3.2	4000		
14	11 28	200	150	30	24	353	80.0	71.0	9.0	71	73	2	20.3	17.1	3.2	4000		
15	11 33	Thermo-valve to radiator opened	200	150	30	24	353	81.5	75.8	5.7	75	77	2	21.3	16.5	4.8	6000	
16	11 45	200	150	30	24	323	82.3	78.5	3.8	78.5	80	1.5	20.8	16.5	4.3	5400		
17	11 49	Engine stopped	200	150	30	24	—	—	—	—	—	—	—	—	—	—	—	

1) Isuzu ZX-75 Type 65-kVA, diesel engine Isuzu DA-640T, turbocharged, 6373 cc.  $N=1500$  rpm. 2) Engine coolant was led to tube side of heat exchanger  $G_h=9600$  kg/h (160 l/min). 3) Cold water to be heated circulated by water pump (Hitachi LOV-MV), measured flow rate  $G_c=12300$  kg/h (205 l/min). 4) Cooling air flow rate to engine radiator  $G_{Ra}=\gamma_a w_a A_R=(1.192)(3.13)(3600)(0.3878)=5215$  kg/h,  $Q_R=c_{pa} G_{Ra} \Delta t_R=0.24(5215) \Delta t_R=1252 \Delta t_R$  kcal/h. 5) Recovered heat  $Q_c=c_w G_c \Delta t_c=12300 \Delta t_c=24600$  kcal/h, heating area  $F_o=17.20$  m<sup>2</sup>. 6) Run No. 1 to Run No. 10 were preliminary running, and Run No. 11 to No. 17 were normal running state with cooling water pump running. 7)  $t_{h1}$ : Coolant inlet temp., °C,  $t_{h2}$ : Coolant outlet temp., °C,  $t_{c1}$ : Water inlet temp., °C,  $t_{c2}$ : Water outlet temp., °C,  $t_R$ : Delivery air temp. from radiator, °C,  $Q_R$ : Heating load of radiator.

the exhaust energy recovering system as shown in Fig. 18. For preventing severe corrosion of exhaust-gas heat exchangers, the water temperature should be kept as high as possible. For this purpose, the horizontal heat exchanger was used as a secondary heat exchanger. In the secondary water-to-water heat exchanger, the heat recovered from the exhaust gas was transferred again to the secondary hot water with a lower temperature than the primary water. The secondary hot water was supplied to eight radiators for room-heating in the living quarters of the JARE-9 engine room. A fan-coil unit radiated 4500 kcal/h of heat. During JARE-20 (1978/80), the waste heat recovery system was rearranged again from that shown in Fig. 18 to that in Fig. 19. In this system, the horizontal heat exchanger, which had been used as a secondary heat exchanger in the exhaust-gas energy recovering system was removed because the hot-water tank in the JARE-9 engine room could supply hot water directly to the exhaust-gas heat exchanger, but the horizontal coolant-to-water heat exchanger in the coolant-heat recovery system has been retained until now.

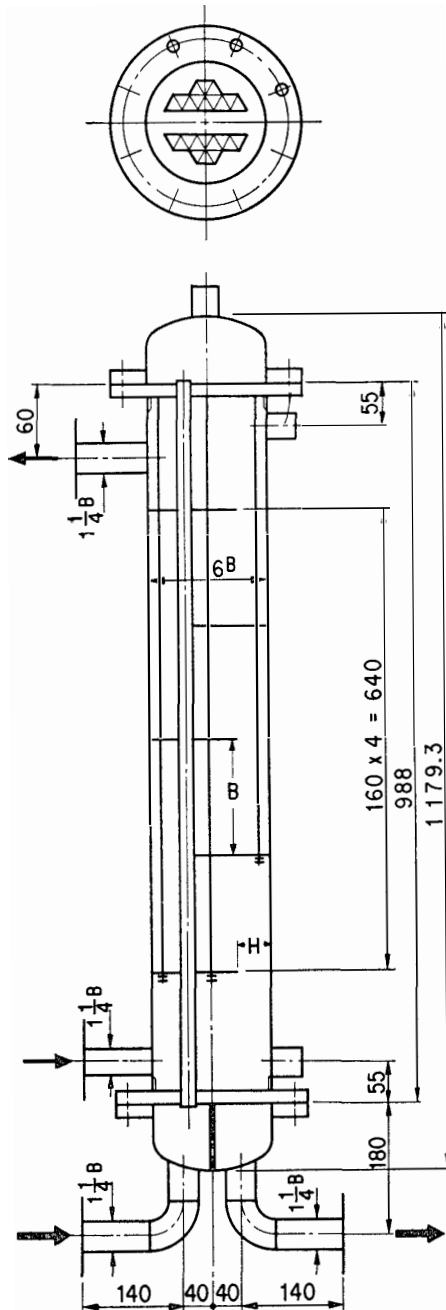


Fig. 55. Vertical shell-and-tube type heat exchanger prepared for JARE-13 (1971/73) as the secondary water-to-water heat exchanger to recover exhaust-gas energy of diesel engine.

## 9.2. Vertical shell-and-tube type water-to-water secondary heat exchanger

For two reasons, the first to protect the heating surface of exhaust-gas heat exchangers from acid corrosion, and the second to remove the radiators submerged in the 130-k/ outdoor cold-water reservoir tank and in the 10-k/ snow-melting tank, a small vertical shell-and-tube type heat exchanger as shown in Fig. 55 was developed by the authors for JARE-13 (1971/73).

Hot water receives heat during its flow through the coil of an exhaust-gas heat

exchanger and is led to the inside of tubes of a vertical water-to-water heat exchanger to warm the cold water of shell side, which recirculates to outdoor water tanks.

This process has been used effectively since JARE-13 up to the present to keep the water in outdoor tanks from freezing.

### 9.3. Estimation of thermal performance of a shell-and-tube heat exchanger

Thermal performance can be estimated by the following method:

Symbols;

- $Q_c$ : recoverd coolant heat, kcal/h,
- $t$ : temperature of water, °C,
- $G$ : flow rate of water, kg/h,
- $F_o$ : total outer heating area, m<sup>2</sup>,
- $d$ : diameter of tubes, m,
- $z$ : total number of tubes,
- $l$ : length of a tube, m,
- $A_i$ : total inner sectional area of tubes, m<sup>2</sup>,
- $D_s$ : inner diameter of shell, m,
- $N$ : number of baffle plates,
- $H$ : height of baffle cut, m,
- $B$ : distance between to baffle plates, m,
- $D_e$ : equivalent diameter for flow at the outside of tubes, m,
- $\alpha$ : heat transfer coefficient, kcal/m<sup>2</sup>h°C,
- $K_o$ : overall coefficient of heat transmission, kcal/m<sup>2</sup>h°C,
- $\Delta t_{lm}$ : logarithmic mean temperature difference, °C,
- $V$ : volume flow rate, m<sup>3</sup>/s,
- $a_s$ : area of minimum flow among three tubes (triangle arrangement) or four tubes (square arrangement), m<sup>2</sup>,
- $\delta_M$ : thickness of tube wall, m,
- $\lambda_M$ : thermal conductivity of tube material, kcal/mh°C,
- $\Phi$ : temperature efficiency,
- $w$ : velocity, m/s,
- $\nu$ : kinematic viscosity, m<sup>2</sup>/s,
- $R_e$ : Reynolds number,  $R_e = wD_e/\nu$ ,
- $P_r$ : Prandtl number,
- $Nu$ : Nusselt number,  $Nu = \alpha D_e/\lambda$ ,
- $\lambda$ : thermal conductivity of water, kcal/mh°C,
- $c$ : specific heat of water, kcal/kg°C

Subscripts;

$i$ : inside of tubes,     $o$ : outside of tubes,  
1: inlet,                    2: outlet.

In a steady state, the following equations of heat balance should be satisfied:

$$Q_c = c_i G_i (t_{i1} - t_{i2}) = c_o G_o (t_{o2} - t_{o1}) \text{ kcal/h,} \quad (70)$$

$$\Phi_i = (t_{i1} - t_{i2}) / (t_{i1} - t_{o1}), \quad (71)$$

$$\Phi_o = (t_{o2} - t_{o1}) / (t_{i1} - t_{o1}). \quad (72)$$

Substituting eqs. (71) and (72) into (70), we get (JSME, 1966)

$$Q_c = c_i G_i \Phi_i (t_{i1} - t_{o1}) = c_o G_o \Phi_o (t_{i1} - t_{o1}) \text{ kcal/h.} \quad (73)$$

The heat transfer coefficient of water flowing through the tubes is given by

$$(Nu)_i = 0.023 (R_e)_i^{0.8} (Pr)_i^{0.4} = \alpha_i d_i / \lambda_i, \quad (74)$$

and the heat transfer coefficient of flow outside of the tubes can be estimated by LYDERSEN (1979)

$$(Nu)_o = 0.224 (R_e)_o^{0.537} (H/D_s)^{-0.4} (Pr)_o^{1/3} = \alpha_o D_e / \lambda_o. \quad (75)$$

In this equation, the equivalent diameter  $D_e$  for the flow across the tube bank can be represented by

(for triangle arrangement with pitch  $P_t$ )

$$D_e = [2\sqrt{3} P_t^2 / (\pi d_o)] - d_o \text{ m,} \quad (76)$$

and

(for square arrangement with pitch  $P_t$ )

$$D_e = [4P_t^2 / (\pi d_o)] - d_o \text{ m.} \quad (77)$$

The velocity  $w_e$  past the tube bank in, or closest to, the center is

$$w_e = V_o / a_s \text{ m/s,} \quad (78)$$

where

$$a_s = (D_s / P_t) (P_t - d_o) B \text{ m}^2, \quad (79)$$

which is the minimum area between two tubes of a flow passage.

The Reynolds number of flow at the outside of tubes is calculated by

$$(R_e)_o = w_e D_e / \nu_o. \quad (80)$$

The overall coefficient of heat transmission  $K_o$  is given as the reciprocal of the total heat resistance of the heat flow through tube wall.

$$K_o = 1/\sum R \text{ kcal/m}^2\text{h}^\circ\text{C}, \quad (81)$$

$$\sum R = (1/\alpha_i)(d_o/d_i) + (1/\alpha_o) + (\delta_M/\lambda_M) \text{ m}^2\text{h}^\circ\text{C/kcal}, \quad (82)$$

and the heat recovered by this heat exchanger is given by

$$Q_c = K_o F_o \Delta t_{lm} \text{ kcal/h.} \quad (83)$$

An example of calculation on the vertical shell-and-tube type water-to-water heat exchanger is shown in Appendix 4. The results of calculations concerning the three kinds of water-to-water heat exchangers are shown in Table 11.

## 10. Coolant Heat Recovery System at Mizuho Station

Mizuho Station was established on continent ice at  $70^{\circ}41'53''\text{S}$  and  $44^{\circ}19'54''\text{E}$  at an elevation of 2230 m, about 270 km inland from Syowa Station, for meteorology and glaciology investigations including the deep core drilling of continental ice.

The weather at Mizuho Station is more severe than that at Syowa Station. In 1978, the observed yearly mean maximum, mean and minimum air temperatures were  $-27.7^{\circ}\text{C}$ ,  $-31.7^{\circ}\text{C}$  and  $-36.0^{\circ}\text{C}$ , respectively, and the yearly mean values of monthly maximum and mean wind velocities were 19.8 m/s and 10.1 m/s, respectively.

JARE-11 built a semi-tubular corrugated steel hut ( $8.5 \times 3.2$  m) in 1970. A living hut ( $19.4 \text{ m}^2$ ) made of prefabricated aluminum panels and three trench rooms, *i. e.*, a glaciology laboratory ( $3.6 \times 3.6$  m), an ice-boring room ( $3.8 \times 4.8$  m), and an engine room ( $4.3 \times 6.8$  m) were added in 1971.

In the trench engine room, a caboose containing a 12-kVA diesel-electric generator (ZX-500B type, 3 phase, 200 V, 50 Hz, Isuzu 221 type diesel engine, 2207 cc) was installed as the main electric power plant.

A coolant heat recovery system for the 12-kVA diesel-electric generator was designed and tested by the authors in 1970 in Tokyo. It was transported to Mizuho Station set as shown in Fig. A-4 in Appendix and operated successfully. The engine ran continuously for 1593 hours from October 1971 to January 1972, consuming 5.4 kJ fuel.

As the engine coolant, 30–50% aqua-solution of ethylene glycol was used to prevent freezing when the engine is stopped. The coolant was bypassed to the headtank installed near the engine and returned directly to the inlet of the engine coolant pump. The hot coolant in the headtank was fed to a tube type heat exchanger submerged in a stainless-steel snow-melting tank (capacity 200 l) and also to a fin-tube type aluminum radiator (measuring  $520 \times 405 \times 98$  mm, fin area  $7.5 \text{ m}^2$ , tube area  $1.9 \text{ m}^2$ ) submerged in a bathtub for heating water and returned to the headtank by a recirculating pump (AC 200 V, 500 W, flow rate 450 l/min). The test results in Tokyo and at Mizuho Station are shown in Tables A-9 and

A-10 in Appendix 5. In the experiment in Tokyo, an exhaust-gas energy recovering system using a shell-and-coil heat exchanger was also examined, but only 4000 kcal/h of the exhaust-gas energy was recovered. This was because of the low gas velocity in the heat exchanger, due to the low flow rate of gas which was only 100 kg/h exhausted from the small engine.

In contrast, the recovered coolant heat reached 15000–20000 kcal/h and was sufficient for supplying heat to three fan-coil units (the capacity of one unit being 4350 kcal/h). For this reason, the coolant heat recovering system at Mizuho Station was utilized only for making washing water by melting snow blocks and also for heating water in the bathtub, but the room-heating system was not put into operation until JARE-17 (1975/77). For heating the living room, a pot-type oil stove was used and drinking water was made by melting snow in a vessel put on the stove. About 10–20 l of kerosene was consumed daily in the oil stove.

In JARE-15 (1973/75), a new observation hut (22.5 m<sup>2</sup>), a trench ice-boring room (17.4 m<sup>2</sup>), and a new trench engine room (15.5 m<sup>2</sup>) were added. The 12-kVA diesel-electric generator was operated only from 15 May 1974 to 2 June 1974 for test running and also from 22 November 1974 to 22 January 1975 for deep ice-boring. Accordingly, the heat-recovery system was also used only during these periods. The total fuel consumption for the 12-kVA diesel was 20 drums, corresponding to 50–57.4 l/day.

Unfortunately, on 29 January 1975, a fire occurred in the trench engine room housing the 12-kVA set. The engine, the coolant heat recovery system, the electric power generator, and other equipment were destroyed. The cause of the accident has not yet been clarified. The camp was used temporarily by JARE-16 (1974/76).

In May 1976, Mizuho Station was reopened with two engine rooms, one for a 16-kVA diesel-electric generator (3-phase, 200 V, 50 Hz, C240 type Isuzu diesel) as an emergency plant and another for a 12-kVA diesel-electric generator (3-phase, 200 V, 50 Hz, DX-500B, C220 type Isuzu diesel) for continuous operation. Until January 1977, the 12-kVA set was operated 6600 h and consumed fuel at a rate of 60–65 l/day, engine oil 1 l/day, and antifreezing liquid 0.6 l/day.

The same coolant heat recovery system as in JARE-12 was prepared again for each of the two diesel-electric generators, and moreover a hot-water heating system using the coolant heat was utilized in a living room and an observation room. A fan-coil unit (single phase, 100 V, 40 W, Hitachi PF-200 type, capacity 4350 kcal/h) was installed for each, and the room temperature was kept between 10°C and 20°C without any other furnaces. The temperature of another observation room had been kept at 20°C by using a 1.5 kW panel heater, but it was replaced by an electric heating source powered by a windmill, as well as warm air transferred from the adjoining electrical instrument observation room by a fan

Table 13. Fuel consumptions in Mizuho Station.

Items	JARE-17 (1975/77)	JARE-18 (1976/78)	JARE-19 (1977/79)
Main engine generators (kVA)	12	12	16
Spare engine generators (kVA)	16	16	12
Yearly mean load (kW)	2.45	2.4	2.6
Maximum peak load (kW)	5.5	4.7	6.3
Number of wintering members	4	4	4
Duration of wintering	29 April 1976 26 Jan. 1977	27 Jan. 1977 1 Feb. 1978	2 Feb. 1978 16 Jan. 1979
Days of wintering (days)	242	371	349
Antarctic gas oil (l)	20300	21600	19000
Antarctic kerosene (l)	5800	600	130
Kerosene (l)	0	0	0
New antarctic engine oil (l)	330	310	420
Antifreezing liquid (l)	270	270	300
Gasoline (l)	0	0	22
Total (l)	26700	22780	19872

at the end of November 1976 (SHIGA, 1977). In the coolant heat recovery system, the engine radiator was removed and all of the hot coolant was conducted to a 60 l headtank, but the other parts of the system remained as before. A pot-type oil heater was installed in the living room, but it was used only for melting snow to make drinking water. The total quantities of fuel consumed in Mizuho Station are shown in Table 13.

During 1977/78, a new research room (18.2 m<sup>2</sup>), a storage hut for machinery, a 1-kVA engine room (4.7 m<sup>2</sup>), and a garage for a snowmobile (7.3 m<sup>2</sup>) were newly built. The 12-kVA and 16-kVA diesel-electric generators were operated 15640 h and 103 h respectively, without any trouble. The 16-kVA engine room was kept at 30°C by coolant heat of the 12-kVA engine and thus readied for easy starting in an emergency. Drinking water was also supplied by the snow-melting tank. The coolant heat recovery system not only saved much fuel (assumed saving 10–13 kl during 278 days) but ensured the safety of the wintering. By this system, the room temperatures of the living and observation rooms were kept between +15°C and +20°C without the aid of other heating sources, although the air temperature of the passage in the trench was –20°C ~ –30°C. During 1978/79, the 16-kVA diesel-electric generator was used as the main source of electricity, and the 12-kVA set was reserved for emergency use. The coolant heat recovery system remained as in the previous year.

Under ordinary conditions, the temperature of the coolant returned to the engine was about 5°C lower than the outlet temperature from the engine. But

the returned coolant temperature was 20–30°C lower than the outlet temperature when a snow block was thrown into the snow-melting tank as shown in Fig. A-5 in Appendix 5, as observed by Mr. TAGA. The extremely low coolant temperature occasionally caused incomplete combustion in the diesel cylinder, some lowering of engine speed, and some diesel knock. These defects were avoided by providing an automatic thermo-valve, which opened at 65°C, on the delivery side of the engine coolant system.

To keep the room air clean, the engine exhaust gas should be conducted to the outside atmosphere through a chimney which was occasionally buried in the deep snow. The snow around the chimney and snow falling on the chimney melted and drained into the engine room through a gap formed around the chimney.

To prevent the drain immersion, an empty drum, its two end plates cut off, was installed around the chimney to prevent snow from hitting the hot chimney directly.

On a part of the exhaust port of the diesel engine, a slight crack was observed. This was probably due to thermal stress caused by contact with the reversed flow of cold air through the chimney. It is advisable to use an exhaust fan which is capable of exhausting hot gases even in blizzards.

Monthly mean and peak electric loads during 1978/79 were 2–3 kW and 3–5.8 kW respectively, and fuel and oil consumption by the 16-kVA set was 48–62 l/day and 0.8–1 l/day, respectively.

## 11. Conclusions

The authors have been involved in the matter of the Antarctic logistics from 1956 to the present and experienced many interesting problems in the special field of engineering in Antarctica. At the start of JARE-1, the Special Committee on Mechanical Engineering, in which one of the authors was included, proposed unifying the fuel to diesel fuel and the main prime mover to diesel engines to save fuel and avoid fire accidents. According to this proposal, diesel engine of the same type was used for the electric generators and snow vehicles.

At the same time, the authors planned and manufactured some fuel-saving systems by utilizing the coolant heat and exhaust-gas energy of the diesel engines driving electric generators as much as possible.

At Syowa Station, the waste heat of the diesel engines, the capacity of which were increased from 20-kVA during JARE-1 to 110-kVA during JARE-19, was fully utilized. For these purposes, many types of exhaust-gas heat exchangers and coolant-heat recovering devices, a snow-melting tank, a hot-water tank, a bathtub, a cold-and-hot water feeding pipe, and a hot-water room-heating system were developed by the authors. By these systems, about 20–30 kl/year of gas oil has been saved at the present.

At Mizuho Station, coolant heat recovery systems for the 12-kVA diesel-electric generator were prepared by the authors. During JARE-15, 1-kVA gasoline engine electric generators were mainly used and a 12-kVA diesel-electric generator was also operated supplementally. Unfortunately, a fire hazard destroyed the 12-kVA engine room, while it was running, and all of the heat recovery systems, so that the camp was unmanned but was used occasionally by JARE-16.

By JARE-17, Mizuho Station was reopened and enlarged, and 12-kVA and 16-kVA diesel electric generators and coolant heat recovery systems were prepared again in the new trench engine rooms. The coolant heat of the diesel engines was supplied not only to a snow-melting tank and a bathtub, but also to fan-coil units in the living and observation rooms. The heat supplied was about 12000 kcal/h, and the room temperature has been held at  $+10^{\circ}\text{C}\sim 20^{\circ}\text{C}$  without any other furnace. With this system at Mizuho Station, about 10–13 kl/year of gas oil has

been saved, and the safety of wintering members in the trench rooms has been assured.

From the experiences during the past 24 years, the following conclusions can be derived:

(a) As the main power source of an antarctic station, a diesel-electric generator is most advisable and gas oil is the safest fuel. The starting of a diesel engine is easier than that of a gasoline engine, especially in cold weather below  $-30^{\circ}\text{C}$ .

However, for starting a diesel engines exposed for a long period to the cold of  $-30^{\circ}\text{C}$ , it was necessary to preheat it by a master heater. It is advisable to keep the emergency engine room above  $+30^{\circ}\text{C}$  at all times.

(b) The coolant heat from diesel engines can be easily recovered, and the quantity of heat is large and stable at any engine load.

(c) The recovery of exhaust-gas energy from diesel engines is more difficult than that of the coolant heat because of the acid corrosion of heating surfaces in heat exchangers and gradual lowering of the recovery efficiency with the increase of carbon soot adhering to the heating surface.

(d) It is most important to increase the gas velocity flowing through an exhaust-gas heat exchanger to increase its heating capacity.

(e) In an exhaust-gas heat exchanger, thermal stress should be prevented in the shell surface of the entrance chamber for hot gas. Maximum thermal stress may occur on a part of the shell against which the inlet hot gas-jet impinges.

(f) To prevent acid corrosion of the heating surfaces of an exhaust-gas heat exchanger, the water temperature should be as high as possible, at least  $50^{\circ}\text{C}$ . For this purpose, a secondary water-to-water heat exchanger is very effective, *i.e.*, cold water should not be heated directly.

(g) Fin-tube type exhaust-gas heat exchangers made of aluminum alloys were developed, which can resist acid corrosion, because of the high temperature of their heating surfaces.

(h) A new bubble type heat exchanger for recovering exhaust-gas energy was developed. The bubble surface itself forms the heating surface, so that the problems of acid corrosion and soot fouling can be overcome completely, and the rate of heat transfer from the bubble to water is very great, but the outlet gas contains much steam vapor.

(i) A new method of estimating the heating capacity and overall coefficient of heat transmission of a heat exchanger from the temperature-time curve of water in a heated bathtub has been introduced.

(j) By means of a waste heat recovering system, about 30–40 kJ/year of fuel can be saved at Syowa and Mizuho Stations.

**Acknowledgments**

The authors wish to thank Dr. E. NISHIBORI, Mr. M. MURAYAMA, Mr. N. MURAKOSHI of JARE, Dr. M. KAWADA and all members of Special Committee on Mechanical Engineering of JSME, and the members of the Machine Shop of Nihon University, for their co-operation in producing the fuel saving systems utilizing waste heat of diesel-electric generators, and also the many wintering members of JARE-1/20 who devoted their efforts to realization and operation of the system successfully in the cold of Antarctica.

The authors are deeply indebted to Isuzu Automobile Industrial Co., Ltd., Meidensha Co., Ltd. and Nakajima Denki Co., Ltd. for preparing the diesel-electric generators and for the testing of them, and especially to Kotobuki Tekkosho for co-operation in designing and manufacturing the heat exchangers. The authors are also deeply grateful for the financial aid rendered by the Ministry of Education, Science and Culture, and by Nihon University.

## References

- AWANO, S. and MAITA, S. (1963): Cold and hot water making equipment utilizing the exhaust-gas energy of diesel engines coupled with electric generators. Symposium on Antarctic Logistics, ed. by National Academy of Sciences-National Research Council, Washington, D.C., 254-280.
- BOŠNJAKOVIĆ, F., VILIČIĆ, M. and SLIPČEVIĆ, B. (1951): Berechnung von Rekuperatoren. VDI-Forschungsh., **432**(17), 1-26.
- ISHIWATA, S., INOUE, M., TAKEUCHI, S. and MAEDA, Y. (1970): Kikai·nenryô. Nihon Nankyoku Chiiki Kansokutai Dai-10-ji Ettôtai Hôkoku 1968-70 (Report of the Wintering Party of the 10th JARE 1968-1970). Tokyo, Nankyoku Chiiki Kansoku Tôgô Suishin Honbu (Headquarters JARE), 135.
- JAPAN SOCIETY OF MECHANICAL ENGINEERS (1966): Heat Transfer JSME Data Book, 2nd ed, Tokyo, 27, 264.
- LYDERSON, A.L. (1979): Fluid Flow and Heat Transfer. New York, J. Wiley, 241.
- OKAMOTO, Y., KANEKO, S., KAKINO, T. and OHIRA, H. (1971): Kikai. Nihon Nankyoku Chiiki Kansoku Dai-11-ji-tai Hôkoku 1969-1971 (Report of the 11th JARE 1969-1971). Tokyo, Nankyoku Chiiki Kansoku Tôgô Suishin Honbu (Headquarters JARE), 226-252.
- SATO, K. (1967): Zôsui oyobi kyû-haisui setsubi. Nihon Nankyoku Chiiki Kansokutai Dai-7-ji Ettôtai Hôkoku 1966-1967 (Report of the Wintering Party of the 7th JARE 1966-1967). Tokyo, Nankyoku Chiiki Kansoku Tôgô Suishin Honbu (Headquarters JARE), 139-144.
- SHIGA, S., KASABA, K., TAKAHASHI, S. and MITSUYAMA, S. (1977): Kikai. Nihon Nankyoku Chiiki Kansokutai Dai-17-ji-tai Hôkoku 1975-1977 (Report of the 17th JARE 1975-1977). Tokyo, Kokuritsu Kyokuchi Kenkyûjo (Nat'l Inst. Polar Res.), 148-153.
- SPECIAL COMMITTEE ON ENGINEERING FOR THE JARE OF JAPAN SOCIETY OF MECHANICAL ENGINEERS AND TECHNICAL MEMBERS OF THE FIRST, SECOND AND THIRD JARE (1959): Report of the Mechanical Engineering Committee for the Japanese Antarctic Research Expedition. Nankyoku Shiryô (Antarct. Rec.), **8**, 57-128.

*(Manuscript received October 18, 1980; Revised manuscript received March 10, 1981)*

## APPENDIX I

**1.1. Experiments on a piping unit prepared for JARE-7 to feed hot and cold water**

The piping unit as shown in Fig. 9a was tested by the authors in the low temperature testing room of the Research Institute of Transportation Technology in August 1965. The equipment for testing is shown in Fig. A-1. The room temperature was kept at about  $-20^{\circ}\text{C} \sim -21.0^{\circ}\text{C}$  by refrigerators. The hot water heated by a 1.5 kW electric heater in a hot-water tank was recirculated by a pump through two aluminum pipes, and cold water was also recirculated by another pump through the remaining two pipes and a cold-water tank. The hot-

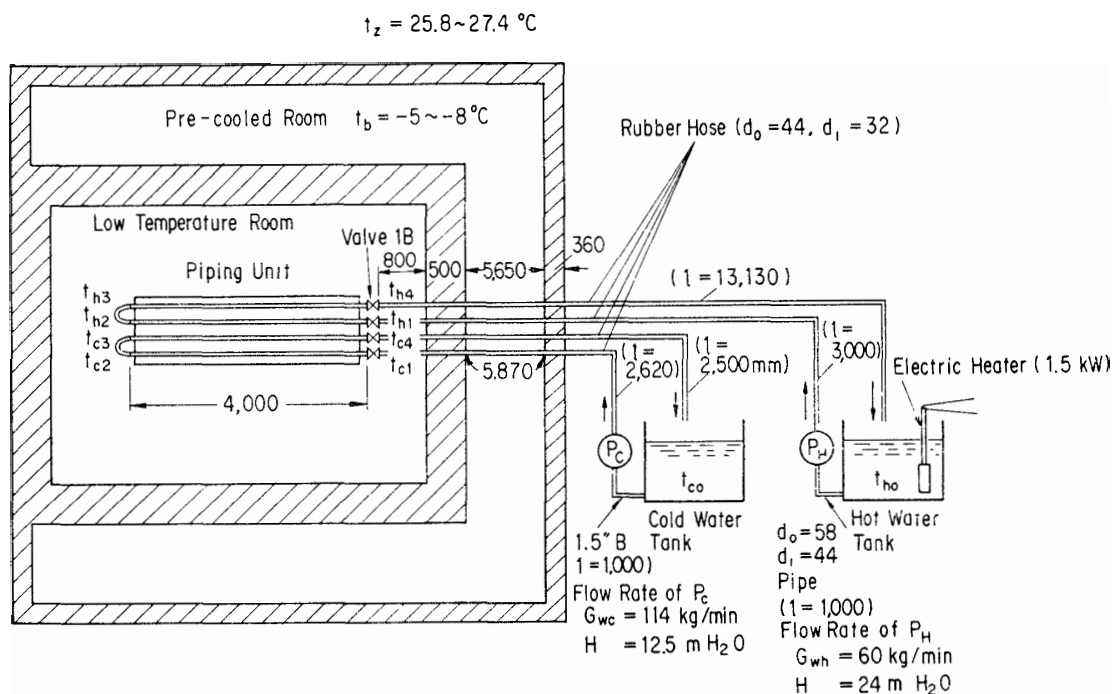


Fig. A-1. Equipment for test pipe unit prepared for JARE-7 for feeding hot and cold water (Low Temperature Testing Room of Research Institute of Transportation Technology, August 1965).

water temperatures  $t_{h1}$ ,  $t_{h2}$ ,  $t_{h3}$ ,  $t_{h4}$  (the mean of which is  $t_h$ ), cold-water temperatures  $t_{c1}$ ,  $t_{c2}$ ,  $t_{c3}$ ,  $t_{c4}$  (the mean of which is  $t_c$ ), and room temperature  $t_a$  were measured for 1.3 h in Exp. No. 1 and 1.8 h in Exp. No. 2.

The experimental results are shown in Table A-1 and Fig. A-2 and indicate that the cold water temperature  $t_c$  can be always kept above the freezing point by using the heat loss from the two hot-water pipes. It was verified experimentally that this heating system was very effective for transporting cold water from the ice-melting tank to living or cooking quarters at Syowa Station.

Table A-1. Results of low-temperature test of piping unit as shown in Fig. 9(a).  
(In low temperature testing room of Res. Inst. of Transportation  
and Technology, Tokyo)

Exp. No. 1 (30 August 1965)  $l=4$  m,  $r_2=0.070$  m,  $r_1=0.014$  m,  $Z_h=Z_c=2$

No.	Time (h)	$t_c$	$t_h$	$t_a$ (°C)	$t_c-t_a$	$t_h-t_a$	$m$	$\xi_h$	Heater input (kW)	Remarks
1	0	—	55.7	-22.2	—	77.9	—	—	1.487	
2	0.300	2.8	54.9	-21.1	23.9	76.0	0.314	0.686	1.530	
3	0.633	2.6	52.7	-20.4	23.0	73.1	0.315	0.685	1.522	
4	0.967	2.5	50.2	-20.1	22.6	70.3	0.321	0.679	1.496	
5	1.300	3.2	48.0	-20.0	23.2	68.0	0.341	0.659	1.496	

Exp. No. 2 (31 August 1965)

No.	Time (h)	$t_c$	$t_h$	$t_a$ (°C)	$t_c-t_a$	$t_h-t_a$	$m$	$\xi_h$	Heater input (kW)	Remarks
1	0	0.6	61.6	-21.0	21.6	82.6	0.262	0.738	1.478	Heater in and pumps start.
2	0.167	0.7	61.7	-21.0	21.7	82.7	0.262	0.738	1.504	
3	0.333	0.9	61.4	-21.0	21.9	82.4	0.266	0.734	1.504	
4	0.500	1.9	61.3	-20.4	22.3	81.7	0.273	0.727	1.470	
5	0.667	4.7	60.7	-20.3	25.0	81.0	0.309	0.691	1.484	
6	1.83	25.1	50.1	-19.3	44.4	69.4	0.640	0.360	0	Heater is cut off, but pumps continue to run.

Flow rate: hot water pump 60 l/min, head  $H=24$  m H<sub>2</sub>O,  
cold water pump 114 l/min, head  $H=12.5$  m H<sub>2</sub>O.

## 1.2. Theoretical analysis of the piping unit

$r_1$ : radius of aluminum pipes,  $r_1=0.014$  m,

$r_2$ : radius of piping unit,  $r_2=0.070$  m,

$l$ : length of aluminum tubes,  $l=4$  m,

$Z_h$ : number of hot-water tubes,  $Z_h=2$ ,

$Z_c$ : number of cold-water tubes,  $Z_c=2$ ,

$t_h$ : mean temperature of hot water, °C,

$t_c$ : mean temperature of cold water, °C,

$t_a$ : room temperature, °C,

$\lambda$ : thermal conductivity of insulating material, kcal/mh°C,

$\alpha_a$ : heat transfer coefficient due to natural convection from the outside of unit to air,  $\alpha_a=2.35$  kcal/m<sup>2</sup>h°C (estimated),

$\xi$ : ratio of heat loss from the external surface of unit to total heat loss of tubes, including the effect of eccentricity between an aluminum tube and an outer tube.

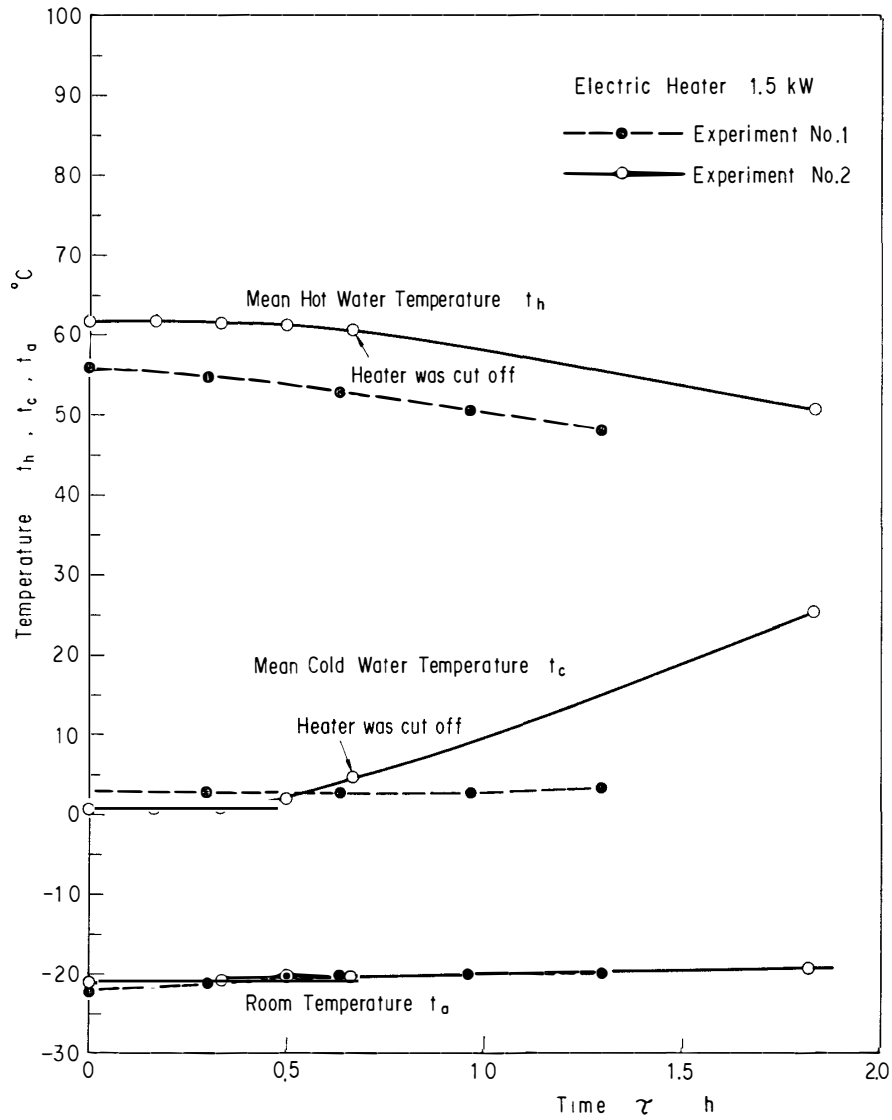


Fig. A-2. Experimental results on pipe unit to feed hot and cold water in low temperature room.

Heat which originated from the hot water transferred to the air by natural convection from the external lower surface of the pipe unit, can be represented approximately as follows:

$$Q_{ha} = 2\pi K r_2 l (t_h - t_a) Z_h \xi_h \text{ kcal/h,} \quad (\text{A-1})$$

where

$$K = 1 / [(1/\alpha_a) + (r_2/\lambda) \ln(r_2/r_1)] \text{ kcal/m}^2\text{h}^\circ\text{C.} \quad (\text{A-2})$$

In the same way, heat which originated from the cold water transferred to air by natural convection from the external upper surface of the pipe unit, can be

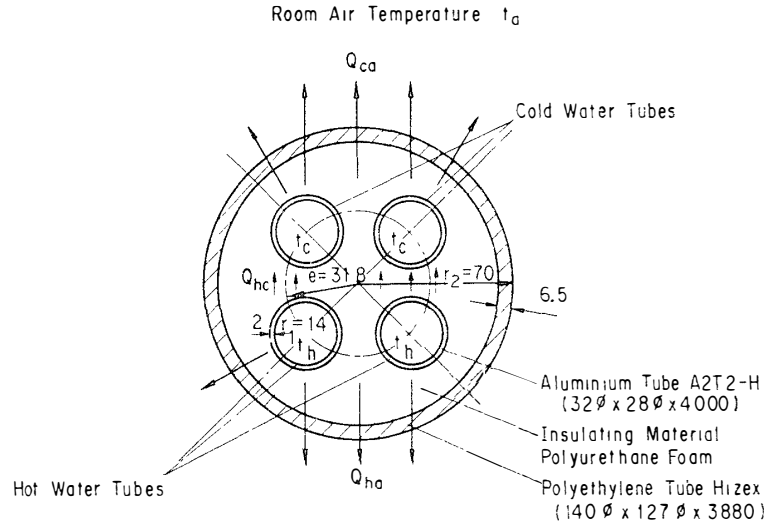


Fig. A-3. Heat flow in an insulated pipe unit to feed hot and cold water in low temperature room.

expressed as:

$$Q_{ca} = 2\pi Kr_2 l (t_c - t_a) Z_c \xi_c \text{ kcal/h,} \quad (\text{A-3})$$

and the heat transferred from hot water to cold water can be represented by

$$Q_{hc} = 2\pi Kr_2 l [(t_h - t_a) Z_h (1 - \xi_h) - (t_c - t_a) Z_c (1 - \xi_c)] \text{ kcal/h.} \quad (\text{A-4})$$

In an equilibrium state, the following condition should be satisfied:

$$Q_{hc} = Q_{ca}. \quad (\text{A-5})$$

From eqs. (A-3), (A-4) and (A-5), we get

$$m = \frac{t_c - t_a}{t_h - t_a} = (1 - \xi_h) \frac{Z_h}{Z_c}, \quad (\text{A-6})$$

$$\xi_h = 1 - m(Z_c/Z_h). \quad (\text{A-7})$$

The temperature of the cold water  $t_c$  should be kept above  $0^\circ\text{C}$ , so that the temperature of the hot water should be higher than the following temperature

$$t_h = -t_a(1 - m)/m \text{ } ^\circ\text{C.} \quad (\text{A-8})$$

As shown in Table A-1, the mean value of  $m$  is 0.323 for Exp. No. 1 and 0.274 for Exp. No. 2. If we adopt a value of  $m=0.274$  to be on the safe side, the hot-water temperature  $t_h$  should be kept higher than the values shown in Table A-2 for any air temperature  $t_a$  in the newly developed piping unit.

As an example, the heat loss from the piping unit and the heat transferred from hot water to cold water is calculated as follows:

Table A-2. Estimated minimum hot-water temperature  $t_h$  at atmospheric air temperature  $t_a$  for avoiding freezing of cold water in piping unit.

$$(Z_h=2, Z_c=2, m=0.274, \xi_h=0.726)$$

Air temp. $t_a$ (°C)	Hot-water temp. $t_h$ (°C)
-40	(106)
-35	93
-30	80
-25	66
-20	53
-15	40
-10	27
- 5	14

$$\begin{aligned}
 t_h &= 61.0^\circ\text{C}, & t_c &= 1.9^\circ\text{C}, & t_a &= -20.4^\circ\text{C}, \\
 Z_h &= Z_c = 2, & m &= 0.274, & \xi_h &= \xi_c = 0.726, \\
 r_2 &= 0.070 \text{ m}, & r_1 &= 0.014 \text{ m}, & r_2/r_1 &= 5, \\
 \ln(r_2/r_1) &= 1.609, & l &= 4 \text{ m}, \\
 \alpha_a &= 2.35 \text{ kcal/m}^2\text{h}^\circ\text{C}, & \lambda &= 0.25 \text{ kcal/mh}^\circ\text{C}, \\
 K &= 1.14 \text{ kcal/m}^2\text{h}^\circ\text{C} \text{ from eq. (A-2)}, \\
 Q_{ha} &= 237 \text{ kcal/h} \text{ calculated from eq. (A-1)}, \\
 Q_{ca} &= 65 \text{ kcal/h} \text{ from eq. (A-3)}, \\
 Q_{hc} &= 65 \text{ kcal/h} \text{ from eq. (A-4)},
 \end{aligned}$$

total heat loss from a piping unit

$$Q_{ha} + Q_{ca} = 237 + 65 = 302 \text{ kcal/h,}$$

total heat loss from hot-water tube

$$Q_{ha} + Q_{hc} = 237 + 65 = 302 \text{ kcal/h.}$$

This example shows that the heat transferred from hot water to cold water in a piping unit is balanced by the heat loss from the cold water to atmospheric air by natural convection. The result of calculation of the heat loss from hot water coincides with the observed results at Syowa Station.

## APPENDIX 2

### 2.1. Theoretical analysis of a shell-and-tube type exhaust-gas heat exchanger

By heat-transfer technology, we can estimate the approximate performance of an exhaust-gas heat exchanger as follows: As shown in eqs. (38), the total

heat resistance  $\sum R$  is composed of the resistance of gas-side boundary layer  $R_g$ , the resistance of adhering soot layer  $R_c$ , the resistance of tube wall  $R_m$ , and the resistance of water-side boundary layer  $R_w$ . The total resistance  $\sum R$  mainly depends on  $R_g$  and  $R_c$  because  $R_m$  and  $R_w$  are smaller than the others. The theoretical calculation on ST-3 will now be set forth as an example (Fig. 36).

### 2.1.1. Estimation of $\alpha_g$

- $w$ : velocity of gas, m/s,  
 $d_o$ : outer diameter of tube,  $d_o=0.0254$  m,  
 $d_i$ : inner diameter of tube,  $d_i=0.0214$  m,  
 $l$ : length of a tube,  $l=0.800 \times 2=1.60$  m,  
 $z$ : number of tubes in a half shell area,  $z=112/2=56$ ,  
 $D_s$ : inner diameter of the shell,  $D_s=0.540$  m,  
 $\delta_c$ : thickness of soot layer adhering on the internal surface of tubes, m,  
 $d_e$ : equivalent diameter, m,  
 $R_e$ : Reynolds number of gas  $R_e=w_g d_e/\nu_g$ ,  
 $\nu_g$ : kinematic viscosity of combustion gas,  $\text{m}^2/\text{s}$ ,  
 $\gamma_{go}$ : specific weight of combustion gas at  $t_g=0^\circ\text{C}$  and 1 atm,  $\text{kg}/\text{m}^3$ ,  
 $\gamma_g$ : specific weight of combustion gas at  $t_{gm}$  and 1 atm,  $\text{kg}/\text{m}^3$ ,  
 $\lambda_g$ : thermal conductivity of combustion gas at  $t_{gm}$ ,  $\lambda_g=0.0325$  kcal/mh $^\circ\text{C}$ ,  
 $\alpha_g$ : coefficient of heat transfer of gas-side boundary layer, kcal/m $^2\text{h}^\circ\text{C}$ ,  
 $Nu$ : Nusselt number,  $Nu=\alpha_g d_e/\lambda_g$ ,  
 $Pr$ : Prandtl number,  $Pr=0.7$  for combustion gas,  
 $G_g$ : weight flow rate of combustion gas,  $G_g=0.121$  kg/s (453.6 kg/h).

For the combustion gas flowing through the inside of tubes

$$\begin{aligned} \gamma_{go} &= 1.296 \text{ kg}/\text{m}^3 \text{ at } t_g=0^\circ\text{C}, \quad p=1 \text{ atm}, \quad \phi=0.45, \\ \gamma_g &= 1.293(273/480)=0.7371 \text{ kg}/\text{m}^3 \text{ at } t_{gm}=207^\circ\text{C}, \\ \eta_g &= \text{viscosity of combustion gas, kg s}/\text{m}^2, \\ \eta_g &= 2.50 \times 10^{-6} \text{ kg s}/\text{m}^2 \text{ for } t_{gm}=207^\circ\text{C} \text{ and } \phi=0.45. \end{aligned}$$

$$g: \text{ gravity acceleration, } g=9.8 \text{ m}/\text{s}^2.$$

Kinematic viscosity of combustion gas

$$\nu_g = \eta_g g / \gamma_g = (2.50 \times 10^{-6}) \times 9.80 / 0.7371 = 33.2 \times 10^{-6} \text{ m}^2/\text{s}.$$

Total internal sectional area of tubes covered with soot of thickness  $\delta_c$  is

$$A_c = z\pi(d_i - 2\delta_c)^2/4, \text{ m}^2.$$

The gas velocity

$$w_g = G_g / (A_c \gamma_g) = 0.121 / (A_c \times 0.7371), \text{ m}/\text{s}. \quad (\text{A-9})$$

Reynolds number

$$R_e = w_g d_e / \nu_g = w_g (d_i - 2\delta_c) / \nu_g. \quad (\text{A-10})$$

For turbulent flow, the following relation should hold:

$$Nu = \alpha_g d_e / \lambda_g = 0.023 R_e^{0.8} Pr^{0.4}, \quad (\text{A-11})$$

where the equivalent diameter is  $d_e = d_i - 2\delta_c$ .

The coefficient of heat transfer on the gas side can be calculated by

$$\alpha_g = \lambda_g Nu / d_e \text{ kcal/m}^2\text{h}^\circ\text{C}. \quad (\text{A-12})$$

### 2.1.2. Estimation of $\alpha_w$

The coefficient of heat transfer on the water side can be estimated as follows:  
The sectional passage area for water  $A_w$  outside of tubes is

$$\begin{aligned} A_w &= (\pi D_s^2 / 8) - (\pi d_o^2 z / 4) = (\pi 0.540^2 / 8) - (\pi 0.0254^2 \times 56 / 4) \\ &= 0.1145 - 0.0284 = 0.0861 \text{ m}^2, \end{aligned}$$

and the wetted perimeter length is

$$P = (\pi D_s / 2) + D_s + \pi d_o z = 5.857 \text{ m}.$$

The equivalent diameter on the water side is

$$d_e = 4 A_w / P = 0.05882 \text{ m}.$$

The kinematic viscosity of water at a mean temperature  $t_{wm} = 54^\circ\text{C}$  is given by

$$\nu_w = 0.514 \times 10^{-6} \text{ m}^2/\text{s}.$$

When the volume flow rate of water supplied by a pump is represented by  $Q_w$  m<sup>3</sup>/s, the water velocity  $w_w$  is

$$w_w = Q_w / [\pi d_e^2 / 4] = 0.001 / 0.002717 = 0.368 \text{ m/s for } Q_w = 0.001 \text{ m}^3/\text{s}.$$

The Reynolds number of the water flow is

$$R_e = w_w d_e / \nu_w = 42100,$$

and for water of  $t_{wm} = 54^\circ\text{C}$ , the Prandtl number  $Pr = 3.4$ , and thermal conductivity  $\lambda_w = 0.556 \text{ kcal/mh}^\circ\text{C}$ , so that the Nusselt number can be calculated by

$$Nu = 0.023 R_e^{0.8} Pr^{0.4} = 0.023 (42100)^{0.8} (3.4)^{0.4} = 188.$$

The coefficient of heat transfer on the water side can be obtained as follows:

$$\alpha_w = \lambda_w Nu / d_e = 0.556 \times 188 / 0.05882 = 1780 \text{ kcal/m}^2\text{h}^\circ\text{C}.$$

### 2.1.3. Heat resistances of tube wall and soot layer

Thermal conductivity of stainless steel	$\lambda_m = 14 \text{ kcal/mh}^\circ\text{C}$ .
Thickness of tubes	$\delta_m = 0.002 \text{ m}$ .
Thermal conductivity of carbon soot layer	$\lambda_c = 0.10 \text{ kcal/mh}^\circ\text{C}$ .
Thickness of soot layer	$\delta_c \text{ m}$ .
Thermal resistance of stainless-steel tube	$R_m = \delta_m/\lambda_m = 0.002/14 = 0.000143$ .
Thermal resistance of soot layer	$R_c = \delta_c/\lambda_c = 10 \delta_c \text{ m}^2\text{h}^\circ\text{C/kcal}$ .

### 2.1.4. Overall coefficient of heat transmission $K_{lm}$

The total heat resistance

$$\sum R = (1/\alpha_w)(d_i/d_o) + (1/\alpha_g)(d_i/d_c) + R_m + R_c. \quad (\text{A-13})$$

Overall coefficient of heat transmission

$$K_{lm} = 1/\sum R \text{ kcal/m}^2\text{h}^\circ\text{C}. \quad (\text{A-14})$$

The total inner surface area of the stainless-steel tubes in a clean state contacting exhaust gas directly, is adopted as a standard heating area

$$F_i = z(\pi d_i l) = 56(\pi \times 0.0214 \times 1.60) = 6.02 \text{ m}^2,$$

sectional area for gas flow

$$A_i = z(\pi d_i^2/4) = 56(\pi \times 0.0214^2/4) = 0.02014 \text{ m}^2,$$

gas velocity

$$w_g = G_g/(A_i \gamma_g) = 0.121/(0.02014 \times 0.7371) = 8.15 \text{ m/s},$$

Reynolds number

$$R_e = w_g d_i / \nu_g = (8.15)(0.0214)/(33.2 \times 10^{-6}) = 5253,$$

Nusselt number

$$Nu = 0.023 R_e^{0.8} Pr^{0.4} = 0.023(5253)^{0.8}(0.7)^{0.4} = 0.023(946.9)(0.867) = 18.9,$$

coefficient of heat transfer on gas side

$$\alpha_g = \lambda_g (Nu)/d_i = (0.0325)(18.9)/(0.0214) = 28.7 \text{ kcal/m}^2\text{h}^\circ\text{C},$$

total heat resistance

$$\begin{aligned} \sum R &= (1/\alpha_w)(d_i/d_o) + R_m + (1/\alpha_g) = (1/1780)(0.0214/0.0254) + (0.000143) + (1/28.7) \\ &= 0.000473 + 0.000143 + 0.03484 = 0.03546 \text{ m}^2\text{h}^\circ\text{C/kcal}, \end{aligned}$$

overall coefficient of heat transmission

Table A-3. Theoretical calculation of the thermal resistance of the shell-and-tube type exhaust-gas heat exchanger ST-3 with soot adhesion.

$\delta_e$ (m)	$d_e$ (m)	$A_c$ (m <sup>2</sup> )	$w_g$ (m/s)	$Re$	$Nu$	$\alpha_g$	$F_c$ (m <sup>2</sup> )	$R_g$	$R_c$	$\Sigma R$	$K_{lm}$ (kcal/m <sup>2</sup> h°C)
0	0.0214	0.02014	8.15	5253	18.9	28.7	6.02	0.0348	0	0.0355	28.2
0.001	0.0194	0.01655	9.92	5797	20.4	34.2	5.46	0.0322	0.010	0.0429	23.2
0.002	0.0174	0.01332	12.3	6446	22.2	41.5	4.90	0.0296	0.020	0.0502	19.9
0.003	0.0154	0.01043	15.7	7283	24.5	51.7	4.34	0.0268	0.030	0.0575	17.4
0.004	0.0134	0.00790	20.8	8395	27.5	66.7	3.77	0.0239	0.040	0.0645	15.5
0.005	0.0114	0.00572	28.7	9855	31.2	88.9	3.21	0.0211	0.050	0.0717	13.9

$$K_{lm} = 1/\Sigma R = 1/0.03546 = 28.2 \text{ kcal/m}^2\text{h}^\circ\text{C}.$$

The heat transferred can be calculated by

$$Q_r = K_{lm} F_i \Delta t_{lm} = (28.2)(6.02) \Delta t_{lm} = 170 \Delta t_{lm} \text{ kcal/h}.$$

In Table A-3 the effect of soot accumulation on the inner surface of tubes on the overall coefficient of heat transmission  $K_{lm}$  is shown, and the decrease of  $K_{lm}$  with soot accumulation coincides with the results shown in Figs. 33 and 34.

### APPENDIX 3

#### 3.1. Experimental data on the performance of shell-and-coil type exhaust-gas heat exchanger

The thermal performance of a shell-and-coil type exhaust-gas heat exchanger, which was used at Syowa Station during JARE-1 and JARE-18 as described in Subsection 6.1, was tested in the Engine Laboratory of Nihon University in Tokyo, by using an Isuzu DA-640 diesel engine. The test results are shown in Table A-4.

#### 3.2. Experimental data on the performance of vertical shell-and-tube type exhaust-gas heat exchanger

As shown in Subsection 6.2, the shell-and-tube type heat exchanger was replaced by the shell-and-coil type from JARE-19 (1977/79) to the present in order to facilitate the scraping off of the soot adhering on the heating surface while the system was in operation. The prototype was ST-1, which was later developed into ST-2 and ST-3. In Tables A-5 and A-6, the test data on ST-2 and ST-3 are shown. Reference is made to Table 9 for the basic design data.

Table A-4. Performance of a shell-and-coil type heat exchanger prepared for JARE-12 (1970/72).

Run No.	Time (min)	Engine speed $N$ (rpm)	Load $W$ (kg)	Output power $L_e$ (PS)	$G_a$ (kg/h)	$G_f$ (kg/h)	$G_g$ (kg/h)	$b_e$ (gr/PSH)	Equivalence ratio $\phi$	$t_{g1}$ ( $^{\circ}\text{C}$ )	$t_{g2}$ ( $^{\circ}\text{C}$ )	$\Delta t_g$ ( $^{\circ}\text{C}$ )	$t_{gm}$ ( $^{\circ}\text{C}$ )	$[c_{pgm}]_{t_{g2}}^{t_{g1}}$ (kcal/kg $^{\circ}\text{C}$ )	$Q_{R1}^*$ (kcal/h)
1	0	1540	0.7	0.54	271	3.60	275	6667	0.189	114	48	66	81	0.244	4430
2	5	1565	10.0	7.83	273	4.36	277	556	0.227	133	53	80	93	0.245	5430
3	10	1540	20.0	15.4	273	5.51	279	355	0.287	150	59	91	105	0.246	6250
4	15	1500	30.5	22.9	269	6.52	276	285	0.344	168	63	105	116	0.248	7190
5	20	1500	40.0	30.0	267	7.27	274	242	0.386	189	72	117	131	0.249	7980
6	25	1520	50.5	38.4	268	8.75	277	228	0.463	214	76	138	145	0.251	9595
7	30	1500	60.5	45.4	267	9.68	277	213	0.515	243	85	158	164	0.254	11120
8	35	1500	70.5	52.9	265	10.9	276	207	0.588	271	93	178	182	0.256	12580
9	40	1485	80.0	59.4	259	11.8	271	199	0.645	297	104	193	201	0.259	13550
10	45	1500	90.0	67.5	259	13.6	273	202	0.746	353	118	235	236	0.263	16870
11	50	1500	100.0	75.0	257	15.7	273	209	0.870	407	128	279	265	0.267	20340

Run No.	Time (min)	$\Delta Q_{R1}$ (kcal/h)	$Q_{R1}$ (kcal/h)	$t_{w1}$ ( $^{\circ}\text{C}$ )	$t_{w2}$ ( $^{\circ}\text{C}$ )	$\Delta t_w$ ( $^{\circ}\text{C}$ )	$Q_{R2}$ (kcal/h)	$\Delta t_{lm}$ ( $^{\circ}\text{C}$ )	$K_{lm}$ (kcal/m $^2$ h $^{\circ}\text{C}$ )	$t_{g1}$ ( $^{\circ}\text{C}$ )	$[c_{pgm}]_0^{t_{g1}}$ (kcal/kg $^{\circ}\text{C}$ )	$Q_{g1}$ (kcal/h)	$\eta_{rec}$	$\phi_g$	$K_{am}$ (kcal/m $^2$ h $^{\circ}\text{C}$ )
1	0	450	3980	31.4	32.2	0.8	3170	41.3	18.0	114	0.243	7610	0.524	0.795	14.5
2	5	540	4890	33.5	34.5	1.0	3960	48.1	19.1	133	0.244	8990	0.544	0.808	15.5
3	10	680	5570	36.3	37.6	1.3	5150	56.2	18.5	150	0.245	10250	0.543	0.798	15.3
4	15	720	6470	38.6	40.2	1.6	6340	62.1	19.5	168	0.247	11450	0.565	0.814	15.3
5	20	855	7125	41.2	43.0	1.8	7130	74.2	18.0	189	0.247	12790	0.557	0.791	15.1
6	25	950	8645	44.3	46.6	2.3	9110	81.7	19.9	214	0.249	14760	0.586	0.812	16.2
7	30	1125	9995	48.5	51.1	2.6	10300	93.2	20.1	243	0.252	16960	0.589	0.814	16.4
8	35	1240	11340	52.3	55.3	3.0	11900	105.3	20.2	271	0.254	19000	0.597	0.813	16.6
9	40	1390	12160	56.3	59.5	3.2	12700	118.7	19.2	297	0.259	20850	0.583	0.801	15.9
10	45	1590	15280	60.4	64.3	3.9	15450	143.8	19.9	353	0.262	25250	0.605	0.802	16.5
11	50	1930	18410	69.7	74.5	4.8	19000	157.0	22.0	407	0.264	29330	0.628	0.828	17.9
									19.5***				0.57**	0.807**	15.9**

Note: 1) Tested at Nihon University in Tokyo (24 Dec. 1973).  
 2) Diesel engine: Isuzu DA-640.  
 3) Flow rate of water  $G_w=3960$  kg/h.  
 4) Atmospheric pressure 769.5 mmHg, temperature 10 $^{\circ}\text{C}$ .

5) Heating area  $F_o=5.33$  m $^2$ , pipe diam.  $d_o=18$  mm,  $d_i=14$  mm.  
 6)  $\Delta Q_{R1}$  is the correction term for heat loss in Eq. (36).  
 \*\* Mean value.



Table A-5b. Overall coefficient of heat transmission  $K_{lm}$ , recovery efficiency  $\eta_{rec}$ , and temperature efficiency  $\phi_g$  of ST-2.

Run No.	Time (min)	$Q_{R1}^*$ (kcal/h)	$t_{gm}$ (°C)	$\Delta Q_{R1}$ (kcal/h)	$Q_{R1}$ (kcal/h)	$\Delta t_{lm}$ (°C)	$K_{lm}$ (kcal/m <sup>2</sup> h°C)	$G_g$ (kg/h)	$t_{g1}$ (°C)	$[c_{pgm}]_0^{t_{g1}}$ (kcal/kg°C)	$Q_{g1}$ (kcal/h)	$\eta_{rec}$	$t_{g1}-t_{g2}$ (°C)	$t_{g1}-t_{w1}$ (°C)	$\phi_g$	$t_{gm}-t_{wm}$ (°C)	$K_{am}$ (kcal/m <sup>2</sup> h°C)
1	0	—	—	—	—	—	—	303	—	—	—	—	—	—	—	—	—
2	5	15400	140	370	15030	70.0	33.2	303	240	0.250	18200	0.826	201	212.5	0.946	115	20.2
3	10	17900	163	441	17460	88.4	30.5	301	280	0.251	21200	0.824	235.5	252.5	0.933	138	19.6
4	15	19100	175	478	18620	99.4	29.0	301	300	0.252	22750	0.836	251	272.5	0.921	151	19.1
5	20	18800	177	485	18320	103.3	27.4	301	300	0.252	22750	0.805	247	272.2	0.907	149	19.0
6	25	18400	179	491	17910	105.1	26.3	300	300	0.252	22680	0.790	242	269.4	0.898	146	19.0
7	30	18100	181	497	17600	102.7	26.5	301	300	0.252	22750	0.774	238.5	264.9	0.900	144	18.9
8	35	17900	182	500	17400	100.3	26.9	301	300	0.252	22750	0.765	235.5	260.9	0.903	141	19.1
9	40	17500	185	509	16990	100.6	26.1	301	300	0.252	22750	0.747	231	257.1	0.898	141	18.6
10	45	17300	186	512	16790	98.3	26.4	301	300	0.252	22750	0.738	227.5	252.6	0.901	138	18.8
11	50	17000	188	518	16480	97.7	26.1	301	300	0.252	22750	0.724	224.5	249.9	0.898	137	18.6
12	55	16800	190	525	16280	95.9	26.2	301	300	0.252	22750	0.716	221	245.8	0.899	135	18.6
13	60	16700	191	528	16170	93.0	26.9	301	300	0.252	22750	0.711	219	242.1	0.905	133	18.8
14	65	16400	192	531	15870	92.4	26.4	301	300	0.252	22750	0.698	216.5	240.0	0.902	130	18.9
15	70	16200	193	534	15670	89.5	27.1	301	300	0.252	22750	0.689	214	235.8	0.908	128	18.9
16	75	16100	195	540	15560	89.8	26.7	303	300	0.252	22900	0.679	211	233.7	0.903	127	18.9
17	80	16000	196	543	15460	87.9	27.2	303	300	0.252	22900	0.675	209	230.8	0.906	125	19.1
18	85	16600	197	546	16050	90.1	27.5	303	310	0.252	23670	0.678	216	238.0	0.908	125	19.8
19	90	16000	196	543	15460	79.1	30.2	303	300	0.252	22900	0.675	209	225.2	0.928	123	19.4
20	95	16600	202	562	16040	78.4	35.2	303	310	0.252	23670	0.678	216	232.1	0.931	124	20.0
21	100	24400	259	738	24330	122.0	30.8	311	410	0.259	33030	0.737	302	330.3	0.914	177	21.2
22	105	24700	268	765	23940	127.4	29.1	311	420	0.259	33830	0.708	305	336.1	0.907	182	20.3
							28.2**					0.737**			0.910**		19.2**

Note: 1)  $Q_{R1}^* = G_g c_{pgm} (t_{g1} - t_{g2})$  kcal/h.2)  $\Delta Q_{R1} = \sum \alpha_a A (t_{gm} - t_a)$  kcal/h (heat loss from gas-side surfaces)  
=  $3.09(t_{gm} - t_a) = 3.09(t_{gm} - 20)$  kcal/h.3) Corrected transferred heat  $Q_{R1} = Q_{R1}^* - \Delta Q_{R1}$ .4)  $\eta_{rec} = Q_{R1} / Q_{g1}$ .5)  $Q_{g1} = G_g c_{pgm} t_{g1}$  kcal/h.6)  $Q_{R1} = K_{lm} F_i \Delta t_{lm}$ .7)  $F_i = 6.47$  m<sup>2</sup>.8)  $K_{lm} = 28.2$  kcal/m<sup>2</sup>h°C.9)  $\eta_{rec} = 0.737$ .10)  $\phi_g = 0.910$ .11)  $K_{am} = 19.2$  kcal/m<sup>2</sup>h°C.

\*\*Mean value.

Table A-6. Performance of a vertical shell-and-tube type exhaust-gas heat exchanger (ST-3) for JARE-21 (1979/81).

Run No.	Time (min)	Engine speed $N$ (rpm)	Load $W$ (kg)	Output power $L_e$ (PS)	$G_a$ (kg/h)	$G_f$ (kg/h)	$b_e$ (gr/PS $h$ )	$t_{g1}$ (°C)	$t_{g2}$ (°C)	$\Delta t_g$ (°C)	$G_g$ (kg/h)	$[c_{pgm}]_{t_{g2}}^{t_{g1}}$ (kcal/kg°C)	$\phi$	$Q_{R1}^*$ (kcal/h)	$\Delta Q_{R1}$ (kcal/h)	$Q_{R1}$ (kcal/h)	$t_{w1}$ (°C)	$t_{w2}$ (°C)	$t_B$ (°C)
1	0	2034	59.5	60.5	428	13.7	227	310	63	247	442	0.254	0.455	27800	510	27300	31.2	35.8	30.8
2	5	2034	58.5	59.5	425	13.2	223	320	72	248	438	0.254	0.442	27700	530	27200	—	—	37.0
3	10	2030	58.0	58.9	421	13.1	223	323	79	244	434	0.254	0.442	27000	550	26450	42.8	47.0	42.7
4	15	2032	57.0	57.9	421	13.0	225	323	85	238	434	0.254	0.441	26300	560	25740	47.8	51.9	47.9
5	20	2034	56.5	57.5	418	12.9	224	323	92	231	431	0.254	0.437	25300	570	24730	52.8	56.9	53.2
6	25	2030	60.0	60.9	418	12.8	214	330	98	232	431	0.255	0.435	25600	590	25000	57.9	62.0	58.5
7	30	2030	59.5	60.4	418	13.2	219	330	102	228	431	0.255	0.455	25100	595	24500	62.6	66.7	63.4
8	35	2030	59.0	59.9	418	13.2	221	330	106	224	431	0.255	0.455	24700	600	24100	67.0	71.0	68.0
9	40	2024	59.0	59.7	418	13.0	218	330	111	219	431	0.255	0.444	24100	610	23500	71.8	75.6	72.5

Run No.	Time (min)	$\Delta t_{lm}$ (°C)	$K_{lm}$ (kcal/m <sup>2</sup> h°C)	$t_{g1}$ (°C)	$[c_{gpm}]_0^{t_{g1}}$ (kcal/kg°C)	$Q_{g1}$ (kcal/h)	$\eta_{rec}$	$t_{g1}-t_{w1}$ (°C)	$\Phi_g$	$t_{gm}$ (°C)	$t_{wm}$ (°C)	$t_{gm}-t_{wm}$ (°C)	$K_{am}$ (kcal/m <sup>2</sup> h°C)
1	0	112.5	40.3	310	0.252	34500	0.791	279	0.885	187	34	153	29.6
2	5	—	—	320	0.252	35300	0.771	—	—	196	—	—	—
3	10	118.1	37.2	323	0.252	35300	0.749	280	0.871	201	45	156	28.2
4	15	117.7	36.3	323	0.252	35300	0.729	275	0.865	204	50	154	27.8
5	20	118.5	34.7	323	0.252	35100	0.705	270	0.855	208	55	153	26.8
6	25	120.0	34.6	330	0.252	35800	0.698	272	0.853	214	60	154	27.0
7	30	117.9	34.5	330	0.252	35800	0.684	267	0.854	216	65	151	27.0
8	35	116.2	34.5	330	0.252	35800	0.673	263	0.852	218	69	149	26.9
9	40	115.1	33.9	330	0.252	35800	0.656	258	0.849	221	74	147	26.6
			35.1**				0.715**		0.860**				26.8**

- Note: 1) Tested at Nihon University in Tokyo (6 October 1979). 2) Diesel engine: Isuzu DA-640. 3) Flow rate of water  $G_w=3600$  kg/h. 4) Water contained in the bathtub, heat exchanger and pipes  $G_B=286.5$  kg. 5) Heating surface area  $F_i=6.02$  m<sup>2</sup> (inner surface area of tubes). 6) Atmospheric pressure and temperatures start  $P_z=759.4$  mmHg  $t_{ad}=19.5^\circ\text{C}$   $t_{aw}=17.1^\circ\text{C}$ , final  $P_z=758.9$  mmHg  $t_{ad}=19.4^\circ\text{C}$   $t_{aw}=17.2^\circ\text{C}$ . 7)  $\Delta Q_{R1}=3.0(t_{gm}-t_a)$  kcal/h. Correction for heat loss. 8) In calculating mean values, No. 1 and No. 2 are omitted. \*\* Mean value.

Table A-7. Performance of a vertical fin-tube type exhaust-gas heat exchanger (AL-F-2) for JARE-21 (1979/81).

Run No.	Time (min)	Engine speed $N$ (rpm)	Load $W$ (kg)	Output power $L_e$ (PS)	$G_a$ (kg/h)	$G_f$ (kg/h)	$G_g$ (kg/h)	$b_e$ (gr/PS h)	Equivalence ratio $\phi$	$t_{g1}$ ( $^{\circ}\text{C}$ )	$t_{g2}$ ( $^{\circ}\text{C}$ )	$\Delta t_g$ ( $^{\circ}\text{C}$ )	$t_{gm}$ ( $^{\circ}\text{C}$ )	$[c_{pgm}]_{t_{g1}}^{t_{g2}}$ (kcal/kg $^{\circ}\text{C}$ )	$Q_{R1}^*$ (kcal/h)	$Q_{R1}$ (kcal/h)	$t_{w1}$ ( $^{\circ}\text{C}$ )	$t_{w2}$ ( $^{\circ}\text{C}$ )
1	0	2028	60.5	61.3	410	13.9	424	226	0.478	305	80	225	193	0.254	24300	23240	31.7	33.8
2	5	2030	60.5	61.4	414	13.7	428	223	0.469	335	123	212	229	0.256	23250	22190	36.8	39.3
3	10	2028	60.0	60.8	410	13.4	423	221	0.465	338	138	200	238	0.257	21800	20740	41.4	44.6
4	15	2028	59.5	60.3	410	13.2	423	220	0.459	338	143	195	241	0.257	21300	20240	45.9	49.2
5	20	2030	59.5	60.4	407	13.2	420	219	0.463	335	148	187	242	0.257	20240	19180	50.9	54.2
6	25	2028	59.0	59.8	407	13.2	420	222	0.463	335	151	184	243	0.257	19900	18840	55.6	58.4
7	30	2028	58.5	50.3	407	13.0	420	219	0.455	335	155	180	245	0.257	19500	18440	59.8	62.5
8	35	2026	58.0	58.8	407	13.0	420	222	0.457	330	157	173	244	0.257	18700	17640	64.3	67.7
9	40	2028	57.5	58.3	407	12.9	420	222	0.450	330	160	170	245	0.257	18400	17340	68.4	71.3

Run No.	Time (min)	$\Delta t_w$ ( $^{\circ}\text{C}$ )	$t_{wm}$ ( $^{\circ}\text{C}$ )	$\Delta t_{tm}$ ( $^{\circ}\text{C}$ )	$K_{tm}$ (kcal/m $^2$ h $^{\circ}\text{C}$ )	$[c_{pgm}]_0^{t_{g1}}$ (kcal/kg $^{\circ}\text{C}$ )	$Q_{g1}$ (kcal/h)	$\eta_{rec}$	$t_{g1}-t_{w1}$ ( $^{\circ}\text{C}$ )	$\phi_g$	$t_{gm}-t_{wm}$ ( $^{\circ}\text{C}$ )	$K_{am}$ (kcal/m $^2$ h $^{\circ}\text{C}$ )	Water temp. in bathtub $t_B$ ( $^{\circ}\text{C}$ )
1	0	2.1	33	129	30.2	0.252	32600	0.713	273	0.824	160	24.3	31.6
2	5	1.5	38	170	21.9	0.253	36280	0.612	298	0.711	191	19.5	36.7
3	10	3.2	43	177	19.6	0.253	36170	0.573	297	0.673	195	17.8	41.0
4	15	3.3	48	176	19.3	0.253	36170	0.560	292	0.668	193	17.6	45.8
5	20	3.3	53	173	18.6	0.253	35600	0.539	284	0.658	189	17.0	50.4
6	25	2.9	57	170	18.6	0.253	35600	0.529	279	0.659	186	17.0	55.0
7	30	2.7	61	169	18.3	0.252	35460	0.520	275	0.655	184	16.8	60.0
8	35	3.4	66	163	18.1	0.252	34930	0.505	266	0.650	178	16.6	64.2
9	40	2.9	70	161	18.0	0.252	34930	0.496	262	0.649	175	16.6	68.2
					18.6**			0.531**				16.9**	

Note: 1) Tested at Nihon University in Tokyo (6 October 1979).

2) Diesel engine: Isuzu DA-640.

3) Flow rate of water  $G_w=3600$  kg/h.4) Water contained in a bathtub 200 (l)  
in the heat exchanger 50 (l)  
in pipe 8.5 (l)

Total 258.5 kg

5) Heating surface area  $F_o=5.971$  m $^2$  (gas side).6)  $\Delta Q_{R1}=1060$  kcal/h (correction for heat loss).7)  $P_a=758.9$  mmHg,  $t_{ad}=19.4^{\circ}\text{C}$ ,  $t_{aw}=17.2^{\circ}\text{C}$ .

\*\* Mean value. In calculating mean values, No. 1 and No. 2 are omitted.

### 3.3. Experimental data on the performance of vertical fin-tube type exhaust-gas heat exchanger

Three kinds of fin-tube type exhaust-gas heat exchangers were developed by the authors as described in Subsection 6.3 and in Table 10. In Table A-7, the test results of AL-F-2 are shown. This type of heat exchanger is now undergoing development. AL-F-3 has a larger heat capacity than AL-F-1 and AL-F-2 because of its large coefficient of heat transfer on the gas side obtained by increasing gas velocity to 2.26 times that of AL-F-1.

## APPENDIX 4

### 4.1. An example of theoretical analysis of a vertical shell-and-tube type water-to-water heat exchanger

As described in Subsection 9.3, a vertical shell-and-tube type water-to-water heat exchanger was developed by the authors for JARE-13 and JARE-20. Its features are shown in Fig. 55, and the design data are as follows:

Inner diameter of shell	$D_s=0.155$ m,
outer diameter of tubes	$d_o=0.018$ m,
inner diameter of tubes	$d_i=0.014$ m,
number of tubes	$z=26$ ,
length of a tube	$l=0.988$ m,
number of baffle plates	$N=5$ ,
height of baffle cut	$H=0.0375$ m $H/D_s=0.242$ ,
triangular pitch	$P_t=0.023$ m,
distance between two baffle plates	$B=0.160$ m.

#### 4.1.1. Hot-water flow inside of the tube

The hot-water is recirculated by a centrifugal pump.

Hot-water pump manufactured by Kawamoto Seisakusho CS-32-CO4T

flow rate 46 l/min with a head of 8 m,

17 l/min with a head of 25 m,

inlet pipe diameter 1·1/2" was reduced to 1".

Estimated flow rate of water  $V_i=1.212$  m<sup>3</sup>/h=0.000337 m<sup>3</sup>/s,

heating surface area  $F_i=\pi d_i l z=\pi(0.014)(0.988)(26)=1.130$  m<sup>2</sup>,

sectional area  $A_i=(\pi/4)d_i^2(z/2)=(\pi/4)(0.014)^2(13)=0.00200$  m<sup>2</sup>,

velocity  $w_i=V_i/A_i=0.000337/0.00200=0.1685$  m/s,

kinematic viscosity  $\nu_i=0.417 \times 10^{-6}$  m<sup>2</sup>/s (70°C),

Prandtl number  $(Pr)_i=2.69$ ,

thermal conductivity  $\lambda_i=0.571$  kcal/mh°C,

Reynolds number  $(Re)_i=w_i d_i/\nu_i=(0.1685 \times 0.014)/(0.417 \times 10^{-6})=5657$ ,

Nusselt number

$$(Nu)_i = 0.023(R_e)_i^{0.8}(Pr)_i^{0.4} = 0.023(5657)^{0.8}(2.69)^{0.4} = 34.3,$$

heat transfer coefficient

$$\alpha_i = \lambda_i(Nu)_i/d_i = 0.571 \times 34.3/0.014 = 1400 \text{ kcal/m}^2\text{h}^\circ\text{C}.$$

#### 4.1.2. Cold-water flow across tube bank

The cold water of the outdoor 130-kl water tank was recirculated by a water pump submerged in the tank.

Manufactured by Sakuragawa Seisakusho V-40F,

inlet diameter 50 mm, motor 400 W,

flow rate 200 l/min, 12000 kg/h,

$V_o = 0.00333 \text{ m}^3/\text{s}$  with a head of 6 m,

total outer heating surface area

$$F_o = \pi d_o l z = \pi(0.018)(0.988)(26) = 1.453 \text{ m}^2,$$

triangular pitch  $P_t = 0.023 \text{ m}$ ,

equivalent diameter

$$\begin{aligned} D_e &= [2\sqrt{3} P_t^2 / (\pi d_o)] - d_o \\ &= [2\sqrt{3} (0.023)^2 / (\pi \times 0.018)] - 0.018 = 0.0144 \text{ m}, \end{aligned}$$

minimum flow area

$$a_s = (D_s/P_t)(P_t - d_o)B = (0.155/0.023)(0.023 - 0.018)0.160 = 0.00539 \text{ m}^2,$$

velocity

$$w_o = V_o/a_s = 0.00333/0.00539 = 0.618 \text{ m/s},$$

kinematic viscosity

$$\nu_o = 1.25 \times 10^{-6} \text{ m}^2/\text{s} (12^\circ\text{C}),$$

thermal conductivity

$$\lambda_o = 0.508 \text{ kcal/mh}^\circ\text{C},$$

Prandtl number

$$(Pr)_o = 8.91,$$

Reynolds number

$$(R_e)_o = w_o D_e / \nu_o = (0.618 \times 0.0144) / (1.25 \times 10^{-6}) = 7120,$$

Nusselt number

$$\begin{aligned} (Nu)_o &= 0.224(R_e)_o^{0.537}(H/D_s)^{-0.4}(Pr)_o^{1/3} \\ &= 0.224(7120)^{0.537}(0.242)^{-0.4}(8.91)^{1/3} = 95.8, \end{aligned}$$

heat transfer coefficient

$$\alpha_o = \lambda_o(Nu)_o/D_e = 0.508 \times 95.8/0.0144 = 3380 \text{ kcal/m}^2\text{h}^\circ\text{C},$$

thickness of tube wall

$$\delta_m = 0.002 \text{ m},$$

thermal conductivity of SUS-28

$$\lambda_m = 14 \text{ kcal/mh}^\circ\text{C},$$

total heat resistance

$$\begin{aligned} \sum R &= (1/\alpha_i)(d_o/d_i) + (1/\alpha_o) + (\delta_m/\lambda_m) \\ &= (1/1400)(0.018/0.014) + (1/3380) + (0.002/14) \\ &= 0.000919 + 0.000296 + 0.000143 = 0.001358 \text{ m}^2\text{h}^\circ\text{C/kcal}, \end{aligned}$$

overall coefficient of heat transmission

$$K_o = 1/\sum R = 1/0.001358 = 736 \text{ kcal/m}^2\text{h}^\circ\text{C},$$

$$K_i = K_o(F_o/F_i) = 736(0.018/0.014) = 947 \text{ kcal/m}^2\text{h}^\circ\text{C},$$

$$\begin{aligned}
W_i &= c_i G_i = (1)(1212) = 1212 \text{ kcal/h}^\circ\text{C}, \\
W_o &= c_o G_o = (1)(12000) = 12000 \text{ kcal/h}^\circ\text{C}, \\
W_i/W_o &= 1212/12000 = 0.101, \\
K_i F_i/W_i &= (947 \times 1.130)/(1212) = 0.883.
\end{aligned}$$

The temperature efficiency  $\Phi_i$  is given by BOŠNJAKOVIĆ *et al.* (1951) in a graph as the function of  $K_i F_i/W_i$  and  $W_i/W_o$ . By the aid of this graph, we can estimate as  $\Phi_i = 0.55$ , and from eqs. (71), we get  $t_{i2} = 40^\circ\text{C}$  by putting  $t_{i1} = 75^\circ\text{C}$ . From eq. (73),

$$W_i \Phi_i = W_o \Phi_o, \quad \Phi_o = \Phi_i (W_i/W_o) = 0.55(0.101) = 0.0556$$

and from eq. (72), we can estimate the outlet temperature of the cold water as follows:

$$t_{o2} = 15.5^\circ\text{C} \text{ for } t_{o1} = 12^\circ\text{C}.$$

The logarithmic mean temperature difference is calculated as  $\Delta t_{lm} = 42^\circ\text{C}$ , and the heat recovered is given by

$$Q_c = K_o F_o \Delta t_{lm} = (736)(1.453)(42) = 45000 \text{ kcal/h}.$$

## APPENDIX 5

### 5.1. Ice-melting experiment in Tokyo utilizing coolant energy of 12-kVA diesel-electric generator to be installed at Mizuho Station

The authors designed and manufactured a waste heat recovery system for utilizing the exhaust gas and coolant energy of a 12-kVA diesel-electric generator for JARE-12 (1970/72), and it was tested at Nakajima Denki Co., Ltd. in Tokyo on 11 November 1970. The test results are given in Table A-8. The first plan for Mizuho Station was as follows:

12-kVA diesel-electric generator set in a caboose: ZX 500B type of Meidensha Co., Ltd.

Diesel engine: Isuzu C221 (total piston displacement volume 2207 cc, 21 PS/1500 rpm).

Electric generator: E-AF type, 12-kVA, 3-phase, AC 200 V, 34.6 A, 50 Hz, power factor 0.8, 9.6 kW/1500 rpm.

Waste heat recovery systems

(1) Exhaust-gas energy recovery system for ice-melting

A shell-and-coil type heat exchanger, ice-melting tank and tube type water-to-water heat exchanger and a recirculating pump (flow rate  $G_w = 41.5 \text{ l/min}$ ).

Table A-8. Results of experiments on the ice-melting system by utilizing the exhaust-gas heat exchanger (shell-and-coil type) and on the hot-water room-heating system by the coolant energy of a 12-kVA diesel-electric generator prepared for Mizuho Station in JARE-12 (1970/72).

Run No.	Time	V	A	kW	$t_{g1}$ (°C)	$t_{g2}$ (°C)	$\Delta t_g$ (°C)	$Q_{R1}$ (kcal/h)	$t_{w1}$ (°C)	$t_{w2}$ (°C)	$\Delta t_w$ (°C)	$Q_{R2}$ (kcal/h)	$t_B$ (°C)	$t_H$ (°C)	$t_{H1}$ (°C)	$t_{H2}$ (°C)	$\Delta t_H$ (°C)	$Q_H$ (kcal/h)	
/	h min 10 42	start	200						14.2	14.0			16.7						
1	10 47	1/4 load	200	6.9	2.21	—	24.3	—	—	19.7	20.7	1.0	2500	17.8					
2	10 50		200	6.9	2.21	154.5	26.6	127.9	2600	22.2	23.2	1.0	2500	19.1	41.2	38.5	33.8	5.7	15400
3	11 05		200	6.9	2.21	154.5	29.9	124.6	2500	25.1	26.0	0.9	2300	20.6	47.0	45.0	39.8	5.2	14000
4	11 15		200	6.9	2.21	154.5	31.4	123.1	2460	27.6	28.5	0.9	2300	23.2	51.0	49.5	43.8	4.3	11600
/	11 17	1/2 load	200	13.6	4.35	—	—	—	—	—	—	—	—	—	—	—	—	—	
5	11 22		200	13.6	4.35	187.5	34.3	153.2	3130	29.8	30.9	1.1	2800	25.6	54.2	52.9	46.5	6.4	17300
6	11 32		200	13.6	4.35	187.5	37.3	150.2	3050	32.8	33.9	1.1	2800	28.7	56.8	55.2	48.8	6.4	17300
/	11 34	3/4 load	200	20.4	6.53	—	—	—	—	—	—	—	—	—	—	—	—	—	
7	11 44		200	20.4	6.53	208.0	43.2	164.8	3320	38.2	39.4	1.2	3000	33.9	61.0	60.5	52.8	7.7	20800
8	11 50		200	20.4	6.53	208.0	44.4	163.6	3280	39.4	40.7	1.3	3200	34.5	62.5	60.6	53.5	7.1	19200
/	11 51	4/4 load	200	30.4	9.73	—	—	—	—	—	—	—	—	—	—	—	—	—	
9	11 56		200	30.4	9.73	245.5	47.4	198.1	4040	42.5	43.9	1.4	3500	37.5	65.0	63.1	55.4	7.7	20800
10	12 01		200	30.4	9.73	245.5	49.3	196.2	3980	44.0	45.5	1.5	3700	38.5	64.2	64.5	56.4	8.1	21900
/	12 14	stop																	

- Note: 1) Tested at Nakajima Denki Co., Ltd. on 12 November 1970 by the authors. Room temperature  $t_a=14.6^\circ\text{C}$  (initial),  $16.9^\circ\text{C}$  (final).  
 2) 12-kVA diesel-electric generator to be installed in Mizuho Station by JARE-12.  
 3) The flow rate of a water pump recirculating the water between the exhaust-gas heat exchanger and a headtank and an ice-melting tank was  $41.5 \text{ l/min}$  ( $2490 \text{ kg/h}$ ). The total weight of water to be heated was  $G_B=54 \text{ kg}$  (in the coil and headtank)+ $90 \text{ kg}$  (in the ice-melting tank)= $144 \text{ kg}$ .  
 4) The coolant was bypassed to a headtank and the hot water in the headtank was fed to three fan-coil units connected in parallel by another water pump having a flow rate of  $45 \text{ l/min}$  ( $2700 \text{ kg/h}$ ). The total weight of the water contained in the fan-coil and recirculating system was  $47.8 \text{ l}$ .  
 5) The air flow of the diesel engine was  $G_a=0.0281 \text{ kg/s}=101 \text{ kg/h}$ . Recovered exhaust-gas energy by the shell-and-coil type heat exchanger can be represented by  $Q_{R1}$  (calculated from gas side) or  $Q_{R2}$  (calculated from water side).  
 6) The temperatures  $t_{w1}$  and  $t_{w2}$  show the inlet and outlet water temperatures of the exhaust-gas heat exchanger.  
 7)  $t_B$ : Water temperature in the ice-melting tank.  $t_H$ : Coolant temperature in a headtank for coolant system.  
 $t_{H1}$ : Feed coolant temperature to fan-coil units.  $t_{H2}$ : Return coolant temperature from fan-coil units.  
 $Q_H$ : Total heat radiated from three fan-coil units as warm air.

- (2) Coolant-heat recovery system for making hot water for room-heating.  
 A headtank for engine coolant.  
 A bathtub and heating radiator.  
 A recirculating pump for coolant (flow rate  $G_{wH} = 41.5$  l/min).  
 Three fan-coil units (1 phase, 100 V, 40 W, 4350 kcal/h).

The experimental results shown in Table A-8 are summarized as follows:

- (1) Exhaust-gas energy recovery system

The recovered exhaust-gas energy was

$$Q_{R1} = 2500 \text{ kcal/h at } 2.2 \text{ kW and } 4000 \text{ kcal/h at } 9.73 \text{ kW.}$$

- (2) Coolant heat recovery system

Three fan-coil units were heated by using the coolant heat of the diesel engine. The heating capacity of one unit was 4350 kcal/h, so that the total available heat was about 13000 kcal/h. The coolant heat was abundant compared with the exhaust-gas energy available and was more easily utilized. At Mizuho Station, only the coolant system was rebuilt during JARE-12 for making cold and hot water, and the room-heating system was put into operation during JARE-17 (1975/77) and has been used successfully thereafter.

## 5.2. Experimental data on a system to melt ice and produce hot water at Mizuho Station in JARE-12

During JARE-12 (1970/72), only the coolant heat recovery system was rebuilt and actually used. The data observed by Mr. TAGA is shown in Table A-9. The experiments were continued from 3:00 of July 12 to 10:30 of July 13, 1971 for 31.5 h.

The system is shown in Fig. A-4. The coolant was bypassed to a headtank and returned to the coolant pump of the engine. The hot water stored in the headtank was recirculated to an ice-melting tank and to a bathtub by a recirculating pump and heated these vessels indirectly through a heating tube and a radiator submerged in each of them.

Six kinds of experiments were continued as shown in Table A-10. In series A, B, C and D, 100 kg of ice, the temperature of which was  $-22^{\circ}\text{C}$ , was thrown into the ice-melting tank containing 100 kg of hot water. The water temperature dropped steeply until the ice block was melted completely, and then it was raised again gradually with time.

The following relations should be held for the heating of water in the ice-melting tank:

- $Q_c$ : transferred heat from coolant to water, kcal/h,  
 $\tau$ : time, h,  
 $t_{cm}^*$ : an ultimate coolant temperature at  $\tau = \infty$ ,  $^{\circ}\text{C}$ ,

Table A-9. Results of tests on the coolant heat recovery system of 12-kVA in Mizuho Station (observed by TAGA in 12-13 July 1971, JARE-12).

Run No.	Time	Load (kW)	$G_{wR}$ (l/min)	$G_{wH}$ (l/min)	Ice-melting tank	$B_o$ (l/h)	kW	Atm. temp. $t_a$ (°C)	Trench temp. (°C)	Caboose temp. (°C)	Coolant outlet temp. (°C)	Temp. return to head-tank (°C)	Temp. in ice-melting tank (°C)	
A	1	1.5 (15.6%)	6 (50%)	6 (50%)	100 kg of ice (−22°C) was put into the ice-melting tank containing 100 l of hot water	1.85	1.4	−31	−4	38	91	89	87	
	2						1.5	−31	−3	36	93	91	89	
	3						1.5	−30	−3	35	72	55	28	4.10 snow-in
	4						1.5	−31	−3	34	60	48	30	
	5						1.5	−32	−6	24	62	56	48	
	6						1.5	−33	−6	24	63	57	50	
	7						1.5	−33	−4	34	94	89	87	
B	8	1.6 (16.7%)	0 (0%)	12 (100%)	Same as No.1	1.88	1.5	−35	−0	34	98	94	92	10.50 snow-in
	9						1.6	−36	−9	14	72	67	60	
	10						1.6	−37	−14	12	87	83	77	
	11						1.7	−38	−8	14	96	92	87	
C	12	3.2 (33.4%)	0 (0%)	12 (100%)	Same as No. 1	2.25	3.2	−40	−14	12	64	54	23	13.56 snow-in
	13						3.2	−41	−13	9	66	60	50	
	14						3.2	−43	−14	12	86	82	75	
	15						3.4	−43	−13	14	94	89	84	
D	16	5.3 (55%)	0 (0%)	12 (100%)	Same as No. 1	2.45	5.2	−43	−15	12	95	90	86	16.50 snow-in
	17						5.3	−43	−17	11	74	62	28	
	18						5.3	−43	−12	13	90	85	78	
E	19	5.2 (54%)	12 (100%)	0 (0%)	Without ice melting	2.34	5.2	−43	−14	13	92	88	80	
	20						5.2	−43	−7	43	79	78	80	
	21						5.2	−43	−7	46	78	77	80	
	22						5.2	−43	−7	39	78	72	78	
F	23	1.9 (20%)	9.6 (80%)	2.4 (20%)	Without ice melting	1.94	2.4	−43	−8	39	72	70	73	9.00 recording was stopped
	24						2.0	−44	−7	40	72	69	70	
	25						2.0	−43	−6	41	72	69	70	
	26						2.0	−43	−6	41	73	68	69	
	27						2.0							
	28						0.2							

Note: 1) Coolant flow rate 18 l/min=1080 kg/h.  
 2)  $G_{wR}$ : Coolant flow rate to the engine radiator l/min.  $G_{wH}$ : Coolant flow rate to the headtank l/min.  
 3)  $B_o$ : Fuel flow rate l/h.

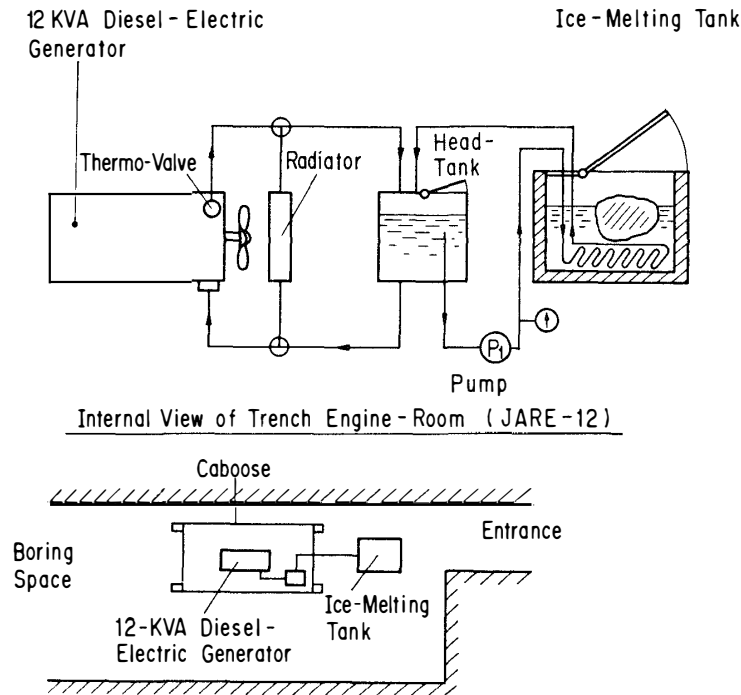


Fig. A-4. System to heat water and melt ice or snow with coolant heat in a trench engine room of Mizuho Station in JARE-12 (1970/72).

- $t$ : an instantaneous water temperature in the ice-melting tank, °C,  
 $c_w$ : specific heat of water, kcal/kg°C,  
 $G_w$ : total weight of water to be heated, kg,  
 $C_M$ : specific heat of tank materials, etc., kcal/kg°C,  
 $G_M$ : weight of tank materials, etc., kg,  
 $\alpha_a$ : coefficient of heat transfer from hot surfaces to atmosphere, kcal/m<sup>2</sup>h°C,  
 $A$ : surface area relating to heat loss of tank, etc., m<sup>2</sup>,  
 $t_a$ : atmospheric air temperature, °C,  
 $K_c$ : overall coefficient of heat transmission of heating coil, referring to  $F_c$  and  $(t_{cm}^* - t)$ , kcal/m<sup>2</sup>h°C,  
 $F_c$ : heating area, m<sup>2</sup>.

The equation of heat balance can be written as follows, similarly as for Section 7(c):

$$Q_c d\tau = K_c F_c (t_{cm}^* - t) d\tau = (c_w G_w + \sum C_M G_M) dt + \sum \alpha_a A (t - t_a) d\tau \quad (\text{A-15})$$

which can be reduced to

$$\frac{dt}{d\tau} = a - bt \quad \text{°C/h}, \quad (\text{A-16})$$

Table A-10. Test results of ice-melting system using waste coolant heat of 12-kVA diesel-electric generator in Mizuho Station in JARE-12 (observed by TAGA in 12-13 July 1971).

Experiment series	A	B	C	D	E	F	Remarks
Engine coolant to radiator $G_{wR}$ (l/min)	6 (50%)	0 (0%)	0 (0%)	0 (0%)	12 (100%)	9.6 (80%)	Refer Fig. A-4 and Table A-9
Engine coolant to headtank $G_{wH}$ (l/min)	6 (50%)	12 (100%)	12 (100%)	12 (100%)	0 (0%)	2.4 (20%)	
Load (kW)	1.5 (15.6%)	1.6 (16.7%)	3.2 (33.3%)	5.3 (55.2%)	5.2 (54.2%)	1.9 (19.8%)	Max. load 9.6 kW (100%)
Fuel consumption							
$B_o$ (l/h)	1.85	1.88	2.25	2.45	2.34	1.94	Specific density $\rho_f=0.82$
$B$ (kg/h)	1.52	1.54	1.85	2.01	1.92	1.59	
Total heat supplied by fuel $Q_f$ (kcal/h)	16500	16700	20000	21800	20800	17200	$H_o=10832$ kcal/kg
Output as electric power (kcal/h)	1290 (7.8%)	1380 (8.3%)	2750 (13.8%)	4560 (20.9%)	4470 (21.5%)	1630 (9.5%)	At $t=70^\circ\text{C}$
Ice-melting power (kcal/h)	1920 (11.6%)	3320 (19.9%)	4580 (22.9%)	4510 (20.7%)			
Efficiency (total)	(19.4%)	(28.2%)	(36.7%)	(41.6%)	(21.5%)	(9.5%)	
Coefficient $b$ (1/h)	0.283	0.408	0.385	0.458			Hot water 100 Ice 100
Total weight of water in ice-melting tank (kg)	200	200	200	200			
$K_c F_c$ (kcal/h $^\circ\text{C}$ )	56.6	81.6	77	91.6			
$t_{cm}^*=b/a$ ( $^\circ\text{C}$ )	104	110.7	129.5	119.2			

where

$$a = (K_c F_c t_{cm}^* + \sum \alpha_a A t_a) / (c_w G_w + \sum c_M G_M) \quad ^\circ\text{C/h}, \quad (\text{A-17})$$

$$b = (K_c F_c + \sum \alpha_a A) / (c_w G_w + \sum c_M G_M) \quad 1/\text{h}, \quad (\text{A-18})$$

$$a/b = (K_c F_c t_{cm}^* + \sum \alpha_a A t_a) / (K_c F_c + \sum \alpha_a A) \doteq t_{cm}^*. \quad (\text{A-19})$$

From eq. (A-18),

$$K_c F_c = b(c_w G_w + \sum c_M G_M) - \sum \alpha_a A \doteq b(c_w G_w) \quad \text{kcal/h}^\circ\text{C}. \quad (\text{A-20})$$

The solution of eq. (A-16) is given as follows:

$$t = (a/b) - [(a/b) - t_o] e^{-b\tau} \doteq t_{cm}^* - [t_{cm}^* - t_o] e^{-b\tau} \quad ^\circ\text{C}, \quad (\text{A-21})$$

and

$$Q_c = K_c F_c (t_{cm}^* - t) \quad \text{kcal/h}. \quad (\text{A-22})$$

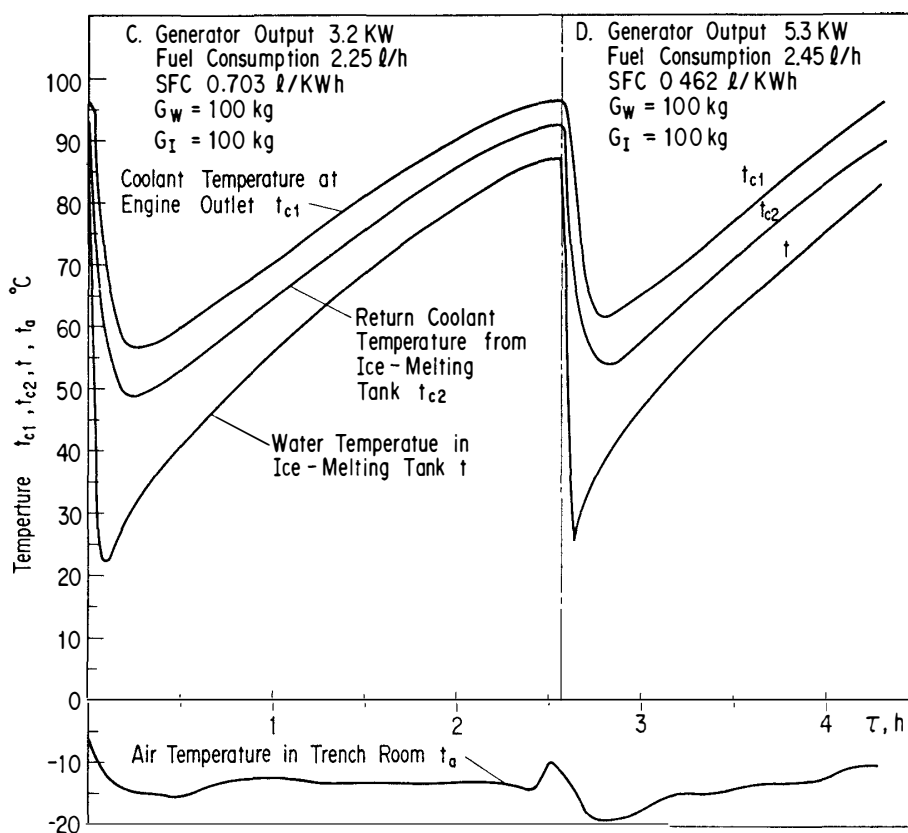


Fig. A-5. Cooling and heating curves of water temperature of ice-melting system using coolant heat of 12-kVA diesel-electric generator (measured by TAGA, 12-13 July 1971).

In eq. (A-21), time  $\tau$  should be calculated from a point on a temperature increasing curve, where the water temperature  $t$  is equal to  $t_o$ .

For series A

$$t = 104 - 57.4 e^{-0.283\tau},$$

$$b = 0.283 \text{ 1/h}, \quad a/b = 104^\circ\text{C}, \quad a = 29.4^\circ\text{C/h},$$

$$G_w = 200 \text{ kg}, \quad c_w = 1.0 \text{ kcal/kg}^\circ\text{C}, \quad t_{cm}^* = 104^\circ\text{C}.$$

From eq. (A-20), we get

$$K_c F_c = b(c_w G_w) = 0.283(200) = 56.6 \text{ kcal/h}^\circ\text{C},$$

$$Q_c = K_c F_c (t_{cm}^* - t) = 56.6(104 - t) = 5886 - 56.6t \text{ kcal/h},$$

$$Q_c = 1924 \text{ kcal/h} (t = 70^\circ\text{C}).$$

For series B

$$t = 110.7 - 54.7 e^{-0.408\tau}, \quad b = 0.408 \text{ 1/h}, \quad a = 45.2^\circ\text{C/h},$$

$$Q_c = 81.6(110.7 - t) = 9033 - 81.6t \text{ kcal/h},$$

$$Q_c = 3321 \text{ kcal/h} (t = 70^\circ\text{C}).$$

For series C

$$t = 129.5 - 82.5 e^{-0.385\tau}, \quad b = 0.385 \text{ 1/h}, \quad a = 49.9^\circ \text{C/h},$$

$$Q_c = 77(129.5 - t) = 9972 - 77t \text{ kcal/h},$$

$$Q_c = 4582 \text{ kcal/h} \quad (t = 70^\circ \text{C}).$$

For series D

$$t = 119.2 - 75.7 e^{-0.458\tau}, \quad b = 0.458 \text{ 1/h}, \quad a = 54.6^\circ \text{C/h},$$

$$Q_c = 91.6(119.2 - t) = 10920 - 91.6t \text{ kcal/h},$$

$$Q_c = 4510 \text{ kcal/h} \quad (t = 70^\circ \text{C}).$$

In Fig. A-5, the cooling and heating curves for series C and D are shown. The summary of the experimental results are shown in Table A-10.